

A. M. Wolde-Tinsae L. F. Greimann P. S. Yang

Nonlinear Pile Behavior in Integral Abutment Bridges

Part 1

February 1982

Iowa DOT Project HR-227
ERI Project 1501
ISU-ERI-Ames 82123

Sponsored by the Iowa Department of Transportation, Highway Division,
and the Iowa Highway Research Board

report

College of
Engineering
Iowa State University

The opinions, findings, and conclusions expressed in this publication are those of the authors and not necessarily those of the Highway Division of the Iowa Department of Transportation.

**A. M. Wolde-Tinsae
L. F. Greimann
P. S. Yang**

in collaboration with
B. Johnson

Final Report

**Nonlinear Pile Behavior in
Integral Abutment Bridges**

February 1982

Submitted to the Highway Division,
Iowa Department of Transportation

Iowa DOT Project HR-227
ERI Project 1501
ISU-ERI-Ames 82123

**DEPARTMENT OF CIVIL ENGINEERING
ENGINEERING RESEARCH INSTITUTE
IOWA STATE UNIVERSITY, AMES**

TABLE OF CONTENTS

	<u>Page</u>
ABSTRACT	vii
LIST OF FIGURES	ix
LIST OF TABLES	xiii
1. INTRODUCTION	1
1.1. Statement of the Problem	1
1.2. Background	2
1.3. Objective and Scope	8
2. SURVEY OF CURRENT PRACTICE	11
2.1. Objective	11
2.2. Method of Investigation	11
2.3. Trends in Responses	13
2.4. Review of Design and Details in Selected States	20
2.4.1. Tennessee	20
2.4.2. Kansas	22
2.4.3. Missouri	22
2.4.4. North Dakota	23
2.4.5. California	24
2.4.6. Iowa	26
2.5. Summary	27
3. REVIEW OF THE LITERATURE	29
3.1. Methods of Analyses	29
3.2. Soil Properties	30
3.2.1. Lateral Resistance - Displacement (p-y) Curves	31
3.2.2. Load-Slip (f-z) Curves	38
3.2.3. Load-Settlement (q-z) Curves	43
3.3. Research on Integral Abutment Bridges	45
3.3.1. California	45
3.3.2. Missouri	50

	<u>Page</u>
3.3.3. South Dakota	52
3.3.4. North Dakota	54
4. MATHEMATICAL MODEL	57
4.1. Mathematical Model Description	57
4.2. Finite Element Idealization	61
4.2.1. Basic Concept of the Finite Element Method	61
4.2.2. Causes of Geometric and Material Nonlinearities	62
4.2.3. Pile (Beam-Column) Model	63
4.2.4. Layering Technique	72
4.2.5. Soil Model	77
4.3. Basic Nonlinear Solution Techniques	86
4.3.1. Convergence Criteria	90
4.4. Verification of Model	90
4.4.1. Beam-Column Problem	91
4.4.2. Short Column Problem	94
4.4.3. Soil Problems	100
4.4.4. Experimentally Loaded Piles	100
5. NUMERICAL RESULTS	119
5.1. Pile Description	119
5.2. Soil Description	119
5.3. Loading Pattern	133
5.4. Results	133
5.5. Behavior of Pile and Soil	143
6. SUMMARY, CONCLUSIONS, AND RECOMMENDATIONS FOR FURTHER STUDY	155
6.1. Summary	155
6.2. Conclusions	158
6.3. Recommendations for Further Study	159
7. ACKNOWLEDGMENT	161
8. REFERENCES	163

	<u>Page</u>
9. APPENDICES	170
9.1. Questionnaire for Bridges with Integral Abutments and Summary of Responses	170
9.2. Memorandum to Designers, Office of Structures Design, California Department of Transportation	179
9.3. Iowa Department of Transportation Foundation Soils Information Chart	184

ABSTRACT

The highway departments of all fifty states were contacted to find the extent of application of integral abutment bridges, to survey the different guidelines used for analysis and design of integral abutment bridges, and to assess the performance of such bridges through the years. The variation in design assumptions and length limitations among the various states in their approach to the use of integral abutments is discussed. The problems associated with lateral displacements at the abutment, and the solutions developed by the different states for most of the ill effects of abutment movements are summarized in the report.

An algorithm based on a state-of-the-art nonlinear finite element procedure was developed and used to study piling stresses and pile-soil interaction in integral abutment bridges. The finite element idealization consists of beam-column elements with geometric and material nonlinearities for the pile and nonlinear springs for the soil. An idealized soil model (modified Ramberg-Osgood model) was introduced in this investigation to obtain the tangent stiffness of the nonlinear spring elements.

Several numerical examples are presented in order to establish the reliability of the finite element model and the computer software developed. Three problems with analytical solutions were first solved and compared with theoretical solutions. A 40 ft H pile (HP 10 × 42) in six typical Iowa soils was then analyzed by first applying a horizontal displacement Δ_H (to simulate bridge motion) and no rotation at the top and then applying a vertical load V incrementally until failure occurred. Based on the numerical results, the failure mechanisms were generalized

to be of two types: (a) lateral type failure and (b) vertical type failure. It appears that most piles in Iowa soils (sand, soft clay and stiff clay) failed when the applied vertical load reached the ultimate soil frictional resistance (vertical type failure). In very stiff clays, however, the lateral type failure occurs before vertical type failure because the soil is sufficiently stiff to force a plastic hinge to form in the pile as the specified lateral displacement is applied.

Preliminary results from this investigation showed that the vertical load-carrying capacity of H piles is not significantly affected by lateral displacements of 2 inches in soft clay, stiff clay, loose sand, medium sand and dense sand. However, in very stiff clay (average blow count of 50 from standard penetration tests), it was found that the vertical load carrying capacity of the H pile is reduced by about 50 percent for 2 inches of lateral displacement and by about 20 percent for lateral displacement of 1 inch.

On the basis of the preliminary results of this investigation, the 265-foot length limitation in Iowa for integral abutment concrete bridges appears to be very conservative.

LIST OF FIGURES

	<u>Page</u>
1. Cross-sectional view through a conventional abutment.	4
2. Integral abutment details.	5
3. Semi-integral abutment details.	9
4. Sketch of Moore engineering integral abutment system.	25
5. Lateral resistance - displacement (p-y) curves.	32
6. Load-slip (f-z) curves.	33
7. Normalized q-z curve (Reese curve).	34
8. Normalized f-z curve (Reese curve).	41
9. Reduction factor α .	42
10. Sample inspection record of structures without expansion joints.	46
11. Calculated versus experimentally determined pile moments.	49
12. A mathematical model of integral abutment bridge with pile/soil interaction.	58
13. Pile finite element model.	59
14. Beam-column element with corotational (x,y) and global (X,Y) coordinates.	65
15. Typical layering system for the H pile about strong axis and weak axis.	73
16. Simulation of resistance-displacement curves by modified Ramberg-Osgood model.	78
17. (a) Nondimensional forms of the modified Ramberg-Osgood model with $E_{sf} = 0$.	80
(b) Nondimensional forms of the modified Ramberg-Osgood model with $E_{sf} = +0.2 E_{si}$.	81
(c) Nondimensional forms of the modified Ramberg-Osgood model with $E_{sf} = -0.2 E_{si}$.	82
18. Linear spring under an applied force f.	83

	<u>Page</u>
19. External and internal forces, and displacements acting on the pile element.	83
20. Increment-iteration or mixed procedure (Newton-Raphson solution of the equation $F = f(D)$).	87
21. Beam-column with a concentrated load, Q .	92
22. Load-displacement curves for beam-column problem.	93
23. Load-displacement curves for beam-column problem (with 2 and 8 finite elements).	95
24. (a) A short column subjected to applied load. (b) Cross section A-A. (c) Stress-strain relation.	96
25. Stress patterns on a cross section as the moment increases.	97
26. $M-\theta$ characteristics for the example in Figure 24.	99
27. HP 14 \times 73 pile used to check soil spring response.	101
28. Iteration path for the example in Figure 27 with applied load, $P = 1000$ kips.	102
29. Iteration path for the example in Figure 27 with applied load, $V = 3000$ kips (no point spring).	103
30. Iteration path for the example in Figure 27 with applied load, $V = 10$ kips (no vertical springs).	104
31. Force in a pile as a function of depth.	107
32. Relationship between tip displacement and load.	108
33. Pile with axial load variation with depth.	108
34. Load settlement curve for HP 14 \times 89 test pile.	111
35. Load settlement curve for HP 14 \times 117 test pile.	112
36. Schematic test setup.	114
37. Comparison between the Reese ($p-y$) curve and modified Ramberg-Osgood model (nondimensional).	116
38. Load-displacement curves, pier 1.	117

	<u>Page</u>
39. Load-displacement curves, pier 2.	118
40. Mathematical model of an integral abutment bridge.	120
41. Comparison between the Reese (f-z) curve and modified Ramberg-Osgood model (nondimensional).	126
42. Comparison between the Reese (q-z) curve and modified Ramberg-Osgood model (nondimensional).	127
43. Comparison between the Reese (p-y) curve and modified Ramberg-Osgood model (nondimensional, soft clay).	128
44. Comparison between the (p-y) curve and modified Ramberg-Osgood model (nondimensional, stiff clay).	129
45. Comparison between the Reese (p-y) curve and modified Ramberg-Osgood model (nondimensional, very stiff clay).	130
46. Comparison between Reese (p-y) curve and modified Ramberg-Osgood model (nondimensional, sand).	131
47. Loading pattern on a single vertical H pile.	134
48. Vertical load-settlement curves with specified lateral displacements, Δ_H (0, 1, 2, 3, 4 in.) for soft clay.	136
49. Vertical load-settlement curves with specified lateral displacements, Δ_H (0, 1, 2, 4 in.) for stiff clay.	137
50. Vertical load-settlement curves with specified lateral displacements, Δ_H (0, 1, 2 in.) for very stiff clay.	138
51. Vertical load-settlement curves with specified lateral displacements, Δ_H (0, 1, 2, 4 in.) for loose sand.	139
52. Vertical load-settlement curves with specified displacements, Δ_H (0, 1, 2, 4 in.) for medium sand.	140
53. Vertical load-settlement curves with specified lateral displacements, Δ_H (0, 1, 2, 4 in.) for dense sand.	141
54. Typical load-settlement curves for (A) friction pile, (B) bearing pile, (C) friction-bearing pile.	142
55. Ultimate vertical load versus lateral specified displacements (clay).	144

	<u>Page</u>
56. Ultimate vertical load versus lateral specified displacements (sand).	145
57. Nondimensional forms of ultimate vertical load versus lateral specified displacements, Δ_H in Iowa soils.	146
58. Deflected shapes in soft clay (a) after Δ_H , (b) after ultimate load, V_{ULT} .	147
59. Deflected shapes in stiff clay (a) after Δ_H , (b) after ultimate load, V_{ULT} .	148
60. Deflected shapes in very stiff clay (a) after Δ_H , (b) after ultimate load, V_{ULT} .	149
61. Deflected shapes in loose sand (a) after Δ_H , (b) after ultimate load, V_{ULT} .	150
62. Deflected shapes in medium sand (a) after Δ_H , (b) after ultimate load, V_{ULT} .	151
63. Deflected shapes in dense sand (a) after Δ_H , (b) after ultimate load, V_{ULT} .	152

LIST OF TABLES

	<u>Page</u>
1. Integral abutment bridge length limitations (1981).	16
2. Constants used in p-y relationships for clays.	36
3. Analytical forms of p-y curves.	39
4. Evaluation of parameters for Table 3.	40
5. Typical and limiting parameters for driven piles in medium dense to dense sand.	44
6. Integral abutment bridge length limitations (1972).	51
7. Comparison between theoretical and numerical results.	105
8. Soil characteristics.	113
9. Cohesionless soils - typical values.	122
10. Cohesive soils - typical values.	122
11. Typical Iowa soils.	123
12. f-z, q-z and p-y curves for clays.	124
13. f-z, q-z and p-y curves for sand.	125
14. Soil parameters in Iowa soils.	132

1. INTRODUCTION

1.1. Statement of the Problem

Integral abutments on concrete bridges came into use in the state of Iowa in 1965 [1].* The current length limitation for such bridges in Iowa is 265 feet for steel H piling, 150 to 200 feet for timber piling with wrapping of flexible material, and under 150 feet for timber piling without wrapping [2]. These length limitations are based on first order theoretical analyses of the effects of thermal expansion and contraction of bridges on piling stresses. Yearly inspection of integral abutment bridges in Iowa for about five years after construction showed no distress associated with lack of expansion joints in the superstructure. Other states, e.g., South Dakota and Tennessee, have been allowing integral abutment bridges significantly longer than 265 feet with apparent success. Long bridges are particularly susceptible to damage from thermal expansion and contraction because of the relatively large displacements associated with annual temperature variations. Historically, a system of expansion joints, roller supports and other structural releases is provided on long bridges to permit thermal expansion. However, providing expansion joints through a bridge leads to substantial increase in the initial cost. The expansion joints are also relatively high sources of deterioration and frequently do not operate as intended; thus, they result in high maintenance costs.

Integral abutment bridges provide an attractive design alternative because expansion joints are not present. Thermal expansion, however,

* Numerals in brackets designate entries in the list of references.

must be relieved or accounted for in some manner. In an integral abutment bridge, the piles are usually the most flexible elements and are expected to accommodate the lateral movements due to thermal expansion. The maximum thermal expansion that can be allowed by the piles without destroying their vertical load-carrying capacity is of primary importance in defining the safe length of integral abutment bridges. If this length can safely be increased, the economic advantages of integral abutments can be realized for longer bridges. There has not been any analytical study to date to determine the effects of such factors as lateral movement and soil-pile interaction on the bearing capacity of piles in integral abutment bridges.

1.2. Background

Prior to World War II most bridges with an overall length of 50 feet or more were constructed with some form of expansion joints. Periodic inspection of these bridges revealed that expansion joints tended to freeze and close and did not operate as intended. Closer inspection of such bridges also indicated that there was no serious distress associated with the frozen or closed expansion joints. This led to the advancement of the case for continuous construction.

Continuity in steel stringer and other types of bridges has been accepted practice since the early 1950s. In addition to the inherent economy of continuous beams, wherein negative moments over interior supports serve to reduce midspan positive moments, one line of bearing devices was automatically eliminated at each interior support. The

predominant problem with these continuous bridges was at the abutments, where some kind of expansion joints were required. An example of such an abutment is shown in Fig. 1 [3]. These joints allowed penetration of water from the backfill and roadway into the bearing areas and onto bridge seats. The joints could then be forced closed, resulting in broken backwalls, sheared anchor bolts, damaged roadway expansion devices and other problems. Maintenance costs associated with these problems accelerated the development of integral abutments.

Figure 2 shows typical integral abutments; each is supported by a single row of vertical piles extending into the abutments [1,4-7]. In addition to being aesthetically pleasing, integral abutments offer the advantage of lower initial cost and lower maintenance cost. Expensive bearings, joint material, piles for horizontal earth loads and leakage of water through the joints are all eliminated.

Kansas, Missouri, Ohio, North Dakota, and Tennessee were some of the early users of integral abutments to tie bridge superstructures to foundation pilings. This method of construction has steadily grown more popular. Today more than half of the state highway agencies have developed design criteria for bridges without expansion joint devices. Most of the states using integral abutments began by building them on bridges less than 100 feet long. Allowable lengths were increased on the basis of good performance of successful connection details. Full-scale field testing and sophisticated rational design methods were not commonly used as a basis for increasing allowable lengths. This led to wide variations in criteria for the use of integral abutments from state to state. In 1974 the variation in maximum allowable length for

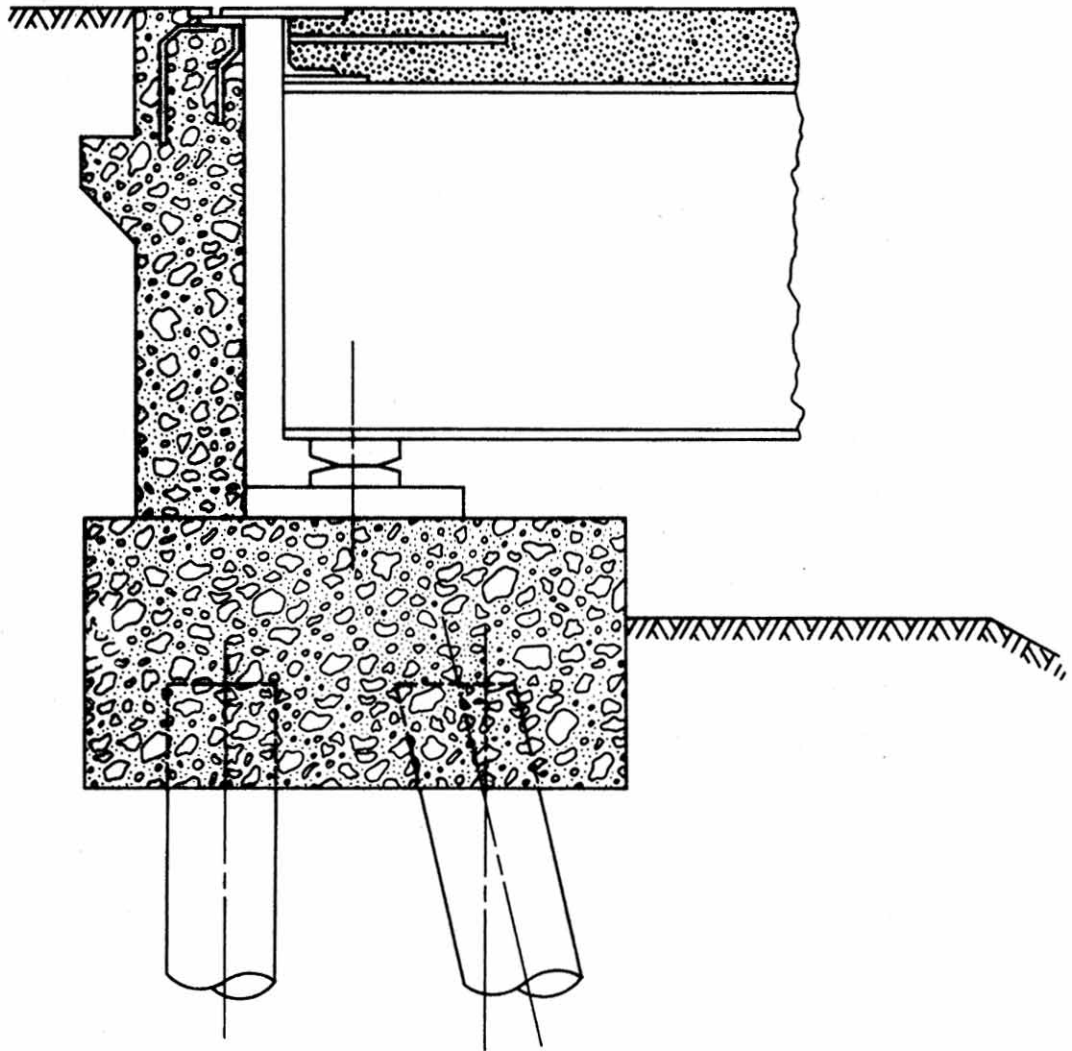
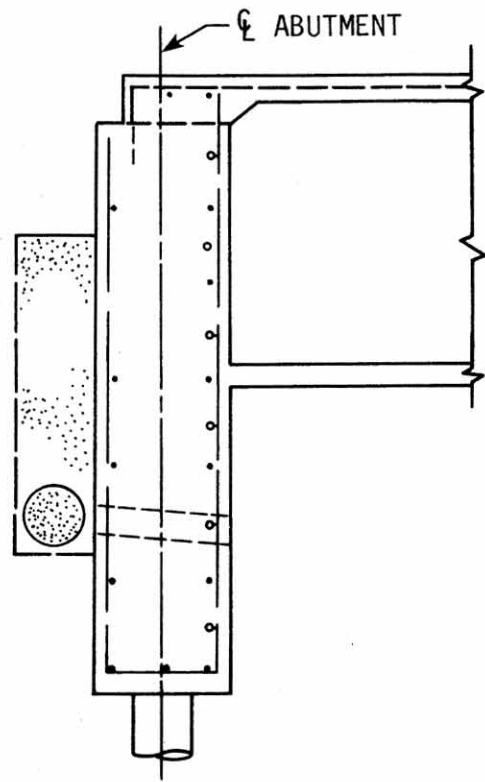
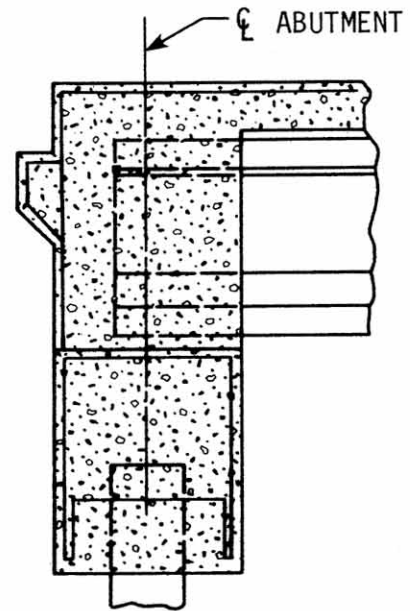


Figure 1. Cross-sectional view through a conventional abutment.

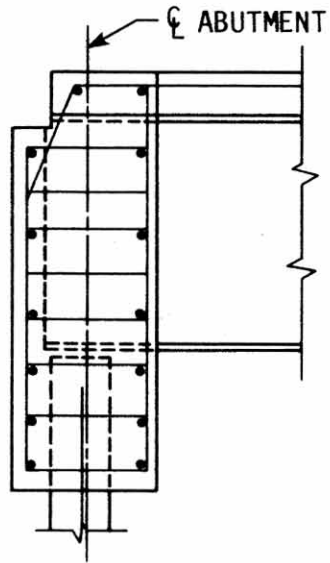


CALIFORNIA
(a)

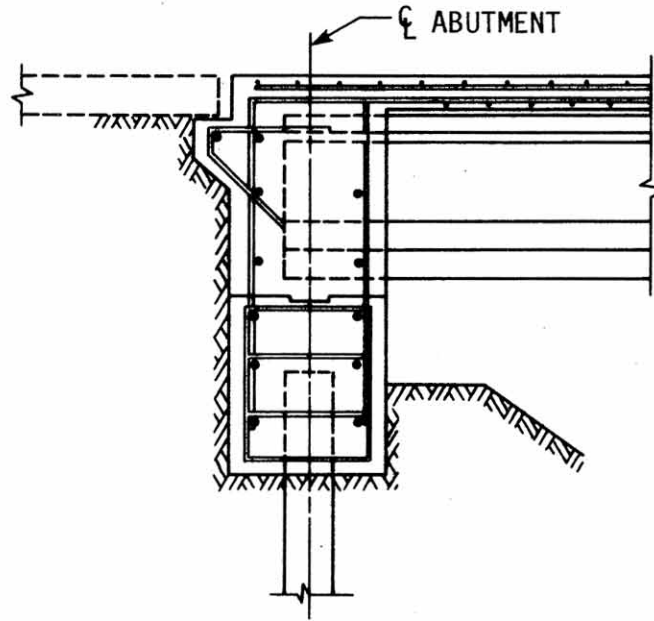


MISSOURI
(b)

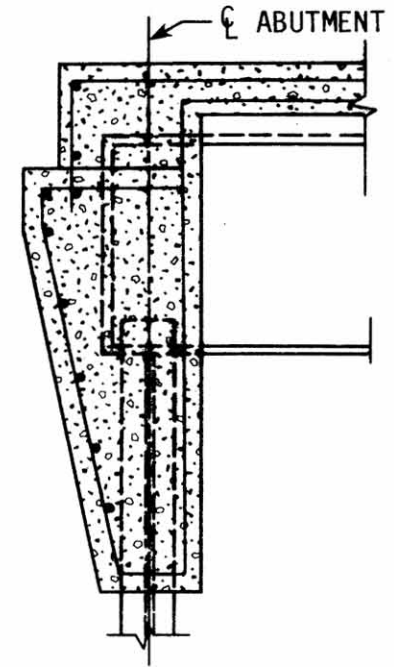
Figure 2. Integral abutment details.



SOUTH DAKOTA
(c)



IOWA
(d)



MISSOURI
(e)

Figure 2. (Continued)

concrete bridges using integral abutments between Kansas and Missouri was 200 feet [1]. A survey conducted by the University of Missouri in 1973 indicated that allowable lengths for integral abutment concrete bridges in some states were 500 feet while in others they were only 100 feet.

Continuous steel bridges with integral abutments have performed successfully for years in the 300 foot range in such states as North Dakota, South Dakota and Tennessee. Continuous concrete structures 500-600 feet long with integral abutments have been constructed in Kansas, California, Colorado and Tennessee [8]. In Iowa the maximum bridge length for which integral abutment construction is allowed has been limited to 265 feet [1]. The Federal Highway Administration recommends integral abutments for steel bridges less than 300 feet long, for pre- or post-tensioned concrete bridges less than 600 feet long, and for unrestrained bridges, that is, bridges where the abutment is free to rotate as with a stub abutment on one row of piles or an abutment hinged at the footing [8].

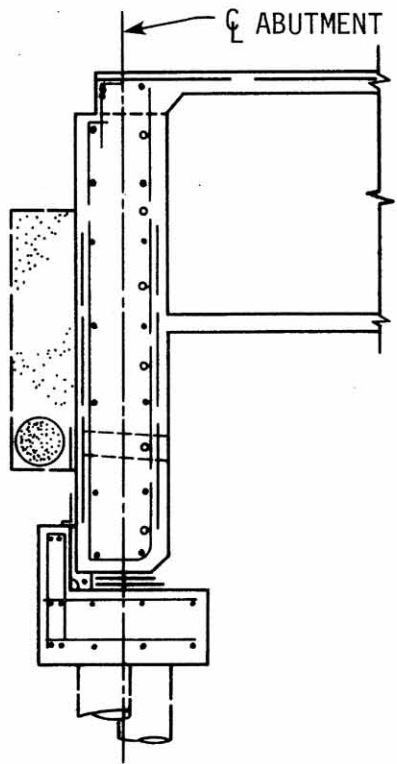
In an integral abutment bridge with flexible piling, the thermal stresses are transferred to the substructure via a rigid connection. Various construction details have been developed to accomplish the transfer as shown in Fig. 2. The abutments contain sufficient bulk to be considered a rigid mass. A positive connection to the girder ends is generally provided by vertical and transverse reinforcing steel. This provides for full transfer of temperature variation and live load rotational displacements to the abutment piling.

The semi-integral abutments shown in Fig. 3 are designed to minimize the transfer of rotational displacements to the piling [4,7]. They do transfer horizontal displacements, and they also allow elimination of the deck expansion joints. Rotation is generally accomplished by using a flexible bearing surface at a selected horizontal interface in the abutment. Allowing rotation at the pile top generally reduces pile loads.

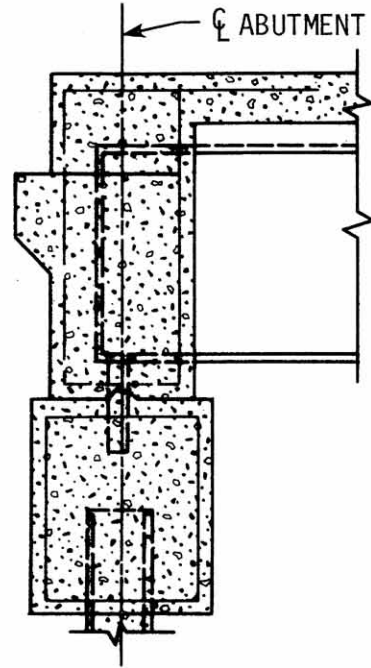
A survey of the fifty states and a review of the literature showed that there has not been a rigorous scientific theoretical or experimental study performed to establish limits for integral abutment bridges. The limit of allowable horizontal movement that will cause objectionable pile stress and what constitutes an objectionable pile stress have not been well defined. This partly explains the wide variation in design criteria for integral abutment bridges that exists among the different state highway agencies.

1.3. Objective and Scope

The objective of this research is to make a preliminary determination of lengths to which bridges with integral abutments can be safely designed. As part of this investigation the highway departments of all the states in the union were contacted to find the extent of application of integral abutment bridges, to survey the different guidelines used for analysis and design of integral abutment bridges, and to assess the performance of such bridges through the years. A state-of-the-art analytical model was devised to study the effect of thermal-induced



CALIFORNIA
(a)



MISSOURI
(b)

Figure 3. Semi-integral abutment details.

lateral movement of the pile on the carrying capacity of the pile. The analytical model was based on the finite element approach and incorporated geometric and material nonlinearities of the pile, nonlinear soil behavior, and soil-pile interaction. The analytical model was verified through correlation of results with experimental data and then applied to Iowa soil conditions to determine maximum safe lengths for steel and concrete integral abutment bridges.

2. SURVEY OF CURRENT PRACTICE

2.1. Objective

As a background to the main objective of this research, which is to establish tentative recommendations on maximum safe lengths for steel and concrete bridges with integral abutments, a survey of the different states was made to obtain information on the design and performance of integral abutment bridges. This chapter summarizes the findings in this aspect of the investigation, including

- Various design criteria and limitations being used;
- Assumptions being made regarding selected design parameters and appropriate level of analysis;
- Specific construction details being used;
- Changes in trends since previous surveys were taken; and
- Long-term performance of bridges with integral abutments.

A more comprehensive report on the survey is included in a research report by Johnson [9].

2.2. Method of Investigation

Surveys concerning the use of integral abutments have previously been conducted [1,7]. They have indicated that there are marked variations in design limitations and criteria for their use. Many states have not felt comfortable using a system that does not contain some "free space" for temperature variation displacements.

Some of the variations among the states occur because of different temperature range criteria. Also, depending on the extent of deicing

salt use, some states may experience greater problems with bridge deck expansion joint devices than others. Naturally, it is difficult to justify altering existing construction techniques by either beginning the use of integral abutments or using them for much longer bridges if the possibility of decreased distress and maintenance are not readily apparent.

A survey questionnaire was prepared in cooperation with the Office of Bridge Design, Highway Division, Iowa Department of Transportation, to obtain information concerning the use and design of integral bridge abutments. Based on a review of the survey, several states were later contacted to gain a better understanding of successful design details and assess the performance of relatively long integral abutment bridges. A summary of the results of correspondence and telephone conversations with bridge engineers in Tennessee, Kansas, Missouri, North Dakota, California, and Iowa is included in Section 2.4 of this report.

Most of the states that use integral abutments, as shown in Appendix 9.1, have developed specific guidelines concerning allowable bridge lengths, design of the backwall, type of piling, etc. The basis of these guidelines is shown to be primarily empirical.

The questionnaire was sent to the 50 states and Puerto Rico. Since the Direct Construction Office, Region 15, Federal Highway Administration is involved in bridge construction on federally owned property, a questionnaire was also sent to the design department in Arlington, Virginia. A copy of the questionnaire and responses from each of these agencies are contained in Appendix 9.1.

The survey questions were directed at limitations in bridge length, type, and skew. The states were also asked what assumptions were made in determining fixity conditions and loads for design of the piling and superstructure. A detailed drawing of the type of integral abutment used in Iowa was included in the questionnaire.

It was hoped that some of the states using integral abutments had performed an analysis regarding anticipated movements and pile stresses. The questions regarding fixity and design loads were included to determine what level of analysis was felt to be appropriate.

Much of the progress in the use of integral abutments has come about by successive extension of limitations based on acceptable performance of prototype installations. In order to learn more from the several states who have pioneered the use of integral abutments, questions were asked regarding costs and performance.

2.3. Trends in Responses

Of the 52 responses received, 29 indicated that their states use integral-type abutments. A few of these, such as New Mexico and Virginia, are just beginning to use them: their first integral abutment bridge was either recently designed or currently under construction.

Of the 23 who did not use these abutments, there were four groups having similar responses.

- Fourteen states have no plans to consider using this type of abutment.
- Five states responded that they have not previously considered the possibility of fixing the girder ends to the abutments.

- Three states have built some integral abutments or semi-integral abutments but currently do not use them in new bridge construction.
- One state indicated that they were presently investigating the possibility of using integral abutments.

The following are some of the reasons given for avoiding the use of integral abutments:

- The possibility of a gap forming between the backwall and the roadway fill (two states);
- Increased substructure loads (one state);
- The possible attenuation of a bump at the ends of the bridge (one state);
- The lack of a rational method for predicting behavior (one state);
- The possible additional stress on approach pavement joints (two states); and
- Cracking of the backwall due to superstructure end span rotation and contraction (two states).

One of the purposes of this study is to present methods of analysis and design details that will reduce the potential ill effects of these concerns. Many of the states currently using integral abutments have effectively solved most of these problems.

The following is a discussion, keyed to the survey question numbers, of the responses received from states using integral abutments. A summary of the responses is contained in Appendix 9.1.

1. Most of the states using integral abutments do so because of cost savings. Typical designs use less piling, have simpler construction details, and eliminate expensive expansion joints. Some states indicated that their primary concern was to eliminate problems with the expansion joint. A few said that simplicity of construction and lower maintenance costs were their motivation.
- 2 and 3. Table 1 shows bridge length limitations currently being used. In summary, 70 percent or more of those states using integral abutments feel comfortable within the following range of limitations: steel, 200-300 feet; concrete, 300-400 feet; and prestressed concrete, 300-450 feet. There are three states using longer limitations for each structure type. They typically have been building integral abutments longer than most states and have had good success with them. The move toward longer bridges is an attempt to achieve the good performance observed on shorter bridges for structures at the maximum practical length limit. This achieves the maximum benefit from what many regard as a very low maintenance, dependable abutment design.

The difference in concrete and steel length limitations reflects the greater propensity of steel to react to temperature changes. Although the coefficients of expansion are nearly equal for both materials, the relatively large mass of most concrete structures makes them less reactive to ambient temperature changes. This is reflected in the design

Table 1. Integral abutment bridge length limitations (1981).

Maximum Length	Number of States		
	Steel	Concrete	Prestressed
800		1	1
500		1	2
450		1	3
400	2	3	4
350	1	3	1
300	8	8	8
250	2	1	
200	5	1	2
150	1		
100		1	

temperature variation specified by the American Association of State Highway and Transportation Officials (AASHTO), which is much lower for concrete.

4. Only a few states responded to the question regarding limitations on piling. Five states use only steel piling with integral abutments. Three others allow concrete and steel but not timber. No length limitations for timber piling were given by states other than Iowa. Timber piling is allowed in Iowa for bridges less than 200 feet in length. If the length is greater than 150 feet, the top of the pile which is embedded in the abutment is wrapped with 1/2 inch to 1 inch thick carpet padding material. This allows some rotation of the abutment, reducing the bending stress on the pile. Only four of the 29 agencies indicated that the webs of steel piles were placed perpendicular to the length of the bridge. In subsequent phone calls to a few other states, it was learned that others also follow this practice. At least one state began using integral abutments with steel piling placed in the usual orientation (with the pile web along the length of the bridge). This led to distress and cracking at the beam-abutment interface, and the state eventually began to rotate the piles by 90 degrees for greater flexibility.
- 5 and 6. Twenty-two states indicated that the superstructure was assumed pinned at the abutments. Five assumed partial fixity, and one assumed total fixity. Seventeen responses noted that at the pile top a pinned assumption was made; four reported a

partial fixity assumption; and five states believe the pile top is totally fixed. Six of the states which assume a pinned condition actually use a detail designed to eliminate moment constraint at the joint. In the absence of a detail which allows rotation, the appropriate assumption depends largely on the relative stiffness of the pile group and the end span superstructure. For example, if a single row of steel pilings with their webs perpendicular to the length of the bridge was used with a very stiff superstructure, the joint would probably behave as if it were pinned in response to dead and live loads and as if it were fixed in response to temperature movements. If the stiffness of the pile group were increased, some degree of partial fixity would result depending on the ratio of stiffnesses.

7. Only a few states consider thermal, shrinkage, and soil pressure forces when calculating pile loads. Several states noted on the questionnaire that only vertical loads are used in design. Of those that do consider pile bending stresses, eight use thermal forces, three use shrinkage forces, and ten consider soil pressure.
8. Most states indicated that bending stresses in abutment pilings were neglected. There were three states, however, that assumed a location for a point of zero moment and used combined bending and axial stresses. Also, prebored holes were used by three states to limit bending stresses by reducing the soil pressure.
9. Most states indicated that a free-draining backfill material is used behind the abutment. Some responses, however, indicated

that problems were encountered such as undermining associated with granular soils. One state said, "Have recently experienced problems with noncohesive material behind this type of abutment. Backfill material should be cohesive and free from cobbles and boulders." Six other states use common roadway fill behind the abutment.

10. All except four states rest the approach pavement on the integral abutment. One state indicated that a positive tie connection was used to connect the slab. No comments regarding the practice of resting the slab on a pavement notch were noted. A few states indicated that they had experienced problems when reinforced approach slabs were not used.
- 11 and 12. All except three states reported lower construction and maintenance costs using integral abutments. One said costs were the same, and two did not respond to the question. The following are some isolated comments that were made about construction and maintenance problems using integral abutments:
 - a. Longer wingwalls may be necessary with cast-in-place, post-tensioned bridges for backwall containment;
 - b. The proper compaction of backfill material is critical;
 - c. Careful consideration of drainage at the end of the bridge is necessary;
 - d. Wingwall concrete should be placed after stressing of cast-in-place, post-tensioned bridges;

- e. The effects of elastic shortening after post-tensioning should be carefully considered, especially on single span bridges;
- f. Proper placement of piles is more critical than for conventional abutments;
- g. Wingwalls may need to be designed for heavier loads to prevent cracking;
- h. Adequate pressure relief joints should be provided in the approach pavement to avoid interference with the functioning of the abutment;
- i. Possible negative friction forces on the piles should be accounted for in the design; and
- j. Wide bridges on high skews require special consideration including strengthening of diaphragms and wingwall-to-abutment connections.

2.4. Review of Design and Details in Selected States

Correspondence and telephone visits were conducted with six states to discuss in greater depth the items covered on the questionnaire and to become more familiar with their design rationale for integral abutments. They were Tennessee, Kansas, Missouri, North Dakota, California, and Iowa. Some of the items covered in the visits are discussed below.

2.4.1. Tennessee

Tennessee has extensive experience with integral abutment construction and performance. It is estimated that over 300 steel and 700

concrete bridges have been built with integral abutments. Mr. Ed Wasserman, Engineer of Structures, Tennessee Department of Transportation, indicated that the state was very pleased with the performance of these structures and has noted no undue stress on the abutments [10].

The maximum length limits using integral abutments were arrived at by setting a limit of expansion or contraction of 1 inch. This figure was developed empirically over a period of several years. By using a simplified column analysis with an unsupported length of 10 feet the state calculated the piling stresses to be just slightly over yield when deflected only 1 inch. Tennessee uses the average AASHTO temperature change of 35 °F for concrete structures and 60 °F for steel. The maximum bridge lengths (2L) for this allowable deflection (Δ) are about 800 feet for concrete and 400 feet for steel.

$$L_{\text{concrete}} = \frac{\Delta}{\alpha_c (\delta T)_c} = \frac{1/12}{(0.0000060)(35)} = 396 \text{ feet} \quad (1)$$

$$L_{\text{steel}} = \frac{\Delta}{\alpha_s (\delta T)_s} = \frac{1/12}{(0.0000065)(60)} = 214 \text{ feet}$$

where:

α_c = Coefficient of thermal expansion for concrete (AASHTO)

$(\delta T)_c$ = Allowable temperature drop or rise for concrete (AASHTO)

α_s = Coefficient of thermal expansion for steel (AASHTO)

$(\delta T)_s$ = Allowable temperature drop or rise for steel (AASHTO)

Tennessee has not completed any research work to verify the assumptions used to develop design criteria other than observing the good

performance of constructed bridges. Abutment details used by Tennessee are very similar to Iowa's. Timber piles are not used.

2.4.2. Kansas

Kansas has not participated in formal research activities to formulate design criteria for integral abutments. The length limitations and details used have been developed empirically through many years of experience. The following length limitations have been established: steel, 300 feet; concrete, 350 feet; and prestressed, 300 feet. Mr. Earl Wilkinson, Bridge Engineer, Kansas State Highway Commission, indicated that a few cast-in-place bridges up to 450 feet long had been built in the past with integral abutments, but this is not the general rule [11].

Point-bearing steel piles with 9000 psi allowable bearing are used most often. Some concrete filled steel shell piling or prestressed concrete piles are occasionally specified.

2.4.3. Missouri

Missouri had planned to instrument the piling of an integral abutment several years ago but was unable to do so because of construction timing. No other investigations of integral abutments have since been planned.

Criteria for use of integral abutments have been developed primarily from following the success of other states, notably Tennessee. The maximum length limit for steel bridges has recently been increased from 300 to 400 feet. Over 100 concrete bridges (mostly prestressed) and over 40 steel bridges have been built with integral abutments over a period of 12-15 years [12].

2.4.4. North Dakota

North Dakota has built over 300 bridges with integral abutments [13]. Most of these have concrete superstructures. They have had good performance except in two areas. First, the superstructure was originally connected to the backwall with dowell bars which were placed with insufficient cover. In some places the concrete over the dowell bars on the inside face of the backwall cracked because of thermal forces caused by contraction of the superstructure. Second, the piles were originally placed with the webs parallel to the long axis of the bridge. Using this orientation caused some distress in the backwall since the piles offered relatively large resistance to lateral bridge movements. The problem was eliminated when the piles were installed with the webs perpendicular to the long axis of the bridge.

North Dakota was an early user of integral abutments. Their design criteria are based mainly on their own experience. No formal analysis methods are employed to calculate stresses in the piles. Steel and concrete bridges are currently limited to 300 feet while prestressed bridges are built up to 450 feet in length.

Last year the state built a 450-foot prestressed concrete box beam bridge on a 0 degree skew near Fargo, North Dakota. The piles in the integral abutments were instrumented with strain gauges and had inclinometer tubes attached. Dr. Jim Jorganson, Civil Engineering Department, North Dakota State University, was commissioned to monitor the movements and strains in the bridge for one year. He had a preliminary report prepared in late summer 1981. It appears that the maximum total movement

at each end is about 2 inches [14]. This is equivalent to a temperature variation of about 117 °F.

The installation contains a unique feature which was designed by Moore Engineering, West Fargo, North Dakota. A special expansion joint material several inches thick is placed behind the abutment backwall. Behind it is a sheet of corrugated metal. The mechanism is designed to reduce passive earth pressures on the abutment and to help reduce the formation of a void space upon contraction of the superstructure. The system is shown in Fig. 4 and discussed further in Section 3.

2.4.5. California

California has engaged in several projects investigating the performance of laterally loaded piles in bridge embankments [15]. This work has been done at California State University at Sacramento and by the California Department of Transportation, Bridge Department, and will be described more fully in the literature review (see Section 3). The research was able to suggest a correlation between the coefficient of subgrade reaction used in an elastic design method to the standard penetration blow count. Maximum bending moments in steel H-piles were predicted within 15 percent of measured values.

California does not analyze pile stresses due to bending at each bridge site. Guidelines have been developed to aid designers in determining the type of abutment to use. They are currently using integral abutments with concrete bridges up to 320 feet long. Because of the effects of elastic shortening on application of post-tensioning forces, the length limitation for prestressed bridges is about 100 feet less.

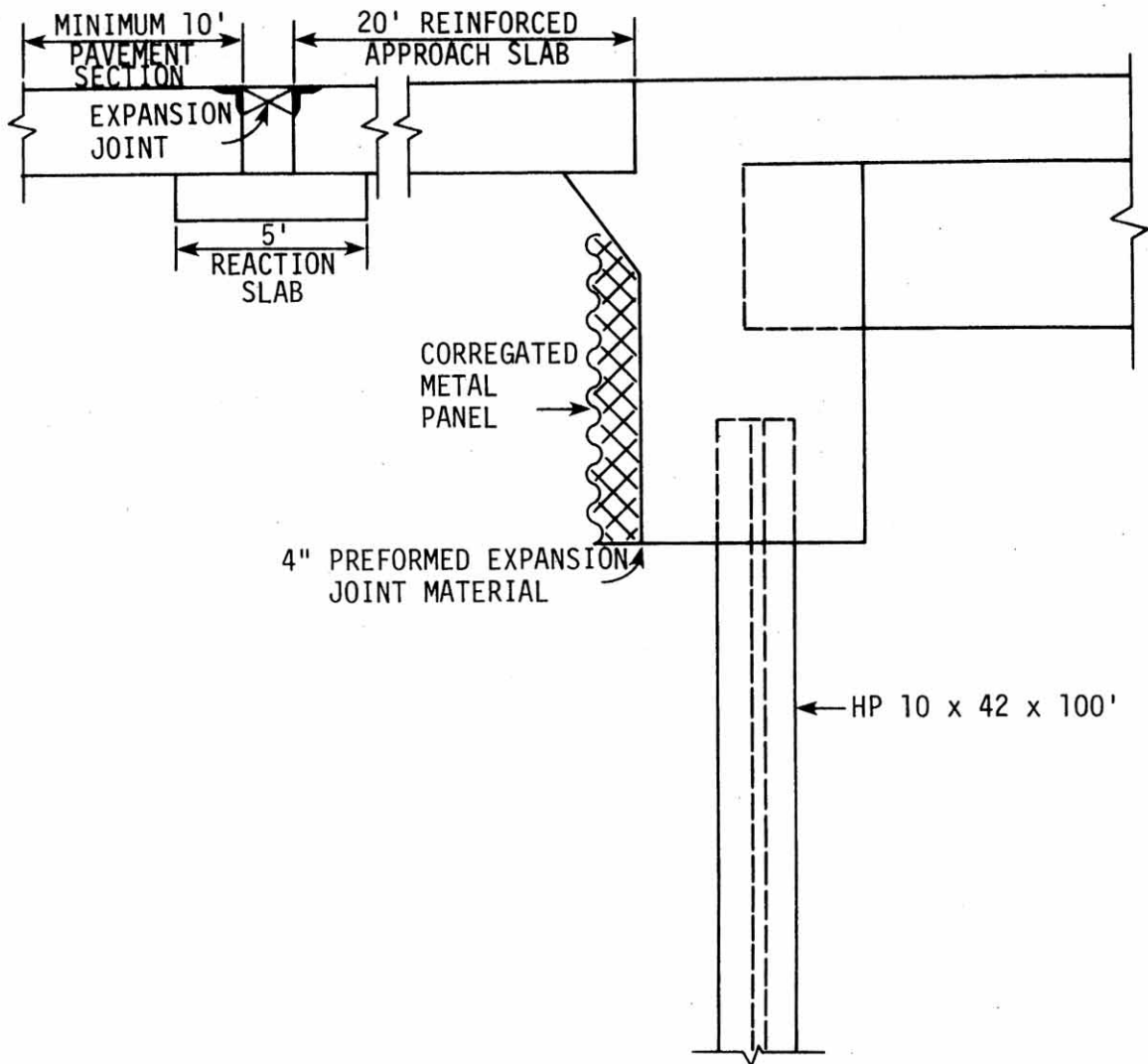


Figure 4. Sketch of Moore engineering integral abutment system.

Design of the endwall is based on specified horizontal loads depending on the type of piling used (see Appendix 9.2).

2.4.6. Iowa

Iowa began building integral abutments on concrete bridges in 1965. One of the first was on Stange Road over Squaw Creek in Ames [16]. This prestressed beam bridge is about 230 feet long with no skew. A visit to this bridge in August 1981 to determine if any apparent distress was evident showed that both approaches were generally in good shape with no major cracking noted. The abutment walls, wingwalls, and beams showed no thermal movement related cracking or distress.

Mr. Henry Gee, Structural Engineer, Office of Bridge Design, Iowa Department of Transportation, inspected at least 20 integral abutment bridges yearly for about 5 years after construction. They varied in length from 138 to 245 feet with skews from 0 to 23 degrees. The inspections were terminated since no distress or problems were found which related to the lack of expansion joints in the superstructure.

Iowa's length limitation for integral abutments in concrete bridges is 265 feet. This is based on an allowable bending stress of 55 percent of yield plus a 30 percent overstress since the loading is due to temperature effects. The moment in the pile was found by a rigid frame analysis which considered the relative stiffness of the superstructure and the piling. The piles were assumed to have an effective length of 10.5 feet, and the soil resistance was not considered. The analysis showed that the allowable pile deflection was about 3/8 inch.

2.5. Summary

There is wide variation in design assumptions and limitations among the various states in their approach to the use of integral abutments. This is largely due to the empirical basis for development of current design criteria. Some states, such as Tennessee and Iowa, have used traditional statics analysis methods for a beam or beam-column to estimate piling stresses. It is recognized, however, that assumptions concerning end fixity and soil reaction may substantially affect the results. A simple rational method of accurately predicting pile stresses would be a valuable addition to the current state of the art in integral abutment design.

The states that use integral abutments are generally satisfied with performance and believe they are economical. Some problems have been reported, however, concerning secondary effects of inevitable lateral displacements at the abutment. These include abutment, wingwall, pavement, distress, and backfill erosion. Only a few states noted that any difficulty had been encountered (see Part 4 of Appendix 9.1). Other states reported that solutions have been developed for most of the ill effects of abutment movements. They include: (1) additional reinforcing and concrete cover in the abutment, (2) more effective pavement joints which allow thermal movements to occur, and (3) positive control of bridge deck and roadway drainage. From the comments of most states, the writers infer that the benefits from using integral abutments are sufficient to justify the additional care in detailing to make them function properly.

Very little work has been done to monitor the actual behavior of integral abutments except in checking for obvious signs of distress in visible elements of the bridge. The research work being done in North Dakota to monitor actual strains and pile displacements in an actual integral abutment installation is one of very few full-scale projects. It is reported on more fully in Section 3 of this report.

Several states have been progressively increasing length limitations for the use of integral abutments over the last 30 years. Improvements in details have also taken place which generally can eliminate the possibility of serious distress occurring with abutment movements of up to 1 inch. These progressive steps in the state of the art of bridge engineering have occurred over the past thirty years and are primarily the result of the observance of satisfactory performance in actual installations.

3. REVIEW OF THE LITERATURE

3.1. Methods of Analyses

The problem of the laterally loaded pile is complex because it involves the interaction between a semirigid structural element and the embedding soil. The problem is further complicated because of the non-homogeneity of most natural soils and the disturbance to the soils caused by installing piles.

In the past, analyses and design of laterally loaded piles were primarily empirical based on data from full-scale tests of laterally loaded piles [17]. However, in recent years, there has been extensive research and development to predict theoretically the behavior of the laterally loaded pile. Two basic approaches have evolved: the subgrade reaction approach and the elastic approach [18].

The subgrade reaction approach was originally proposed by Winkler in 1867 when he represented the soil as a series of unconnected linearly elastic springs. In this method the continuous nature of the soil medium is ignored. Such factors as nonlinearity, variation of soil stiffness with depth and layering of the soil profile can be incorporated into the method [18]. Several methods have been used to account for soil nonlinearity [19-21], including an elasto-plastic Winkler model [19]. One of the more widely used approaches has been to use a series of p-y (pressure-deflection) curves for the soil at various points along the pile and a finite difference solution of the following differential equation:

$$\frac{d^2M}{dz^2} + (P_z) \frac{d^2y}{dz^2} - p = 0 \quad (2)$$

where

y = deflection;

M = moment at depth z in pile

z = depth;

P_z = axial load on pile at depth z; and

p = soil reaction per unit length

The elastic approach in which the soil is considered as an elastic continuum has been described by several authors [22-24]. The elastic method can be modified to make allowance for soil yield and can also be used to give approximate solutions for varying soil modulus with depth and for layered systems [18].

A versatile method of analysis which permits the inclusion of all the factors mentioned above and which also makes a three-dimensional formulation possible is the finite element method. A detailed description of the finite element formulation used in this investigation is given in Section 4.

3.2. Soil Properties

Soil properties and characterization of soil-pile interaction are needed as input for the nonlinear finite element analysis of pile capacity. The soil response can be characterized by three different types of curves: lateral resistance - displacement (p-y) curves, load-slip (f-z) curves and load-settlement (q-z) curves for the tip of the

pile. Typical p-y [25], f-z [26], q-z [27] curves are shown in Figs. 5-7. Numerous methods exist for estimating these curves for different types of soils. A brief discussion on some of these methods follows.

3.2.1. Lateral Resistance - Displacement (p-y) Curves

Probably the most accurate method of developing p-y curves is to use sensitive instruments to measure pile deflection and earth pressure directly in a full-scale lateral load test. Although the necessary equipment could probably be obtained given the level of current technology, the method would be expensive and time consuming.

Another potentially accurate method is to place electric strain gauges along the length of the pile. After calculating pile stresses and bending moments from the strain readings, the soil pressure (p) and lateral displacement (y) can be found from Eqs. (3) and (4):

$$y = \iint M/EI \, dx \quad (3)$$

$$p = d^2M/dx^2 \quad (4)$$

where:

M = applied moment in the pile

This method is also quite expensive and requires extreme care in taking measurements since the deflection is extremely sensitive to variations in the bending moment [28].

It is possible to obtain approximate values for p-y variations along the pile by knowing the load, moment, deflection, and rotation

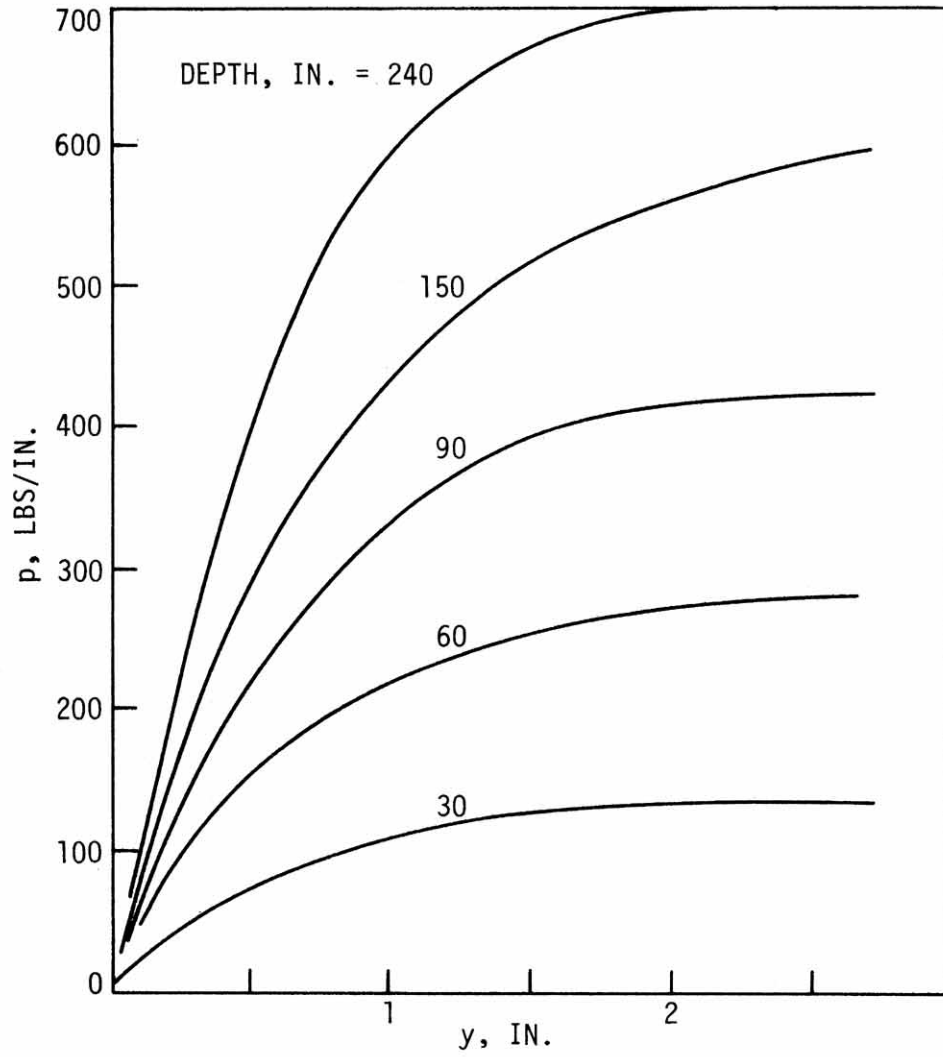


Figure 5. Lateral resistance - displacement (p-y) curves.

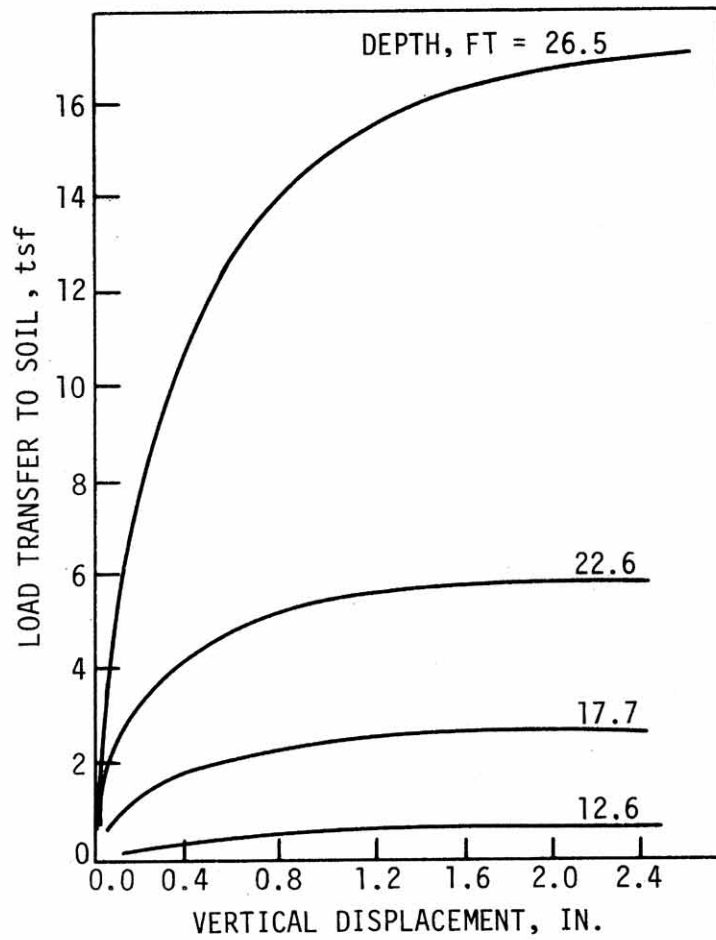


Figure 6. Load-slip (f-z) curves.

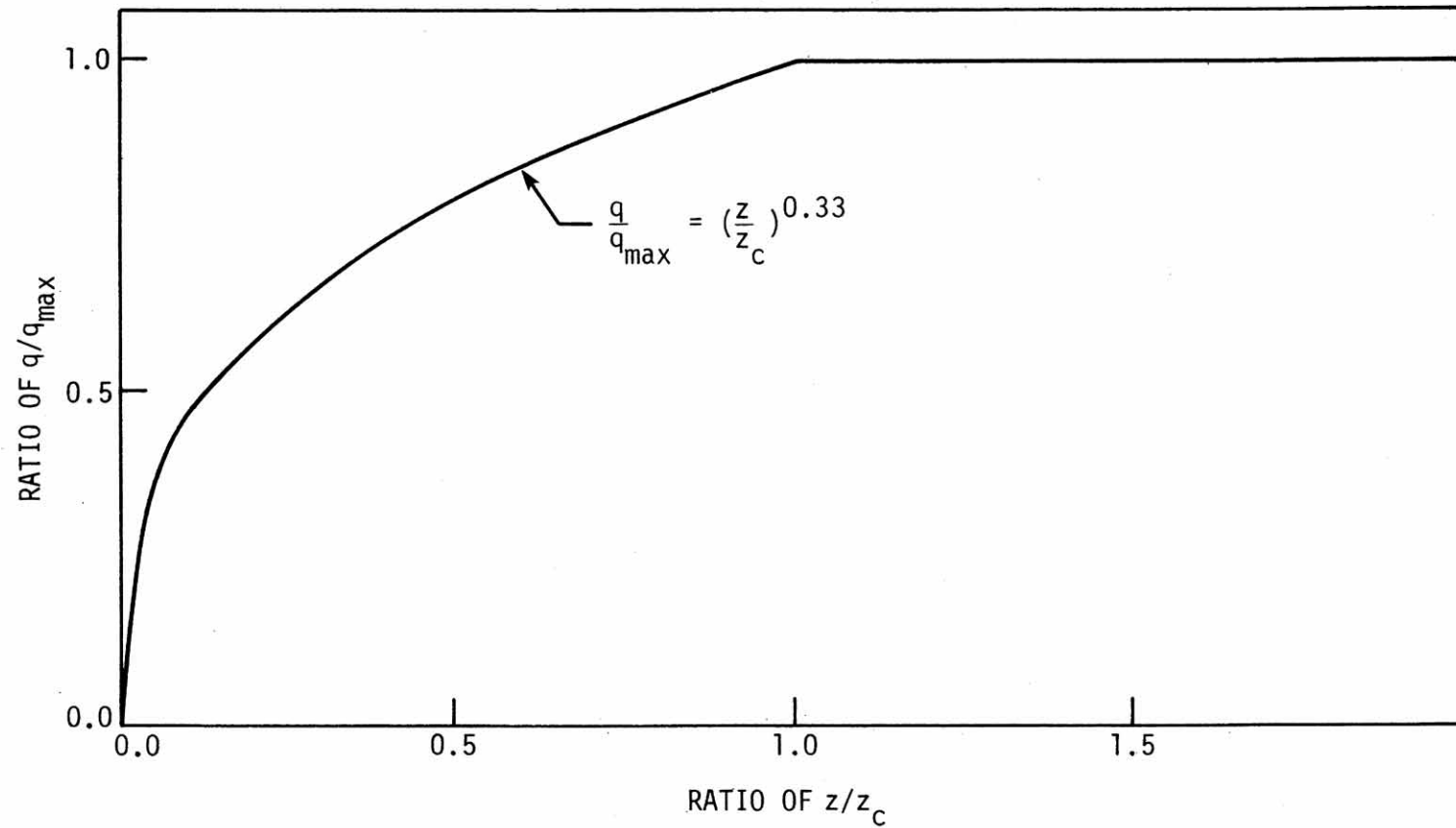


Figure 7. Normalized q-z curve (Reese curve).

at the top of a test pile. This simple test requires only that a pile be driven beyond the point below which the soil has no appreciable effect on pile-top deflections and a lateral load be applied while measurements are periodically recorded. The method is based on Reese and Matlock's nondimensional solutions [29] which assume a linear variation of soil modulus with depth. Relatively accurate information can be obtained, but the method [30] does require actual field measurements to be taken.

Several investigators [28,31,32,33,34] have attempted to correlate a lateral load-deflection response with laboratory soil tests. The form of the equation normally used in clay is shown in Eq. (5):

$$\frac{p}{p_u} = 0.5 \left(\frac{y}{y_{50}} \right)^{1/n} \quad (5)$$

where:

p = soil resistance per unit length of pile

p_u = ultimate soil resistance per unit length of pile

y = displacement corresponding to p

y_{50} = displacement at one-half ultimate soil reaction

n = a constant relating soil resistance to pile deflection

Possible functional relations and values for n are shown in Table

2. The following specific values for a soft clay have been suggested by Reese:

$$\frac{p}{p_u} = 0.5 \left(\frac{y}{y_{50}} \right)^{1/3} \quad (6)$$

Table 2. Constants used in p-y relationships for clays.

	Soft Clay	Firm Clay	Very Stiff Clay
n	3	4	2
C_1	2.5	2.5	2.0
J	0.5	0.5	2.0

where:

$$p_u = \begin{cases} \left(3 + \frac{\gamma x}{c} + J \frac{x}{b}\right) cb & (7) \\ 9cb & \text{(use smaller value)} \end{cases} \quad (8)$$

$$y_{50} = C_1 b \varepsilon_{50} \quad (9)$$

J = a constant which controls the depth at which p_u reaches 9 cb for clays

b = pile diameter

c = average undrained shear strength of soil from ground surface to depth x

x = depth at which p_u is computed

γ = average effective unit weight of soil within the depth x

C_1 = a constant relating pile deflection to laboratory strain

ε_{50} = strain at 50 percent of the maximum principal stress difference, $(\sigma_1 - \sigma_3)_{\max}/2$

The Iowa Department of Transportation's current soil investigation procedure at bridge sites includes taking a split tube sample if compressible layers are found in the area of the approach fill. Soil strength, unit weight, and compressibility data are routinely obtained on these samples by performing triaxial, density, and consolidation tests. If three split tube samples were taken, sufficient information would be available to predict the soil response with reasonable accuracy to a depth of about 15 feet. Since soil conditions below about 15 feet have little effect on bending stresses in laterally loaded piles [35,36], sample depths of 3, 7, and 12 feet would seem to be convenient choices.

If stiff clay and very stiff clay are encountered, the equations are modified slightly. Generally, ε_{50} will be somewhat lower and the exponent is changed from 1/3 to 1/4 and 1/2, respectively.

A summary of the p-y curves used in this investigation, including p-y curves for sand, is given in Table 3. Descriptions of the parameters used in Table 3 are provided in Table 4. The p-y formulations used in this investigation are similar to those summarized by Welch and Reese [21].

3.2.2. Load-Slip (f-z) Curves

Several methods have been proposed for estimating the load-slip behavior of single piles. The criteria used in this investigation follow the formulations summarized by Ha and O'Neill [37]. An f-z curve based on load tests of single piles is shown in Fig. 8. The figure shows a curve normalized with respect to the maximum shear stress developed between pile and soil (f_{\max}) and the relative displacement (z_c) required to affect f_{\max} . The methods adopted for estimating f_{\max} are summarized below.

For piles in clay soil and sand, f_{\max} may be estimated using [37]:

$$f_{\max} = \begin{cases} \alpha C_u & \text{for clay soil} \\ 0.04N \text{ (ksf)} & \text{for sand} \end{cases} \quad (10)$$

where

α = shear strength reduction factor

C_u = undrained cohesion of the clay soil (see Fig. 9), and

N = average standard penetration blow count

For purposes of this investigation, C_u was correlated to standard penetration blow count, N , values from soil test data of Iowa soils [9]. Data from nineteen sites in four Iowa counties (Blackhawk, Benton, Buchanan, and Linn) were analyzed and a simple linear prediction model

Table 3. Analytical forms of p-y curves.

Case	Basic p-y Curves Equations	y_{50}	p_u (use lesser value)	E_{si}	E_m
Soft Clay, Static Load	$p/p_u = 0.5 (y/y_{50})^{1/3}$	$2.5 B\epsilon_{50}$	$p_u = 9 C_u B$ $p_u = (3 + \frac{\gamma}{C_u} x + \frac{0.5}{B} x) C_u B$	---	---
Stiff Clay, Static Load	$p/p_u = 0.5 (y/y_{50})^{1/4}$	$2.5 B\epsilon_{50}$	$p_u = 9 C_u B$ $p_u = (e + \frac{\gamma}{C_u} x + \frac{0.5}{B} x) C_u B$	---	---
Very Stiff Clay, Static Load	$p/p_u = 0.5 (y/y_{50})^{1/2}$	$2.0 B\epsilon_{50}$	$p_u = 9 C_u B$ $p_u = (3 + \frac{\gamma}{C_u} x + \frac{2.0}{B} x) C_u B$	---	---
Sand, Static Load	$p/p_u = \tanh(E_{si} y/p_u)$	---	$p_u = \gamma x [B(k_p - k_a) +$ $x k_p \tan \alpha (\tan \beta) +$ $x k_o \tan \beta (\tan \phi - \tan \alpha)]$ $p_u = \gamma x (k_p^3 + 2k_p^2 k_o \tan \phi - k_a) B$	$E_m/1.35$	$J\gamma x$

Table 4. Evaluation of parameters for Table 3.

Parameter	Evaluation
ϵ_{50}	From laboratory triaxial test, or use = 0.02 for soft clay = 0.01 for stiff clay = 0.005 for very stiff clay (Axial strain at 0.5 times peak stress difference)
C_u	Undrained cohesion indicated for UU laboratory test
B	pile width
γ	Effective unit soil weight
x	Depth from soil surface
ϕ	Angle of internal friction
k_p	$= \tan^2(45^\circ + \frac{\phi}{2})$
k_a	$= \tan^2(45^\circ - \frac{\phi}{2})$
k_o	$= 1 - \sin\phi$
α	$= \frac{\phi}{2}$ for dense or medium sand $= \frac{\phi}{3}$ for loose sand
β	$= 45^\circ + \frac{\phi}{2}$
J	= 200 for loose sand = 600 for medium sand = 1500 for dense sand

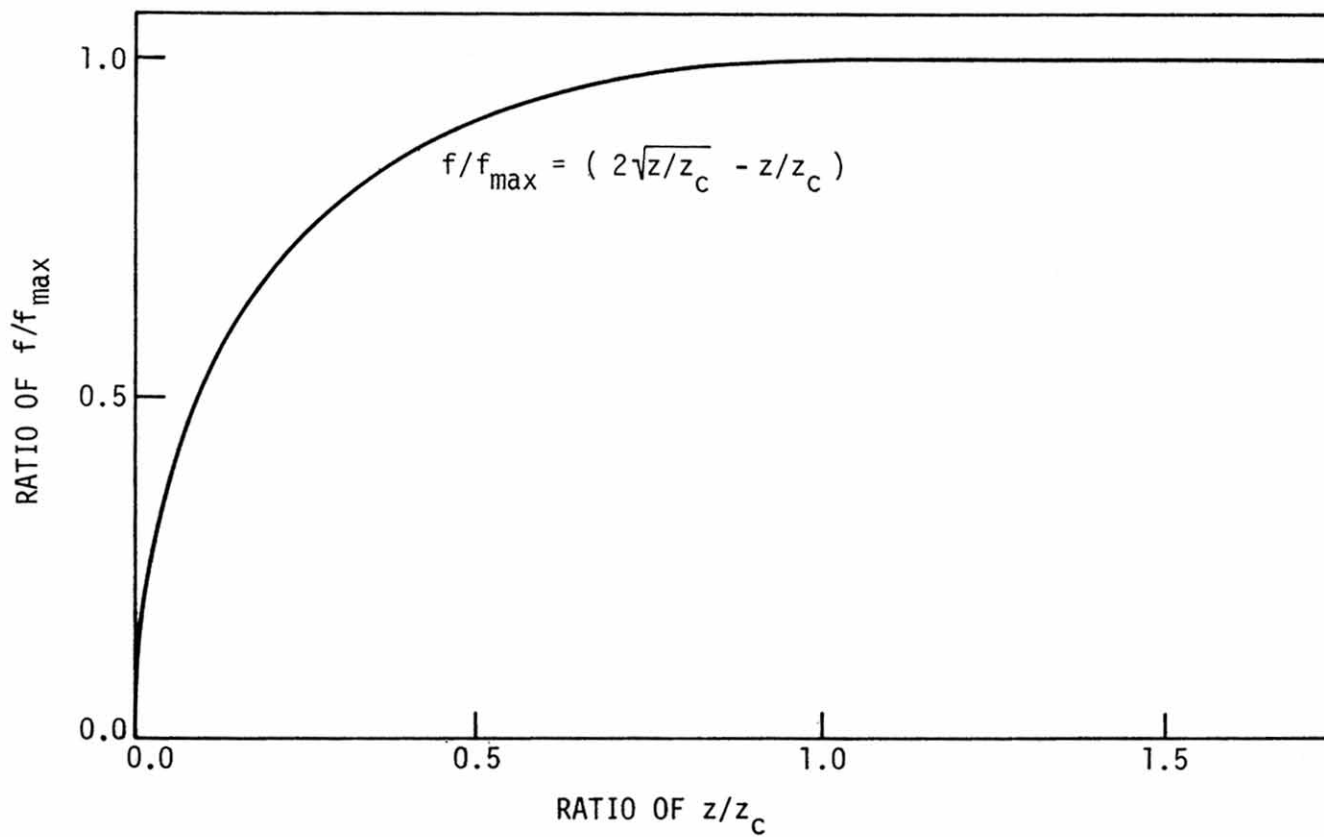


Figure 8. Normalized f-z curve (Reese curve).

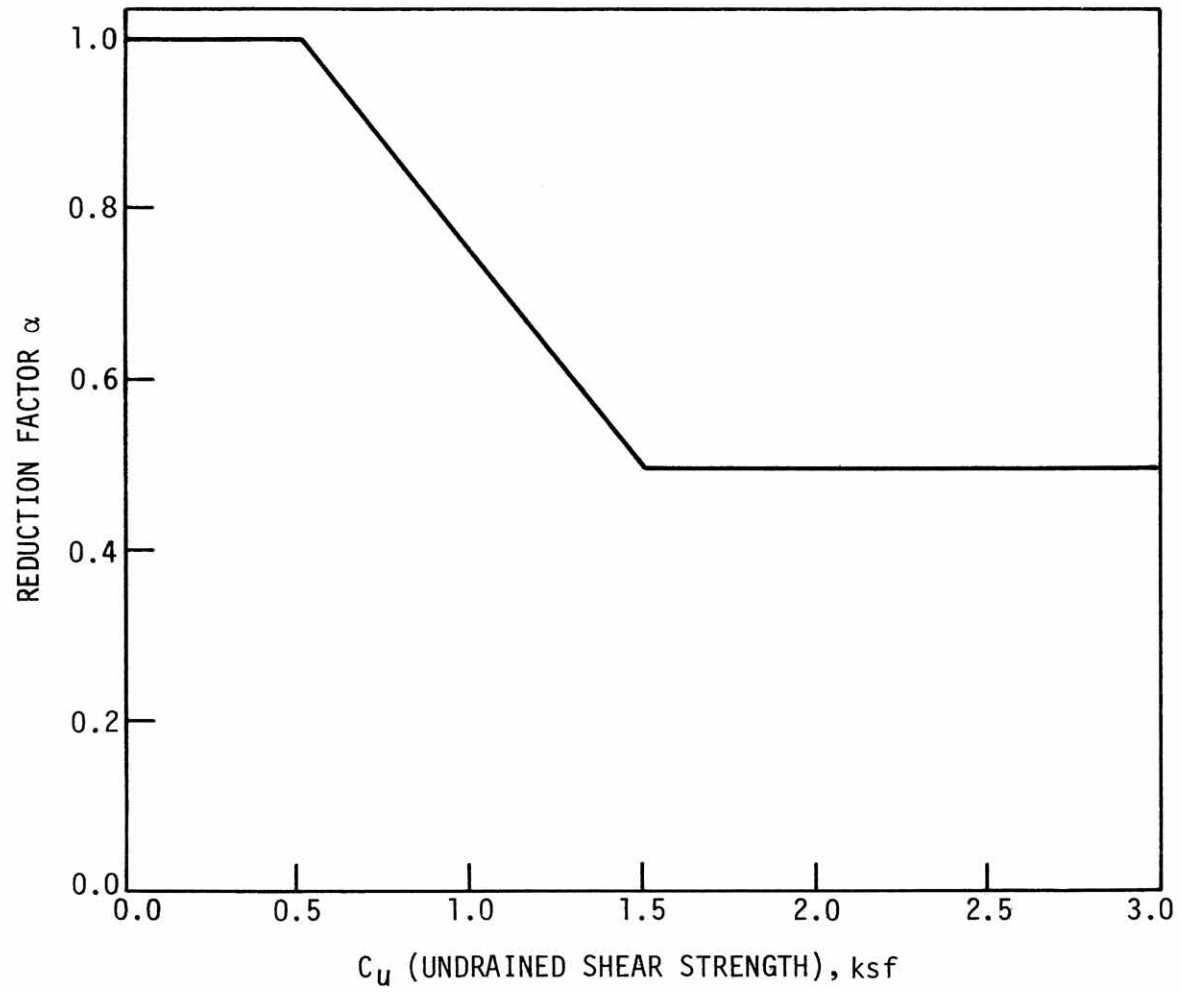


Figure 9. Reduction factor α .

was devised. The best fit equation given below had a correlation of 0.82 with the actual data,

$$C_u = 97.0N + 114.0 \text{ (lbs/ft}^2\text{)} \quad (11)$$

3.2.3. Load-Settlement (q-z) Curves

A typical q-z curve is shown normalized in Fig. 7 [38]. The curve is defined by estimating the bearing capacity of the pile tip, Q_{\max} , and the corresponding vertical deflection, Z_c .

For end bearing piles in clay ($\phi = 0$) and sand the following formulations may be used for estimating Q_{\max} [39]:

$$\begin{aligned} \text{For clay, } Q_{\max} &= 9 C_u A_B \text{ and} \\ \text{For sand, } Q_{\max} &= N_q \bar{\sigma}_v A_B \end{aligned} \quad (12)$$

where

$$\begin{aligned} C_u &= \text{undrained cohesion of soil at pile tip} \\ A_B &= \text{tip area} \\ \bar{\sigma}_v &= \text{vertical effective stress at pile tip} \\ N_q &= \text{bearing capacity factor} \end{aligned}$$

N_q depends, among other factors, on angle of internal friction, degree of compressibility and ratio of horizontal to vertical stress.

N_q may be approximated by [40]

$$N_q = (1 + \tan\phi) e^{\pi \tan\phi} \tan^2(45^\circ + \phi/2) \quad (13)$$

Limiting values of $q_{\max} = N_q \bar{\sigma}_v$ are given in Table 5 [40].

Table 5. Typical and limiting parameters for driven piles in medium dense to dense sand.

Soil Type	δ (degrees)*	Limiting f_{\max} (kips/ft ²)	Limiting q_{\max} (kips/ft ²)
Clean Sand	30	2.0	200
Silty Sand	25	1.7	100
Sandy Silty	20	1.4	60
Silt	15	1.0	40

* δ = angle of pile-soil friction.

q_{\max} may also be obtained from SPT (standard penetration test) and CPT (cone penetrometer test) tests. q_{\max} may be approximated by [41].

$$q_{\max} = 8 N_{\text{corr}} \text{ kips/ft}^2 \quad (14)$$

where

$$\begin{aligned} N_{\text{corr}} &= \text{corrected SPT blow count at depth of pile tip} \\ &= N \text{ (uncorrected) if } N \leq 15 \\ &= 15 + 0.5 (N - 15) \text{ if } N > 15 \end{aligned}$$

Z_c corresponding to q_{\max} may be related to cross-sectional properties. Z_c may be estimated to be in the range of 0.02-0.05 (0.05 in the absence of any data) times the tip diameter of the pile [37].

3.3. Research on Integral Abutment Bridges

3.3.1. California

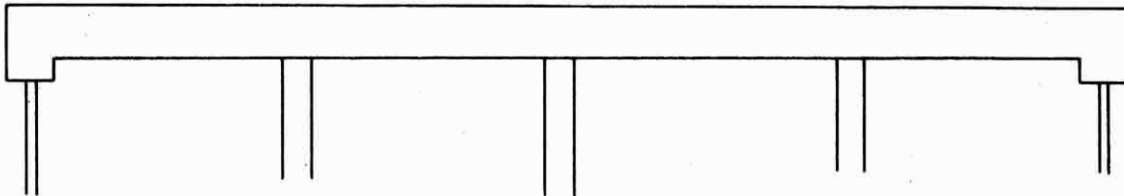
California [42] began informal studies of some of their long structures without expansion joints about 15 years ago. Their efforts consisted of identifying appropriate structures and conducting periodic inspections to monitor performance. Twenty-seven bridges were studied. They varied in length from 269 feet to 566 feet. About 18 of the bridges had integral abutments while the others had semi-integral abutments. An example of a typical inspection record [43] is shown in Fig. 10.

Although a final report on this study will not be available until 1982, the Structures Office, California Department of Transportation, has reported the following interim findings [15]:

SAMPLE
INSPECTION RECORD
OF
STRUCTURES WITHOUT EXPANSION JOINTS

Date 5-1-67

Br 53-1671 Name Fairfax On Ramp Co-Rte LA-10
 Type RCB Length 352' Skew Var. Year Built 1964



ELEVATION

APPROACH PAVEMENT

Type: AC

Condition: The Westerly approach appears to have been patched twice, it is now in good condition. Easterly approach has settled slightly, it has never been patched. A 1/16" wide transverse crack has occurred in the Easterly approach about 8' from the abutment for most of the width. The crack has been filled with latex.

STRUCTURAL DEFECTS

Space between structure and PCC curb: 1/2" Westerly, 3/8" Easterly.

Deck surface has a few transverse cracks over the bents, otherwise crack free.

No cracks found in soffit, webs, abutment walls, or columns.

There is a 1/2" crack between fill and backwall of Westerly abutment.

COMMENTS

Traffic volume appears to be light to moderate.

Figure 10. Sample inspection record of structures without expansion joints.

- There is no apparent distress at end bent columns;
- There is no cracking on girder soffits related to the lack of deck joints;
- No structural distress is apparent at the abutments;
- Some problems have occurred from erosion and piping of abutment support soils due to small amounts of water flowing down behind the abutments; and
- There are no apparent deck cracking problems associated with expansion stresses.

The interim report recommends that a reinforced concrete approach slab be used with all jointless structures.

In 1971 and 1972 the California Department of Transportation and the Federal Highway Administration sponsored a research project to correlate theoretical solutions for laterally loaded piles to full-scale field tests in bridge embankments. Most of the work was done by W. S. Yee at the University of California at Sacramento.

Yee worked with two available solutions for laterally loaded piles. The first was the nondimensional solutions with soil modulus proportional to depth developed by Reese and Matlock [29]. This method allows analysis of variable fixity conditions at the pile top and can be used in an iterative solution for other than linear variations of the soil modulus. Yee also used the finite difference solution to the general differential equation. Since the pile is separated into small elements in this solution, any discrete variation in the soil modulus can be accommodated.

In Yee's study, however, a linear variation was assumed. The coefficient of soil modulus (n_h) was determined by measuring the deflection

and rotation at the top of a laterally loaded pile as described by Davisson [44].

Load tests were performed on instrumented pilings at three actual bridge construction sites. Using strain gauge measurements, the moment in the pile was calculated and compared to calculated moments using the experimentally determined n_h value. A typical example of the results is shown in Fig. 11 [39].

Yee [39] concluded that:

- Reliable predictions of bending moments and pile stresses could be found using experimentally determined n_h values and either the nondimensional solution or the finite difference method;
- The use of a linear variation in soil modulus with depth is a good approximation;
- The influence of the soil below about 12 to 20 feet on pile stresses was practically negligible; and
- The effective length of the pile was about 15 feet for a free-head condition and about 21 feet for a fixed-head condition.

The results of this research were used to develop guidelines for the use of integral abutments in California. They are used when up to 1 1/2 inches of total movement due to thermal forces is expected in a reinforced concrete bridge. Also to avoid rotation problems at the abutment, the end span is limited to 160 feet. The use of integral abutments is limited on prestressed bridges to those where the elastic

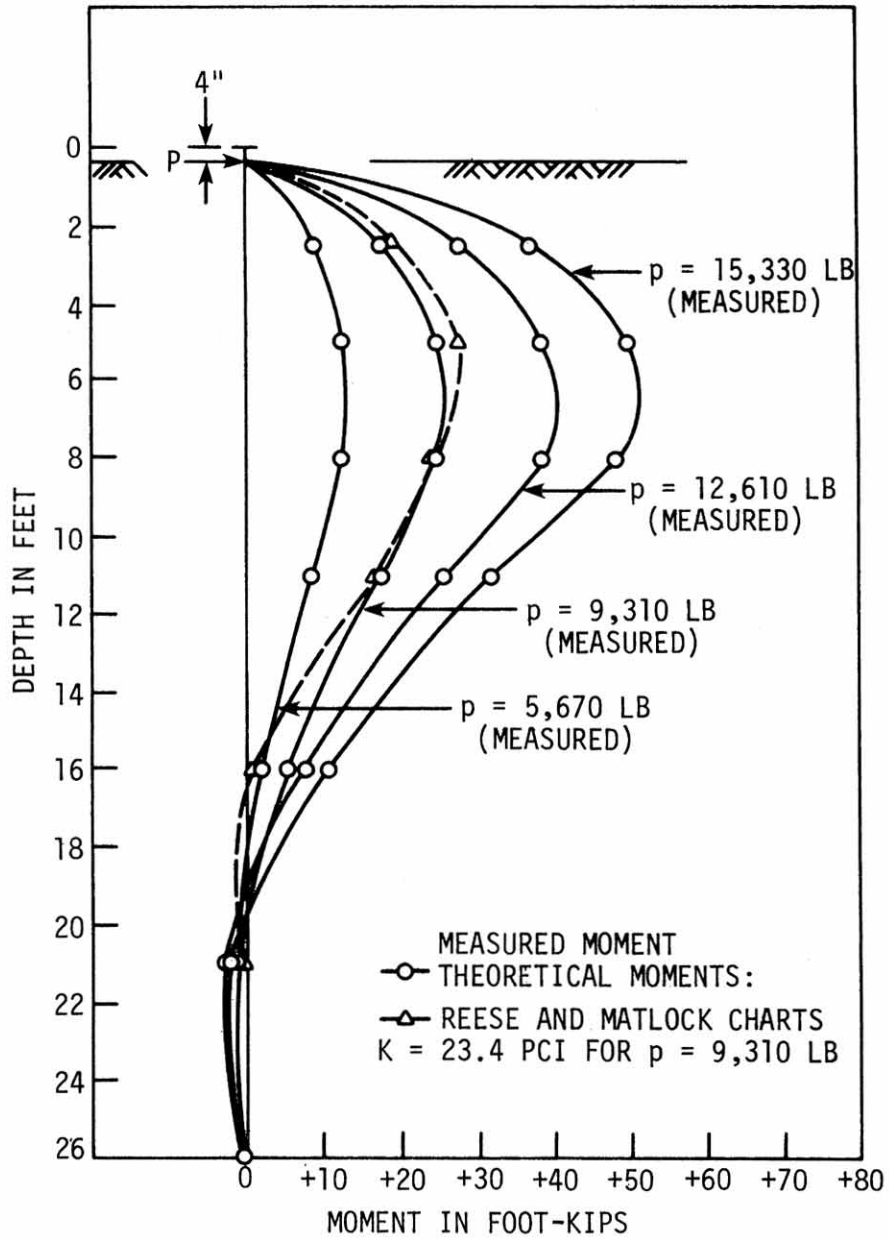


Figure 11. Calculated versus experimentally determined pile moments.

shortening due to post-tensioning is less than 3/8 inch, and the end span is less than 115 feet (see Appendix 9.2).

3.3.2. Missouri

In 1972 the University of Missouri conducted a survey and feasibility study of integral and semi-integral abutments. The work was sponsored by the Missouri State Highway Department and the Federal Highway Administration [7]. The survey was undertaken to determine current design methods and limitations used by state highway agencies and the feasibility of instrumenting a jointless bridge to obtain thermal-induced stresses.

The survey indicated that 13 states were using integral abutments with steel bridges and 24 were using them with concrete bridges. The distribution of length limitations was as shown in Table 6. Three states allowed the use of integral abutments for nonskewed bridges only; none used them with skews over 30 degrees.

The survey concluded that:

- The use of superstructures connected to flexible substructures was becoming generally acceptable;
- Design limitations were more restrictive for steel bridges than for concrete;
- There was no simple design criteria which accounted for shrinkage, creep, temperature, or substructure flexibility;
- Induced stresses resulting from thermal effects, creep, shrinkage, backfill movement, etc., are recognized by bridge engineers as potentially significant, but there is a wide variance in method for considering them; and

Table 6. Integral abutment bridge length limitations (1972).

Maximum Length (feet)	Number of States	
	Steel	Concrete
100	2	4
200	8	6
300	2	7
400		2
450		2
500		1

- Bridge design engineers are interested in induced stresses and associated problems, are generally uncertain as to the significance of and suitable methods for consideration of these stresses, and would welcome simple, rational design criteria and specific recommendations as to design details.

In the feasibility study a temperature distribution model was developed and superstructure stresses were calculated for a wide range of temperature variations. The nondimensional solutions for laterally loaded piles developed by Reese and Matlock [29] were used with an assumed value of the modulus of soil reaction. Instrumentation procedures were recommended for a field test to verify the theoretical results. The field test, however, was not carried out and no further work has been done on the project.

3.3.3. South Dakota

In 1973 South Dakota State University conducted full-scale model tests on integral abutments to determine induced stresses in the superstructure and the upper portion on the piling [1]. The model consisted of two HP 10 × 42 steel piles on 8-foot 6-inch centers cast into a rigid concrete abutment with two plate girders about 26 feet long. The 32-foot piles were driven into silty clay over glacial till to a bearing capacity of 23 tons. The pile tops were welded to the bottom flanges of the girders.

Various lateral displacements within plus or minus 1 inch were induced at the abutment by jacking at the free end during four construction stages. The results of interest are with the slab and backfill in place. Strains were measured corresponding to stresses of up to 42 kips

per square inch in the piling. This occurred just below the bottom of the concrete abutment. Several conclusions--called qualitative results which would require further study to verify--were drawn by the investigators:

- Stresses were induced into the girders which in some cases were additive with dead and live load stresses. The induced stresses were generally within the 40 percent overstress allowed by AASHTO.
- Horizontal movements over about 1/2 inch will cause yielding in the piles.
- Free draining backfill is recommended since frozen soil against the abutment can greatly increase induced girder stresses by limiting free movement.
- The use of approach slabs which allow rotation and translation of the abutment and, if possible, avoid continuing compaction of the backfill by traffic is recommended.

As part of this study a questionnaire was sent to ten states in the north central part of the United States. Two trends can be identified when the survey is compared to the responses of these states to the survey recently conducted by Iowa. Four of the states (Idaho, Missouri, North Dakota, and South Dakota) have substantially increased their length limitations for use with integral abutments. Four of the states (Iowa, Kansas, Nebraska, and Wisconsin) have retained the same limits, and two states still do not routinely use integral abutments. Also of interest is the fact that three of the states have been routinely using integral

abutments with steel bridges since 1973; four of them already did and one still does not.

3.3.4. North Dakota

A recently constructed county road bridge near Fargo, North Dakota, was instrumented and monitored for temperature-induced stresses by North Dakota State University [14]. The study is being conducted by J. Jorgenson, Chairman of the Civil Engineering Department, and is sponsored by the State Highway Department.

The bridge is a 450-foot by 30-foot prestressed concrete box girder with six 75-foot spans and no skew angle. It was designed by Moore Engineering, West Fargo, North Dakota and built in August 1979 on a very low volume gravel road. Since the bridge length was at the limit for the use of integral abutments in North Dakota, a unique system was used to limit the passive earth pressure on the backwall. A diagrammatic representative of the abutment is shown in Fig. 4 [14].

The purpose of the expansion joint material behind the abutment is to hold back the soil during thermal contraction of the superstructure and to provide a collapsible mass to work against during expansion. Jorgenson informed the writer that the maximum lateral movement measured at the pile top has been about 2 inches. No distress has been noted which could reasonably be attributed to this movement. Jorgenson also reported that the bridge approach to superstructure transition was still very smooth.

The pilings are founded in a deep glacial clay layer. Soft clay deposits exist near the surface and down to the limit of influence on the temperature stresses in the pile. Actual stresses in the piles

are being determined from strain gauge readings for various temperature ranges throughout the year. The results of this analysis were to be available in the late summer of 1981. Based on the results of the South Dakota study, it seems likely that the piles are being stressed above yield with the reported off-center deflections of up to 1 inch occurring.

MATHEMATICAL MODEL

4.1. Mathematical Model Description

The purpose of this section is to describe a state-of-art mathematical model that can be used to help evaluate the safety of piles in bridges with integral abutments. As illustrated schematically in Fig. 12, if an integral abutment bridge is subjected to a change in temperature, thermal expansion and/or thermal stresses will occur. Since the piles are usually the most flexible elements, they will be displaced laterally and their vertical load carrying capacity could be affected.

The mathematical model developed in this investigation was limited to defining the behavior of the piles as part of the bridge system. Thus, a significant portion of the work focused on an accurate description of the laterally and vertically loaded piles. A combination of a one-dimensional idealization for the piles (beam-column) and an equivalent spring idealization for the soil, which included (a) vertical spring, (b) lateral spring, and (c) point spring for the foundation, are shown in Fig. 13. Important parameters for this analysis were the pile and soil characteristics. Pile characteristics can be represented by the beam-column element with geometric and material nonlinearity. Soil characteristics can be divided into two parts, described below.

- Axial Behavior. A unique relationship is assumed to exist between unit skin friction (f), i.e., shear stress, and the relative deflection between the pile and the soil at each depth

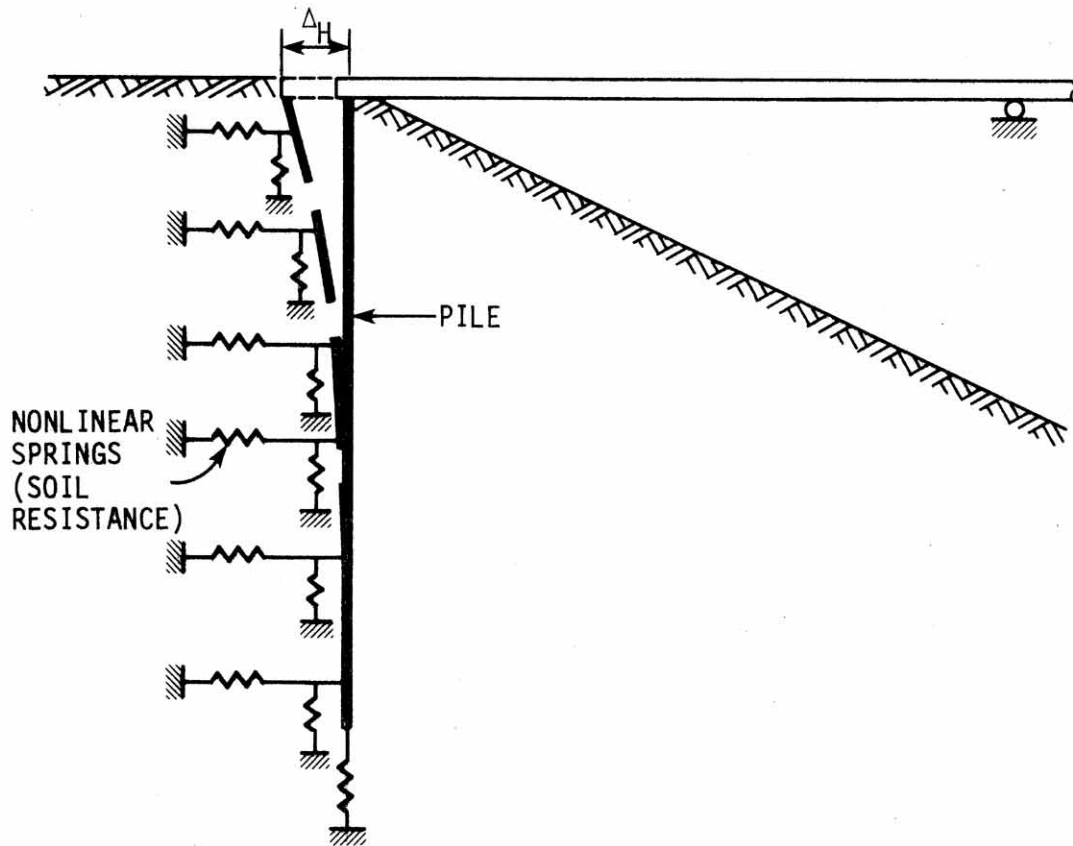


Figure 12. A mathematical model of integral abutment bridge with pile/soil interaction.

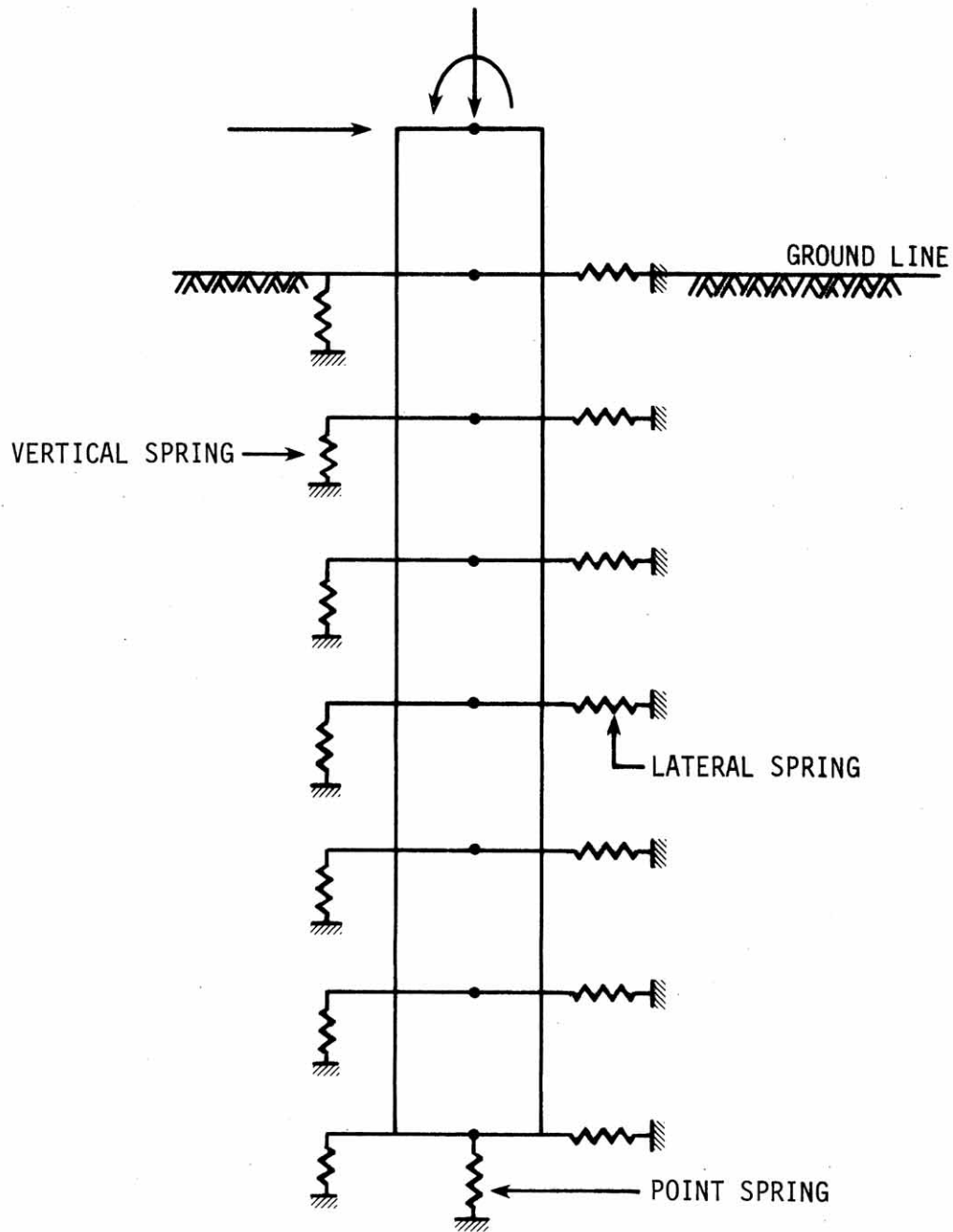


Figure 13. Pile finite element model.

(z). This relationship, denoted by the f - z curve, can vary from depth to depth, if necessary, in order to model, for example, nonuniform or layered soils or installation procedures that may produce gradation effects. Also, a unique relationship, the q - z curve, is assumed to exist between stress load at the pile tip (q) and tip deflection relative to the soil (z). Several criteria exist with respect to the synthesis of f - z and q - z curves (see Section 3.2).

- Lateral Behavior. Lateral soil pressure (transverse to the pile axis) will exist against a pile if the pile is battered or has lateral loading in the form of shear or moments applied to the top of the pile. The lateral soil reactions are represented by lateral nonlinear springs (p - y functions) which relate lateral soil reaction in force per unit length of the pile (p) to lateral pile displacement (y). The p - y curves can vary from depth to depth, especially for layered soils (see Section 3.2).

The set of curves, f - z , q - z , and p - y , seem to imply that the behavior of the soil at a particular depth is independent of the soil behavior at all other depths. That assumption, of course, is not strictly true. However, it has been found by experiments [45] that, for the patterns of pile deflections which can occur in practice, the soil reaction at a point is dependent essentially on the pile deflection at that point and independent of the pile deflections above or below. Thus, for purposes of analysis, the soil can be replaced by a set of

discrete nonlinear soil springs with load-deflection characteristics of the character of the f - z , q - z and p - y curves.

4.2. Finite Element Idealization

The initial development of the finite element method for aerospace and structural engineering was soon followed by application of the method to problems in soil and rock mechanics. The nature of soils and rocks, however, is highly complex and required different considerations from the material used in structures. A realistic appraisal of the complexities imposed by such natural causes as joints and other discontinuities would often require that soils and rocks be treated as discontinua. Nevertheless, approximate but acceptable solutions can be obtained by considering them as continuous mass [46]. In most applications of the finite element method, the continuum approach is used; hence we shall restrict our attention to this idealization. Furthermore, we shall consider only those aspects of soil and rock mechanics directly related to the applications of the finite element method. Several books [47-49] dealing exclusively with the fundamentals of the finite element method and its application to a wide class of problems have been published. Consequently, the basic concepts of the method will only be reviewed very briefly and the formulations that are of direct relevance to the present study will be presented.

4.2.1. Basic Concept of the Finite Element Method

The finite element method is based upon the general principle known as going from a part to the whole. In engineering many problems cannot

be solved in closed form, that is, as a "whole." Therefore, we consider the physical medium as an assemblage of many small parts. Analysis of the basic part forms the first step toward a solution. The structure is idealized as an assemblage of separate elements interconnected at nodes. The type of element, the number of elements and the arrangement of the elements can be selected properly on the basis of the accuracy needed and the available computer facilities.

Regardless of the shape or the type of the finite element the analysis is carried out using the same basic principles. In the displacement approach, the displacements within an element are approximated by a function of the nodal displacements following a simple pattern, usually polynomials. This assumed displacement function can then be used to derive the stiffness matrices for the elements using the principle of virtual work. The element stiffnesses are appropriately added to form the total stiffness matrix for the structure. The resulting simultaneous algebraic equations which relate nodal forces to nodal displacements are then solved. From the known nodal displacements, using the assumed displacement functions, the displacements, strains and stresses at any point within the element can be calculated.

4.2.2. Causes of Geometric and Material Nonlinearities

All phenomena in solid mechanics are nonlinear. In many applications, however, it is practical and convenient to use linear formulations for problems to obtain engineering solutions. On the other hand, some problems definitely require nonlinear analysis if realistic results are to be obtained. Some examples of situations in the latter category include the postyielding and large deflection behavior of structures,

the postbuckling deformations of beams, plates, and shells and nearly all problems in soil and rock mechanics. The type of nonlinearity can be classified as geometric nonlinearity and/or material nonlinearity depending on the distinct phenomena.

Geometric nonlinearity is ascribed to large-deflection problems in which the deformed configuration must be used to write equilibrium equations and to problems related to structural stability. In this case, the pile is in compression and geometric nonlinearities are important. Material nonlinearity is due to nonlinear stress-strain relationships of the materials that make up the structure. For the present problem, the soil and, possibly, the steel may exhibit nonlinear material behavior. It is possible in an analysis to include nonlinearity due to either or both material or geometric causes. Both nonlinearities will be included in this soil-structure interaction problem.

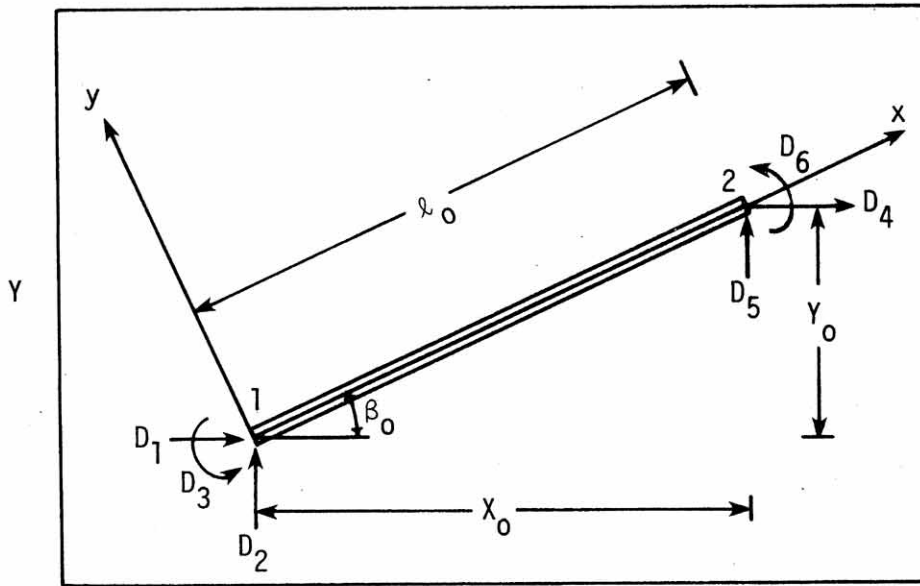
4.2.3. Pile (Beam-Column) Model

A large-displacement, geometrical, nonlinearity problem can be analyzed in Lagrangian coordinates or in Eulerian coordinates.

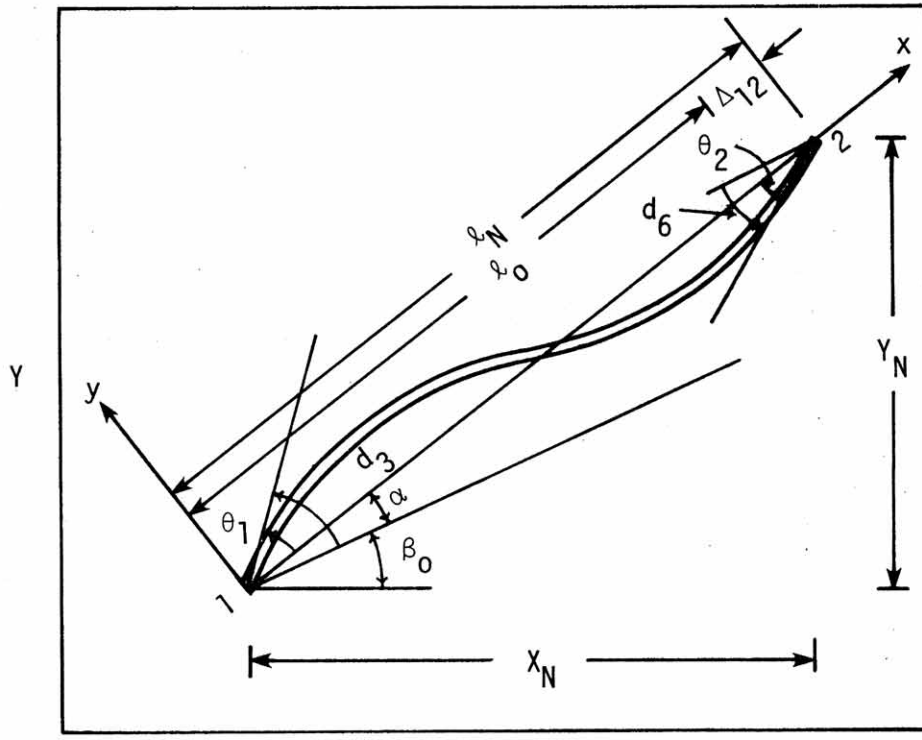
The Lagrangian approach is called "stationary Lagrangian" and total Lagrangian. In this approach the original reference frame remains stationary and everything is referred to it regardless of how large the strains and rotations become. Displacements, differentiations and integrations are all with respect to the original frame. As displacements become larger and larger, more and more terms must be added to the strain-displacement relations in order to account for nonlinearities [50].

The Eulerian approach involves convected coordinates: a reference frame that deforms with the structures so that the (convected) coordinates of a point never change [49]. As actually implemented, the Eulerian approach takes a form that is usually called the "updated Lagrangian" approach. It can be described as follows. A local coordinate system, called a corotational system, is attached to each element. The local system moves with the element and therefore shares its rigid-body motion. Differentiations and integrations are performed with respect to local coordinates. The current deformed state is used as the reference state prior to the next incremental step of the solution. The local coordinates are updated to produce a new reference state as the solution proceeds. Local coordinates of material points do change, so the method is not strictly Eulerian. Essential nonlinearities are accounted for by tracking the orientations of the several local systems. The equations are developed in terms of displacement increments.

The updated Lagrangian (corotational) coordinate system for the beam-column element is defined so that the x axis is and remains coincident with a line joining the endpoints of the element, as shown in Fig. 14. The origin is taken to coincide with node 1 of the element, and the y axis is perpendicular to the x axis. Thus, in the local x,y system, only three nodal displacements are considered: that is, Δ_{12} , θ_1 , θ_2 . All degrees of freedom (d.o.f.) in the global directions, D_1 to D_6 (see Fig. 14), are generally nonzero. The global coordinate system denoted as X,Y is also shown in Fig. 14.



(A) UNDEFORMED STATE



(B) DEFORMED STATE

Figure 14. Beam-column element with corotational (x, y) and global (X, Y) coordinates.

In this updated Lagrangian formulation, the displacement fields of each element, u and v , are additively decomposed into rigid body deformation displacements; that is

$$\begin{aligned} u &= u^r + u^d \\ v &= v^r + v^d \end{aligned} \quad (15)$$

Now the rigid body displacements can be easily observed by giving any displaced configuration of the beam. The orientation of the updated Lagrangian coordinate is immediately specified by the x axis which always connects the endpoints. The translation and rotation needed to update the Lagrangian coordinate system are the rigid body displacements. Any remaining displacements are deformation displacements.

The strain-displacement equation is determined from the large-deflection strain-displacement equation by assuming planes remain plane during bending:

$$\varepsilon = \frac{\partial u^d}{\partial x} + \frac{1}{2} \left(\frac{\partial u^d}{\partial x} \right)^2 - y \frac{\partial^2 u^d}{\partial x^2} \quad (16)$$

For the beam-column element, the linear and cubic shape functions are assumed to represent the deformation displacements, u^d and v^d , in x and y directions respectively. This deformational displacement field is given by

$$\begin{aligned} \begin{Bmatrix} u^d \\ v^d \end{Bmatrix} &= \begin{bmatrix} \xi & 0 & 0 \\ 0 & \ell_N(\xi^3 - 2\xi^2 + \xi) & \ell_N(\xi^3 - \xi^2) \end{bmatrix} \begin{Bmatrix} d^d \end{Bmatrix} \\ &= [N] \{d^d\} \end{aligned} \quad (17)$$

where

$$\xi = \frac{x}{\ell_N}$$

and ℓ_N is the distance between nodes 1 and 2 of the beam-column element at any stage, and the deformation nodal displacements are

$$\{d^d\}^T = \{\Delta_{12}, \theta_1, \theta_2\} \quad (18)$$

and the corresponding nodal forces are

$$\{f^d\}^T = \{f_1^d, f_2^d, f_3^d\} \quad (19)$$

This deformation is then followed by a rigid body rotation α and translation. Thus, if the nodal rotations in the local system are d_3 and d_6 , it follows that

$$\theta_1 = d_3 - \alpha \quad \theta_2 = d_6 - \alpha \quad (20)$$

The elongation, Δ_{12} , and the rigid body rotation, α , can be computed by [51]:

$$\Delta_{12} = \frac{1}{\ell_N + \ell_o} \left[2X_{21}D_{41} + 2Y_{21}D_{52} + (D_{41})^2 + (D_{52})^2 \right] \quad (21)$$

and

$$\sin\alpha = \frac{D_{52}X_{21} - D_{41}Y_{21}}{\ell_N \ell_o} \quad (22)$$

in which

$$X_{21} = X_2 - X_1, Y_{21} = Y_2 - Y_1, D_{41} = D_4 - D_1, \text{ etc.}$$

$$l_0^2 = X_0^2 + Y_0^2 \text{ (refer to Fig. 14)}$$

From Eqs. (16) and (17), the strain and deformation nodal displacements can be related as

$$\varepsilon = \left([B_L] + \frac{1}{2} [B_{NL}] \right) \{d^d\} \quad (23)$$

in which

$$[B_L] = \frac{-y}{l_N} \left[-\frac{1}{y}, 6\xi - 4, 6\xi - 2 \right] \quad (24)$$

$$[B_{NL}] = \frac{\partial v^d}{\partial x} [G] \quad (25)$$

where

$$[G] = [0, 3\xi^2 - 4\xi + 1, 3\xi^2 - 2\xi]$$

$$\frac{\partial v^d}{\partial x} = [G] \{d^d\}$$

For general nonlinear problems, the solution algorithm (Newton-Raphson method) is based upon the application of a small increment of load. For this technique, it is necessary to relate the rate of change of force with displacement, i.e., the tangent stiffness. From Eq. (23) the rate of strain, $\Delta\varepsilon$, can be found as

$$\Delta\varepsilon = ([B_N] + [B_{NL}]) \{\Delta d^d\} \quad (26)$$

or

$$\Delta \varepsilon = [B] \{\Delta d^d\}$$

Once the strains are known, the stresses are computed by the constitutive law [46]. The stress-strain relationship for the beam material will be restricted to elastic-perfectly-plastic material laws [46] or

$$\Delta \sigma = E_T \Delta \varepsilon \quad (27)$$

$$E_T = \begin{cases} E & \text{if } |\sigma| \leq \sigma_y \text{ or } \sigma \cdot \Delta \sigma \leq 0 \\ 0 & \text{otherwise} \end{cases} \quad (28)$$

where E is the modulus of elasticity, σ and σ_y are the corotational stress and yield stress, respectively.

Using the principle of minimum potential energy [46], the nodal forces can be found as

$$\{f^d\} = \int_V [B]^T \sigma dV \quad (29)$$

where V is the volume of the element. The rate form of these nodal forces is found as

$$\begin{aligned} \{\Delta f^d\} &= \int_V [\Delta B]^T \sigma dV + \int_V [B]^T \Delta \sigma dV \\ &= [k^d]_T \{\Delta d^d\} \end{aligned} \quad (30)$$

where, from Eqs. (25) and (26),

$$[\Delta B]^T = [\Delta B_{NL}]^T = [G]^T [G] \{\Delta d^d\} \quad (31)$$

The deformed tangent stiffness $[k^d]_T$ can be expressed by the following equation:

$$[k^d]_T = [k_G^d] + [k_o^d] + [k_L^d] \quad (32)$$

The first term of the right-hand side of Eq. (30) becomes $[k_G^d] \{\Delta d^d\}$ and the second term will give $([k_o^d] + [k_L^d])\{\Delta d^d\}$. (Explicit formulations for each term will be given presently.) The matrix $[k_o^d]$ is known as the small displacement stiffness matrix or the conventional stiffness matrix; $[k_G^d]$ is known as the initial stress stiffness matrix or the geometric stiffness matrix, which depends linearly on the deformation nodal displacements; and $[k_L^d]$ represents the large displacement stiffness matrix which depends on quadratic terms of the deformation nodal displacements. The updated Lagrangian strain approach makes the strains and rotations in the local system (updated Lagrangian coordinate system) small enough (for reasonably small increments) that $[k_L^d]$ can be omitted [50,52]. Eq. (32) can then be reduced to

$$[k^d]_T = [k_o^d] + [k_G^d] \quad (33)$$

and also

$$\{\Delta f^d\} = [k^d]_T \{\Delta d^d\} \quad (34)$$

The following definitions are made in order to obtain the expressions for $[k_o^d]$ and $[k_G^d]$.

$$P_i = \int_A \sigma dA \quad (35)$$

$$M_i = \int_A \sigma y dA \quad (36)$$

$$(EA)_{Ti} = \int_A E_T dA \quad (37)$$

$$(EK)_{Ti} = \int_A E_T y dA \quad (38)$$

$$(EI)_{Ti} = \int_A E_T y^2 dA \quad (39)$$

where $i = 1, 2$ denotes $\xi = 0$ and 1 , respectively and A refers to the beam cross-sectional area. The quantities P_i , M_i , $(EA)_{Ti}$, $(EK)_{Ti}$, and $(EI)_{Ti}$ are assumed to be linear functions of ξ , for example,

$$P(\xi) = (P_2 - P_1)\xi + P_1 \quad (40)$$

$$M(\xi) = (M_2 - M_1)\xi + M_1, \text{ etc.} \quad (41)$$

The small displacement stiffness matrix is obtained by evaluating the integral (see Eq. 30).

$$[k_o^d] = \int_V [B_N]^T E_T [B_N] dV \quad (42)$$

Using the definitions of Eq. (37)-(39) gives

$$[k_o^d] = \begin{bmatrix} \frac{1}{\ell_N} \left(\frac{1}{2}(EA)_{T1} + \frac{1}{2}(EA)_{T2} \right) & \frac{1}{\ell_N} (EK)_{T1} & -\frac{1}{\ell_N} (EK)_{T2} \\ \frac{1}{\ell_N} (EK)_{T1} & \frac{1}{\ell_N} (3(EI)_{T1} + (EI)_{T2}) & \frac{1}{\ell_N} ((EI)_{T1} + (EI)_{T2}) \\ -\frac{1}{\ell_N} (EK)_{T2} & \frac{1}{\ell_N} ((EI)_{T1} + (EI)_{T2}) & \frac{1}{\ell_N} ((EI)_{T1} + 3(EI)_{T2}) \end{bmatrix} \quad (43)$$

The geometric stiffness is obtained by evaluating the first integral in Eq. (30) with appropriate substitution of Eq. (31) with the definitions in Eq. (35) and (36).

$$[k_G^d] = \frac{\ell_N}{60} \begin{bmatrix} 0 & 0 & 0 \\ 0 & 6P_1 + 2P_2 & -P_1 - P_2 \\ 0 & -P_1 - P_2 & 2P_1 + 6P_2 \end{bmatrix} \quad (44)$$

4.2.4. Layering Technique

The integrals in Eqs. (35)-(39) must be evaluated numerically since the cross section may be partially plastic. Numerical methods are introduced to calculate the strains and stresses in different layers of the cross section. The cross-sectional area is correspondingly divided into a number of layers over the depth as shown in Fig. 15. The number of layers used must be sufficient to follow the variation of material properties and stress over the depth. Each layer is assumed to have uniform material properties and the strain is evaluated at the centroid of the layer. For elastic-perfectly-plastic material if the strain, ϵ , exceeds the yield strain, ϵ_y , then the stress will be equal to yield stress and $(EA)_T$, $(EK)_T$, $(EI)_T$ will become zero. If the entire cross section is at yield, the maximum load at this location has been reached

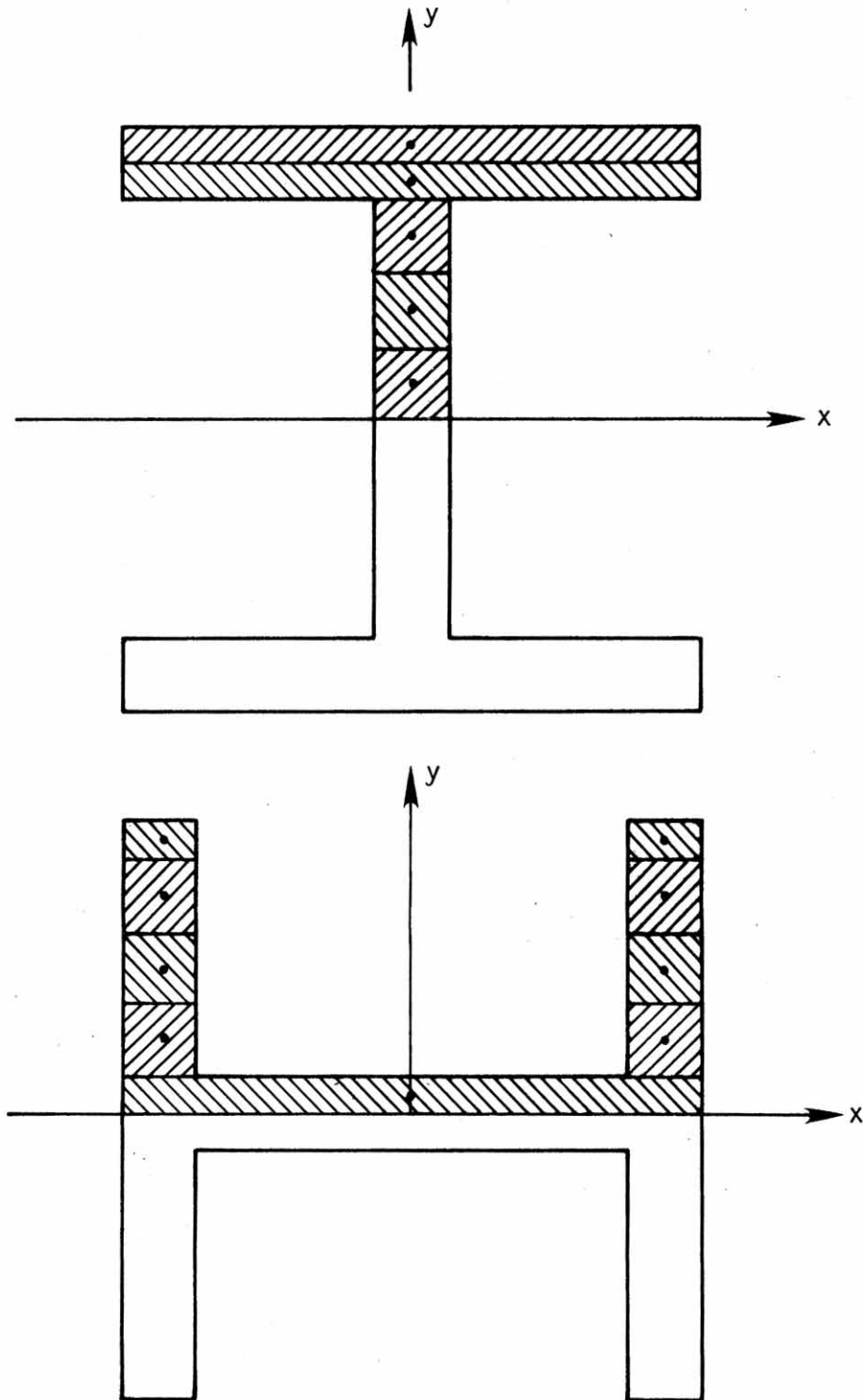


Figure 15. Typical layering system for the H pile about strong axis and weak axis.

and the tangent stiffness for additional displacement increments is zero.

The total deformation nodal force in Eq. (29) can be evaluated (after introduction of [B] from Eq. (26) and the definitions in Eq. (35) and (36)) as

$$\{f^d\} = [A_L] \{p\} + [A_{NL}] \{p\} \quad (45)$$

where

$$\{p\} = \begin{Bmatrix} P_1 \\ P_2 \\ M_1 \\ M_2 \end{Bmatrix} \quad (46)$$

$$[A_L] = \begin{bmatrix} 1/2 & 1/2 & 0 & 0 \\ 0 & 0 & -1 & 0 \\ 0 & 0 & 0 & 1 \end{bmatrix} \quad (47)$$

$$[A_{NL}] = \frac{l_N}{60} \begin{bmatrix} 0 & 0 & 0 & 0 \\ 6\theta_1 - \theta_2 & 2\theta_1 - \theta_2 & 0 & 0 \\ -\theta_1 + 2\theta_2 & -\theta_1 + 6\theta_2 & 0 & 0 \end{bmatrix} \quad (48)$$

The nodal forces, $\{f\}$, in the local system can be obtained from the deformation nodal forces, $\{f^d\}$, through equilibrium of the element, as

$$f_1 = -f_4 = -f_1^d \quad (49)$$

$$f_2 = -f_5 = \frac{(f_2^d + f_3^d)}{l_N} \quad (50)$$

$$f_3 = f_2^d \quad (51)$$

$$f_6 = f_3^d \quad (52)$$

or

$$\{f\} = [R] \{f^d\} \quad (53)$$

where

$$[R] = \begin{bmatrix} -1 & 0 & 0 \\ 0 & \frac{1}{l_N} & \frac{1}{l_N} \\ 0 & 1 & 0 \\ 1 & 0 & 0 \\ 0 & -\frac{1}{l_N} & -\frac{1}{l_N} \\ 0 & 0 & 1 \end{bmatrix} \quad (54)$$

The increment of nodal forces in local coordinates can be obtained from Eq. (53) as

$$\{\Delta f\} = [R] \{\Delta f^d\} \quad (55)$$

The transformation of deformation nodal displacements, $\{\Delta d^d\}$, can be derived by equating work expressed in deformed coordinates to work expressed in local coordinates as (principle of contragradience)

$$\{\Delta d^d\} = [R]^T \{\Delta d\} \quad (56)$$

Let $[T]$ be the transformation matrix from local coordinates to global systems and be defined as follows:

$$[T] = \begin{bmatrix} \cos(\alpha + \beta_o) & -\sin(\alpha + \beta_o) & 0 & 0 & 0 & 0 \\ \sin(\alpha + \beta_o) & \cos(\alpha + \beta_o) & 0 & 0 & 0 & 0 \\ 0 & 0 & 1 & 0 & 0 & 0 \\ 0 & 0 & 0 & \cos(\alpha + \beta_o) & -\sin(\alpha + \beta_o) & 0 \\ 0 & 0 & 0 & \sin(\alpha + \beta_o) & \cos(\alpha + \beta_o) & 0 \\ 0 & 0 & 0 & 0 & 0 & 1 \end{bmatrix} \quad (57)$$

The nodal forces and displacements in the global system can be related to the local system as

$$\{F\} = [T] \{f\} \quad (58)$$

$$\{d\} = [T]^T \{D\} \quad (59)$$

Differentiating Eq. (58), the incremental nodal forces in the global system can be found:

$$\{\Delta F\} = [\Delta T] \{f\} + [T] \{\Delta f\} \quad (60)$$

Since the updated Lagrangian (temporary stationary) method was applied, $[\Delta T]$ is zero and Eq. (60) becomes

$$\{\Delta F\} = [T] \{\Delta f\} \quad (61)$$

Substituting Eqs. (34), (55), and (56) into Eq. (61) yields the tangent stiffness in the local and global systems, $[k]_T$ and $[K]_T$, respectively:

$$\{\Delta F\} = [K]_T \{\Delta D\} \quad (62)$$

where

$$[k]_T = [R] [k^d]_T [R]^T \quad (63)$$

$$[K]_T = [T] [k]_T [T]^T \quad (64)$$

Thus, the tangent stiffness matrix for beam-column element, $[K]_T$, was derived by using an incremental formulation approach. One must keep in mind that $[K]_T$ can be applied for only small displacement increments.

4.2.5. Soil Model

4.2.5.1. Modified Ramberg-Osgood Model

The soil response is assumed to be nonlinear. The nonlinear characteristics are expressed by the concept of soil resistance versus displacement, such as f-z, q-z, p-y curves. Fig. 16 shows a typical representation of resistance-displacement curves in vertical or lateral directions. A set of f-z, q-z and p-y curves are formed on the basis of criteria presented in Section 3.2. These curves can be approximated by various mathematical formulas. The most frequently used mathematical functions are parabolas, hyperbolas, splines and the Ramberg-Osgood functions [53-57]. A general function similar to the Ramberg-Osgood model for simulation of resistance-displacement curves will be used here. This model offers certain advantages over the other models and also includes the commonly used hyperbola as a special case. According to this model, a function can be approximated by a four-parameter curve as

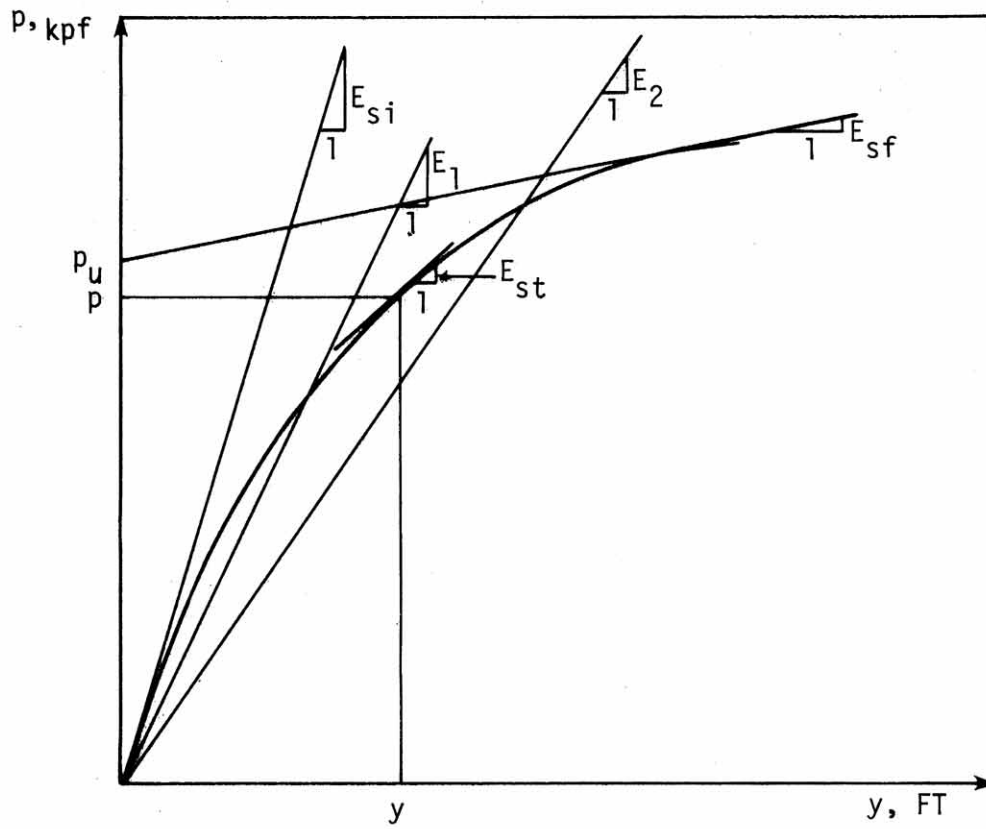


Figure 16. Simulation of resistance-displacement curves by modified Ramberg-Osgood model.

$$p = \frac{(E_{si} - E_{sf})y}{\left(1 + \left|\frac{(E_{si} - E_{sf})y}{p_u}\right|^n\right)^{1/n}} + E_{sf} y \quad (65)$$

where

- E_{si} = initial tangent modulus
- E_{sf} = final tangent modulus
- p = generalized soil resistance
- p_u = ultimate soil resistance
- n = shape parameter
- y = generalized displacement

The expression for the tangent modulus is obtained by differentiating Eq. (65) with respect to displacement, y :

$$E_{st} = \frac{(E_{si} - E_{sf})}{\left(1 + \left|\frac{(E_{si} - E_{sf})y}{p_u}\right|^n\right)^{n/n+1}} + E_{sf} \quad (66)$$

Details of evaluation of the parameters together with a computer code are given by [58]. Fig. 17 illustrates a set of curves which come from Eq. 65 to show various nondimensional forms of the modified Ramberg-Osgood model.

4.2.5.2. Soil Springs

Fig. 18 shows a linear spring with spring constant k_s under a load of f . The spring deflects by the amount d under the load. The equilibrium equation or load-displacement relation for the loaded spring can be obtained by using the minimum potential energy

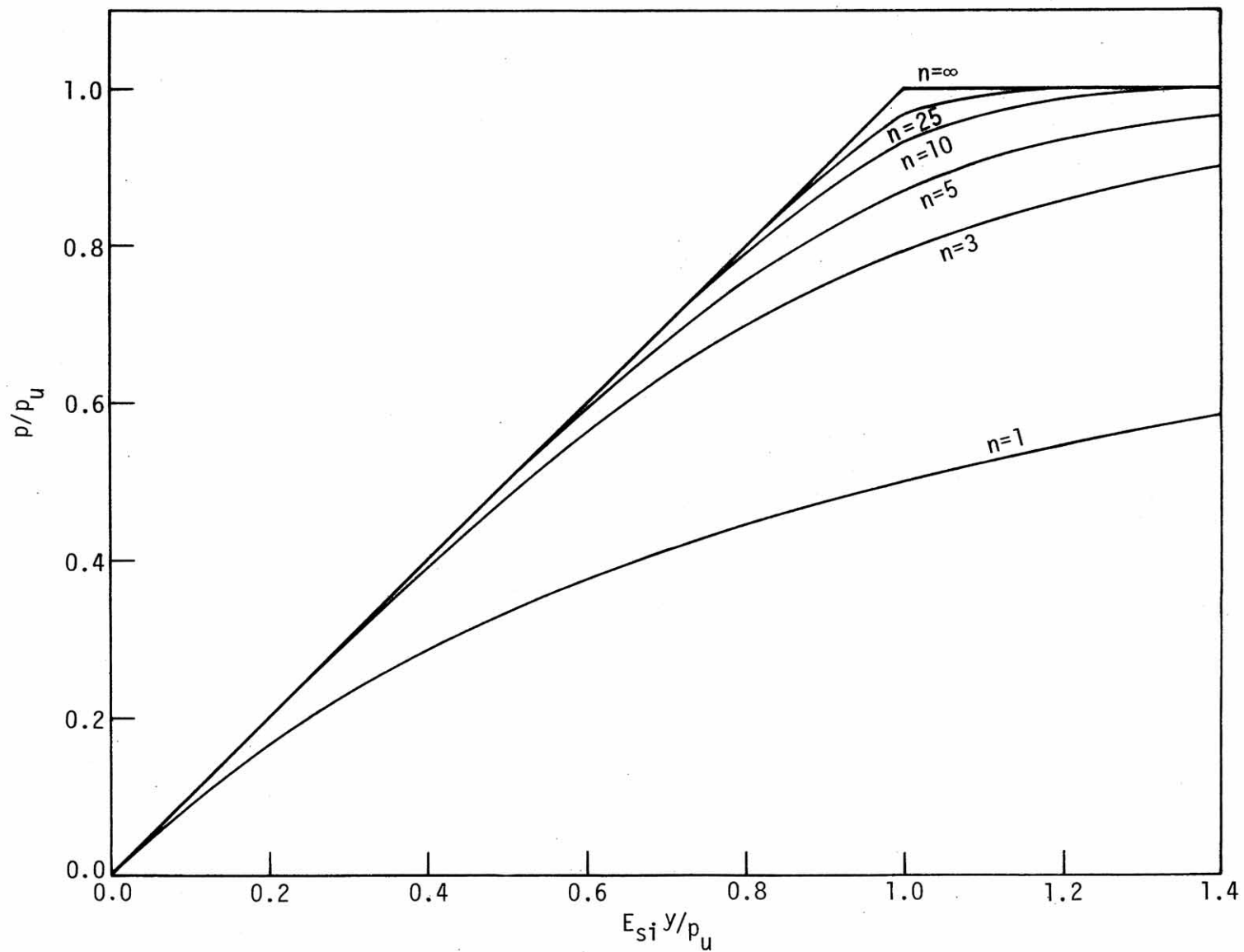


Figure 17. (a) Nondimensional forms of the modified Ramberg-Osgood model with $E_{sf} = 0$.

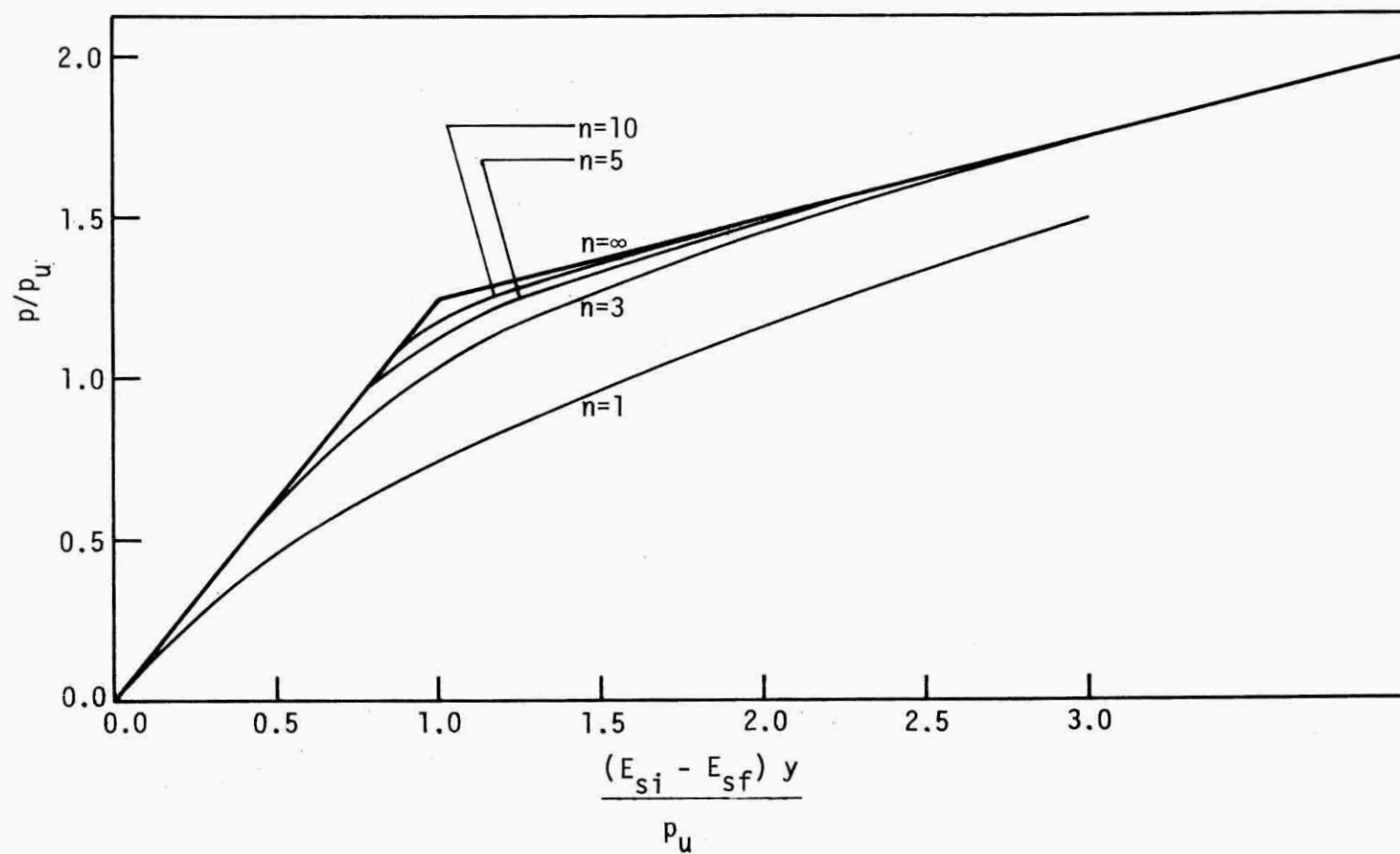


Figure 17. (b) Nondimensional forms of the modified Ramberg-Osgood model with $E_{sf} = +0.2 E_{si}$

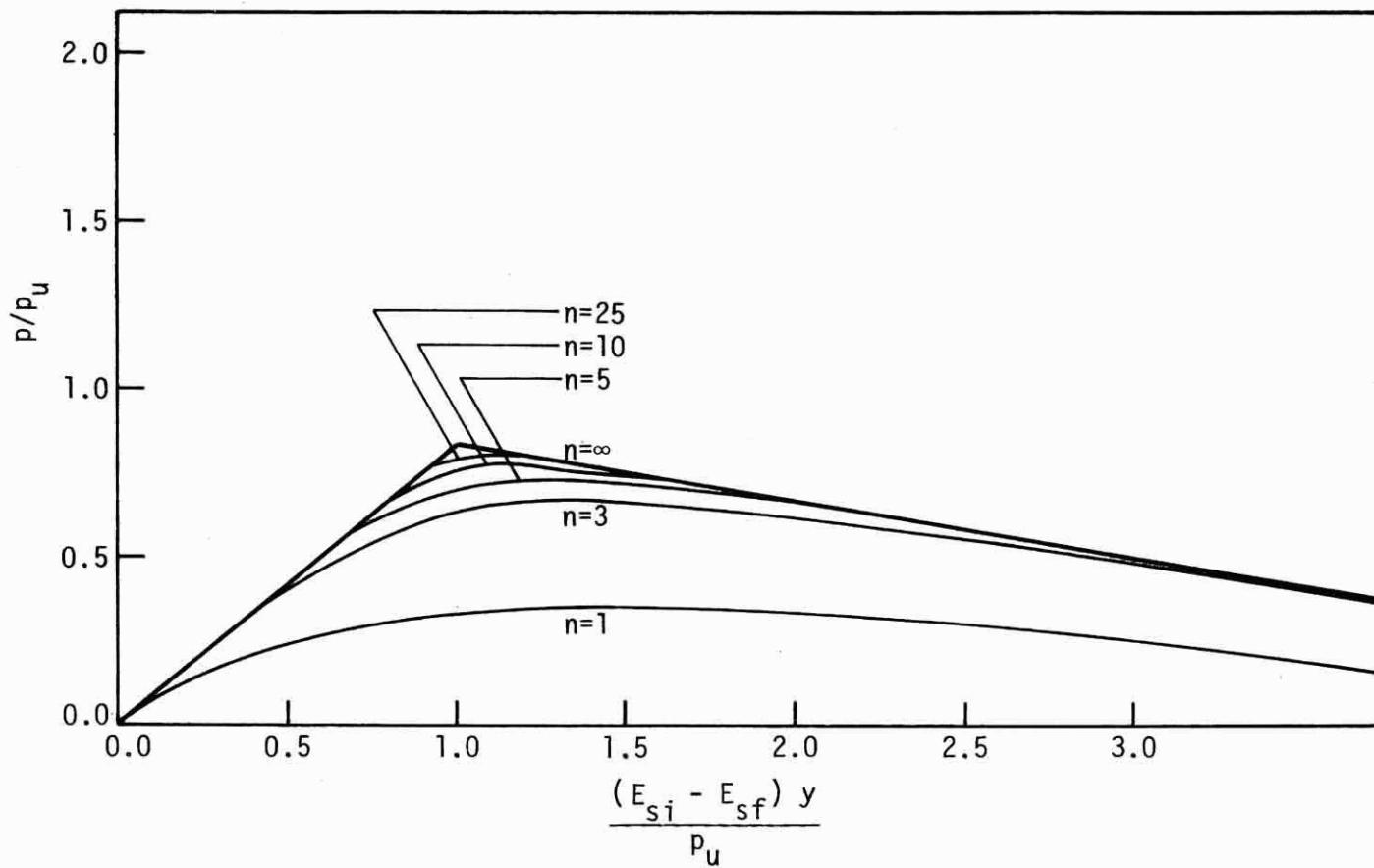


Figure 17. (c) Nondimensional forms of the modified Ramberg-Osgood model with $E_{sf} = -0.2 E_{si}$.

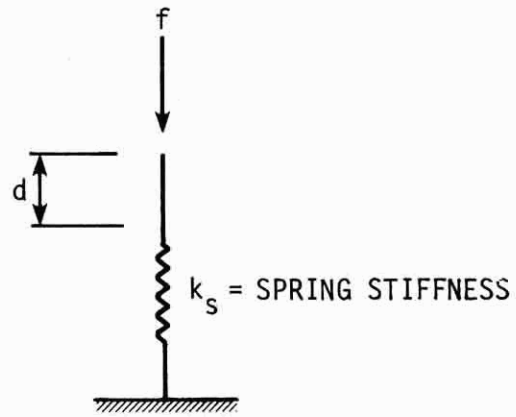


Figure 18. Linear spring under an applied force f .

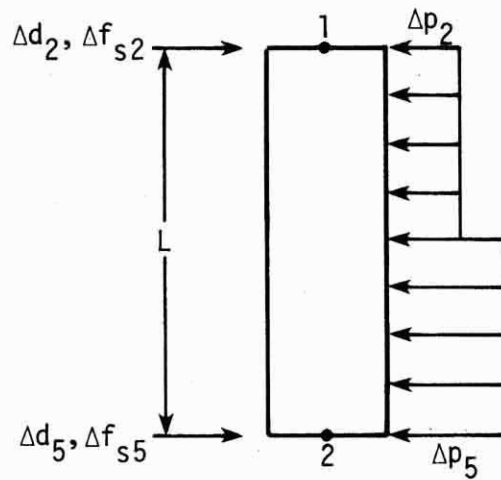


Figure 19. External and internal forces and displacements acting on the pile element.

$$f = k_s d \quad (67)$$

where

k_s = the stiffness of the soil spring element

If nonlinear soil behavior is considered, then the spring stiffness is not constant and instead is a function of displacement. Only the lateral spring element will be discussed in detail here since the others would follow the same derivations. As discussed in the previous section, a set of p-y curves can be represented by the modified Ramberg-Osgood model as shown in Fig. 17. The lateral soil resistance per unit length of pile, p, is assumed to be uniformly distributed on the top half of the element and dependent only upon the displacement at the top node and distributed similarly on the bottom half of the pile element. Fig. 19 shows the assumed distribution for the lateral soil resistance per unit length. In this figure, the following quantities are illustrated.

l = pile element length

Δf_s = force increment acting on the node

Δp = resistance increment per unit length

Δd = displacement increment

From Fig. 19,

$$\Delta f_{s2} = \Delta p_2 l/2 \quad (68)$$

$$\Delta f_{s5} = \Delta p_5 l/2 \quad (69)$$

For incremental loading, the relationship between soil resistance-displacement can be expressed by Eq. (66) as

$$\Delta p = E_{hzt} \Delta d \quad (70)$$

where

$$E_{hzt} = \text{tangent modulus from p-y curve}$$

With Eqs. (68), (69), and (70), the tangent stiffness of the nonlinear lateral spring element, k_{hst} , can be expressed as follows:

$$\Delta f_{s2} = \Delta p_2 \frac{\ell}{2} = \left(E_{hzt} \frac{\ell}{2} \right) \Delta d_2 \quad (71)$$

$$\Delta f_{s5} = \Delta p_5 \frac{\ell}{2} = \left(E_{hzt} \frac{\ell}{2} \right) \Delta d_5$$

where

$$k_{hst} = \frac{E_{hzt} \ell}{2} \quad (72)$$

If the same approach is used on the nonlinear vertical and point spring elements, the tangent stiffness of the nonlinear vertical and point spring elements, k_{vst} and k_{pst} , respectively, will be given as follows:

$$k_{vst} = E_{vzt} C \ell/2 \quad (73)$$

$$k_{pst} = E_{pzt} A_B \quad (74)$$

where

$$\begin{aligned}
 E_{vzt} &= \text{tangent modulus from } f\text{-}z \text{ curve} \\
 E_{pzt} &= \text{tangent modulus from } q\text{-}z \text{ curve} \\
 C &= \text{pile perimeter} \\
 A_B &= \text{effective pile tip area} \\
 &\quad (\text{for H pile, treated as rectangular section})
 \end{aligned}$$

Combining the tangent stiffness of the spring elements with the tangent stiffness of the beam-column element in the local system yields

$$[k]_T = [R] \left([k_o^d] + [k_G^d] \right) [R]^T + [k_s]_T \quad (75)$$

Transforming $[k]_T$ to the global system yields $[K]_T$ (see Eq. (64)).

4.3. Basic Nonlinear Solution Techniques

The solution of nonlinear problems by the finite element method is usually attempted by one of three basic techniques: incremental or stepwise procedures, iterative or Newton methods, or increment-iteration or mixed procedures. The increment-iteration procedures will be adopted in this investigation as shown in Fig. 20. Here the load is applied incrementally, and, after each increment, successive iterations are performed until convergence to a specified tolerance occurs. Two versions of the numerical procedure, the basic Newton-Raphson method and the modified Newton-Raphson method, are widely used. The choice of any one of these methods depends upon its computational efficiency when applied to the particular nonlinear problem under consideration. The basic Newton-Raphson method will be applied to this problem.

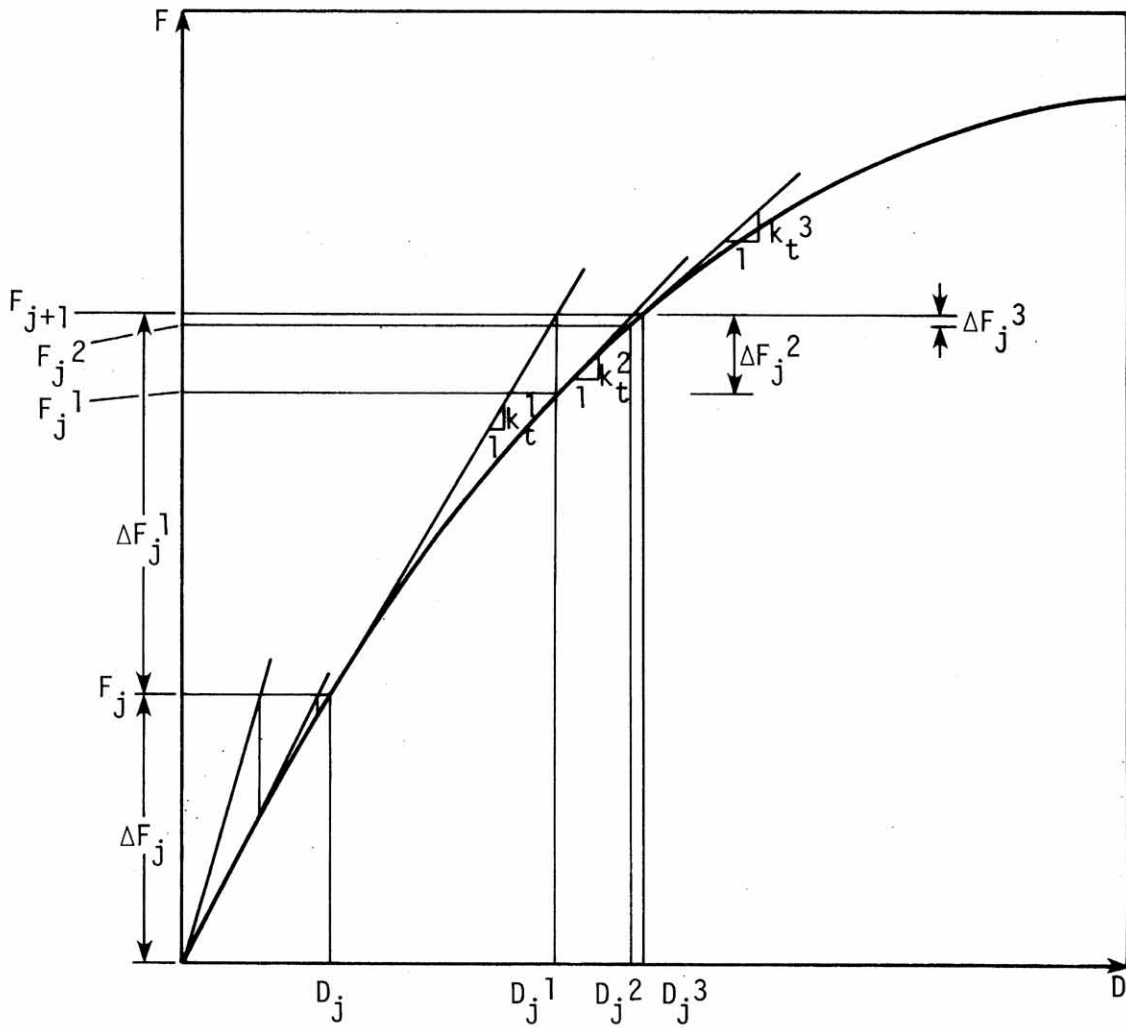


Figure 20. Increment-iteration or mixed procedure
(Newton-Raphson solution of the equation $F=f(D)$).

In the basic Newton-Raphson procedure the most current information available concerning the structure is used to calculate the incremental quantities at any step. In other words, the tangent stiffness matrix at the start of each iteration is used to estimate the next incremental quantities. It requires the formation of the element tangent stiffness transformed into global coordinates at the start of each iteration.

Suppose that currently $\{\epsilon_j^i\}$, $\{\sigma_j^i\}$, $\{f_j^i\}$, $\{F_j^i\}$, $\{X_j^i\}$, $\{Y_j^i\}$, $\{D_j^i\}$, $\{d_j^i\}$, and $\{P_j^i\}$ are given at the j th increment and the i th iteration. The condition $i = 1$ and $j = 1$ is the initial stage in the nonlinear problem. Thus, except for $\{X_1^1\}$, $\{Y_1^1\}$, the above vectors are null. To generate the $i+1$ th iteration by the updated Lagrangian method, the following steps will be followed.

Step 1: Calculate the current unbalanced forces in the global system:

$$\{\Delta F_j^{i+1}\} = \{F_{j+1}\} - \{F_j^i\} \quad (76)$$

where

$$\begin{aligned} \{F_{j+1}\} &= \text{forces for } j+1\text{th load increment} \\ \{F_j^i\} &= \text{forces from previous iteration } i \end{aligned}$$

Step 2: Establish the current local coordinates x, y for the element at hand.

Step 3: Generate the structural tangent stiffness in current coordinates $\{X_j^i\}$ and $\{Y_j^i\}$.

- (a) establish E_T at each integration point through the cross-section (with the current strain information)

- (b) perform $(EA)_T$, $(EK)_T$, $(EI)_T$ integrals at each end
- (c) determined $[k_{oj}^i]$, also with current $\{p_j^i\}$, find $[k_{Gj}^i]$
- (d) generate $[k_j^i]_T$ by adding $[k_{sj}^i]_T$
- (e) transform $[k_j^i]_T$ into global coordinates to get $[K_j^i]_T$
- (f) assemble $[K_j^i]_T$ into the structural tangent stiffness $\Sigma[K_j^i]_T$

Step 4: Solve for incremental displacements with current unbalanced forces $\{\Delta F_j^{i+1}\}$:

$$\{\Delta D_j^{i+1}\} = \left(\Sigma[K_j^i]_T \right)^{-1} \{\Delta F_j^{i+1}\} \quad (77)$$

Step 5: Update coordinates.

- (a) update coordinates, $\{X_j^{i+1}\} = \{X_j^i\} + \{\Delta D_j^{i+1}\}$
- (b) update displacements, $\{D_j^{i+1}\} = \{D_j^i\} + \{\Delta D_j^{i+1}\}$

Step 6: Calculate the updated strains and stresses.

- (a) find $\{d_j^d{}^{i+1}\}$ from Eqs. (18), (20), (21), (22)
- (b) compute $\{\epsilon_j^{i+1}\}$ from Eq. (23)
- (c) compute $\{\Delta \epsilon_j^{i+1}\} = \{\epsilon_j^{i+1}\} - \{\epsilon_j^i\}$
- (d) compute $\{\Delta \sigma_j^{i+1}\}$ from Eq. (27)
- (e) compute $\{\sigma_j^{i+1}\} = \{\sigma_j^i\} + \{\Delta \sigma_j^{i+1}\}$

Step 7: Compute element nodal forces in the local system

- (a) perform area integral to find $\{p_j^{i+1}\}$ from Eqs. (35) and (36)
- (b) compute $\{f_j^d{}^{i+1}\}$ from Eq. (45)
- (c) compute $\{f_j^{i+1}\}$ from Eq. (53)

Step 8: Find the equilibrium external nodal forces in global coordinates:

$$\{F_j^{i+1}\} = \Sigma[T_j^{i+1}] \{f_j^{i+1}\} \quad (78)$$

Step 9: Test for convergence. If not satisfied, return to Step 1. Otherwise go to the next increment of load $\{F_{j+2}\}$. Each step of this algorithm is tangent to the load versus displacement curve, as suggested before. The process is interpreted graphically in Fig. 20.

4.3.1. Convergence Criteria

In the adaptation of the basic Newton-Raphson method, specification of certain convergence criteria is necessary to terminate the iterations at a load increment. Convergence could be defined in terms of the relation between load imbalance and the total externally applied load. A criterion based on displacements is preferable [50]. In this work, convergence is assumed to have occurred when the maximum displacement increment is less than a specified value (typically 0.001 ft):

$$|\Delta D|_{\max} < 0.001 \text{ ft} \quad (79)$$

4.4. Verification of Model

Based on the theory outlined above, a computer program Yang 5 (or YANG 5) has been developed to solve the nonlinear pile-soil problems. A number of examples have been analyzed to establish its reliability. Three problems with analytical solutions were first solved: (a) a beam-column problem was used to check geometric nonlinearity of the pile; (b) a short, thick column problem was used to check material nonlinearity, and (c) a simple soil problem was used to check soil nonlinearity. Finally, the data obtained from two experimentally loaded piles tested in the field were compared with the analytical results.

4.4.1. Beam-Column Problem

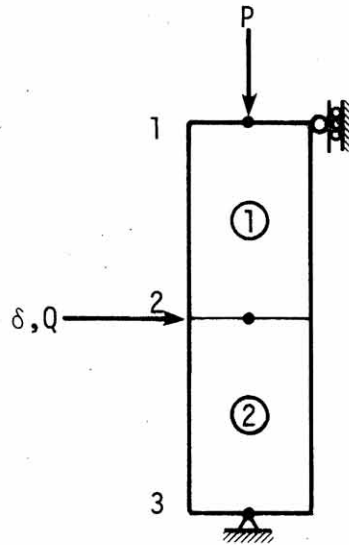
Figure 21 shows a beam-column with a concentrated lateral load, Q , acting on the midspan. To avoid material nonlinearity, the yield strain ϵ_y and yield stress are taken to be very large. The theoretical displacement at the midspan δ can be evaluated by solving the classic differential equation for beam columns [59] to obtain (refer to Fig. 21).

$$\delta = \frac{Q\ell^3}{48EI} \frac{3(\tan u - u)}{u^3} \quad (80)$$

$$P_{cr} = \frac{\pi^2 EI}{\ell^2} \quad (81)$$

$$u = \frac{\pi}{2} \sqrt{\frac{P}{P_{cr}}} \quad (82)$$

Equation (80) indicates that the displacement at the midspan, δ , is equal to $Q\ell^3/48EI$, the deflection that would exist if only Q were acting, multiplied by an amplification factor that depends on the ratio P/P_{cr} . If P/P_{cr} approaches unity, then the displacement at the midspan of the beam-column increases without bound. Figure 22 shows the relation between P and δ , if P is allowed to increase. The load-displacement relation is not linear. This is true regardless of whether Q remains constant (solid line) or increases proportionally with P (dashed curve). The displacement of a beam-column is, thus, a linear function of Q but a nonlinear function of P . The results obtained by running the Yang 5 computer program (two beam elements) are also plotted in Fig. 22. Significant differences between these results and the classical beam



USE HP 14 x 73

DATA : $A = 21.15 \text{ in}^2$

$b_f = 14.586 \text{ in}$

$d = 13.64 \text{ in}$

$t_f = 0.506 \text{ in}$

$t_w = 0.506 \text{ in}$

$I_{x-x} = 721.8044 \text{ in}^4$

$Z_{x-x} = 117.1082 \text{ in}^3$

$C = \text{perimeter} = 4.7 \text{ ft}$

$P_{cr} = \text{critical load} = 3710.377 \text{ kips}$

Figure 21. Beam-column with a concentrated load, Q.

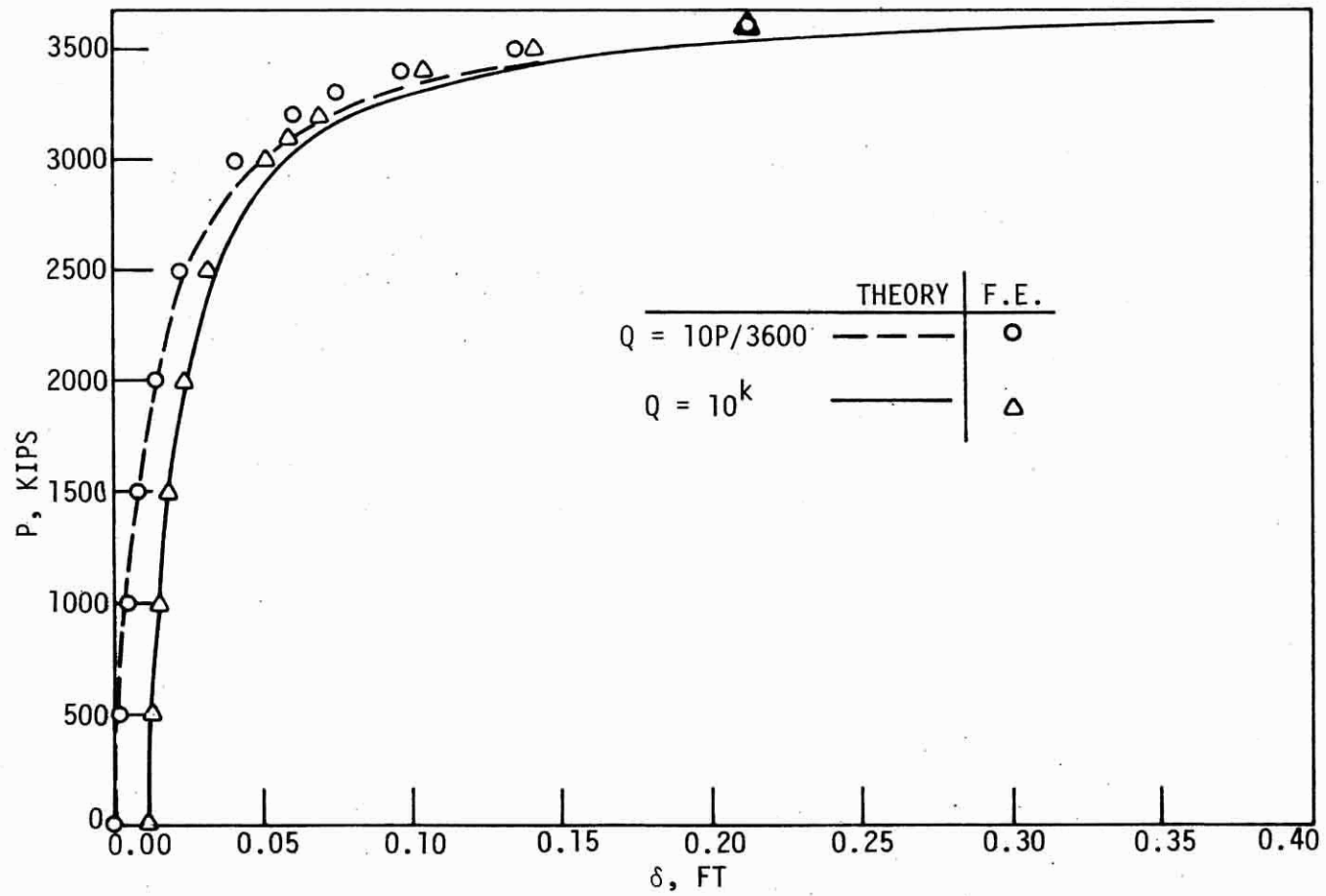


Figure 22. Load-displacement curves for beam-column problem.

column solution occur only when P approaches P_{cr} . Better results could be obtained by increasing the number of elements, e.g., eight elements in Fig. 23, by decreasing the load increment, and/or by reducing the tolerance of convergence. The reader will also note that, because displacements became large near P_{cr} , the classical solution is increasingly invalid.

4.4.2. Short Column Problem

Figure 24 shows a short, thick column with its material properties. A short, thick column is used in this example so that the geometric effect can be neglected and only the material nonlinearity will be considered.

Simple plastic theory assumes that a member subjected to bending moment will sustain a certain limiting bending moment value (the "plastic moment," M_p) that is dependent only on the geometrical properties of the cross section and the yield stress of the material. When this maximum moment is approached, curvature increases infinitely and a plastic hinge occurs. When enough hinges have formed to produce a mechanism, the structure will fail. If a member is subjected to the combined action of bending moment and axial forces, the available plastic moment capacity is reduced from the full value of M_p to a lesser value that can be designated as M_{pc} . Theoretical analyses have been presented in several books [60-62] and formulas of M_{pc} for different cross sections have been derived. Figure 25 illustrates stress patterns on a cross-sectional element as the moment increases (a) without axial force and (b) with axial force.

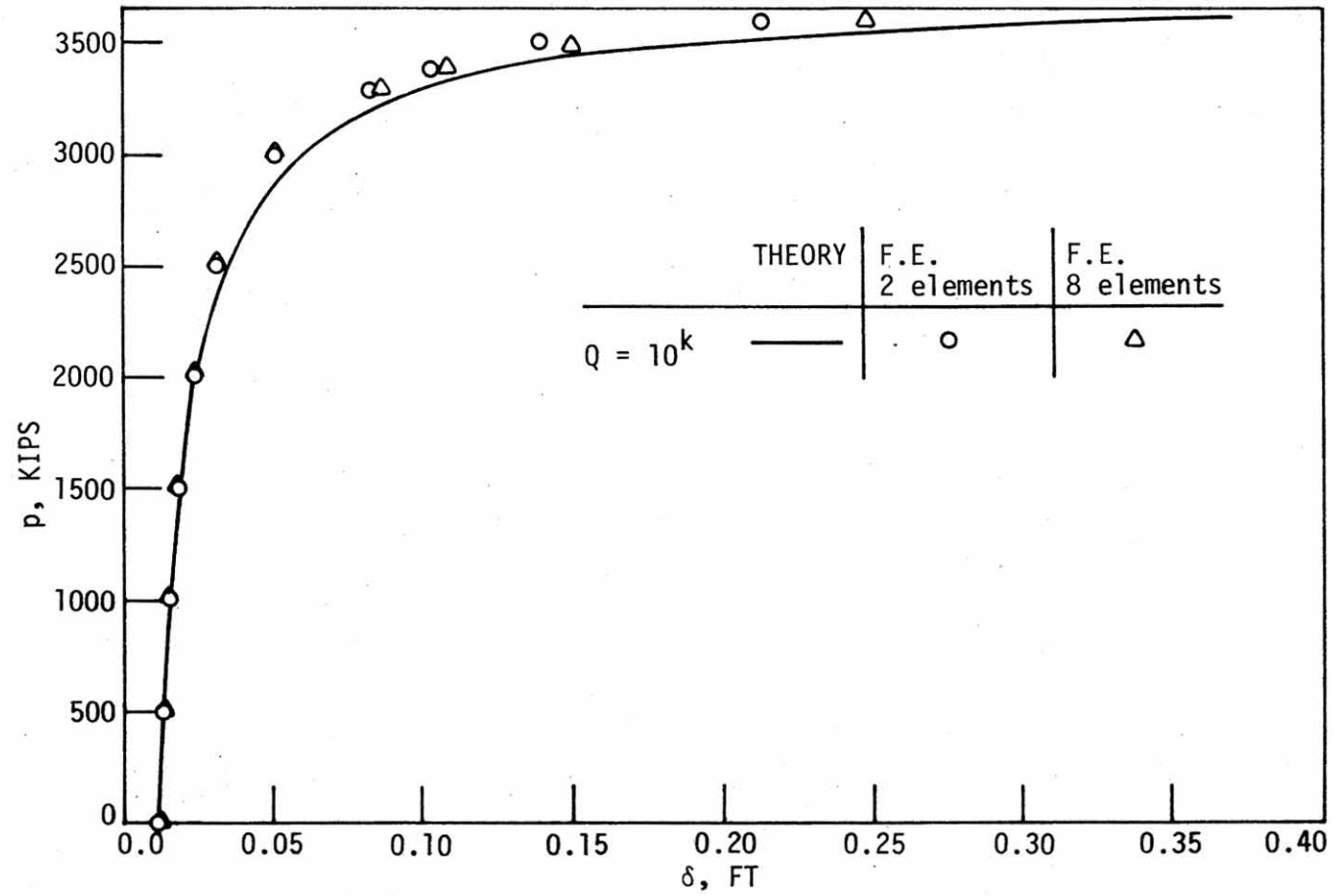
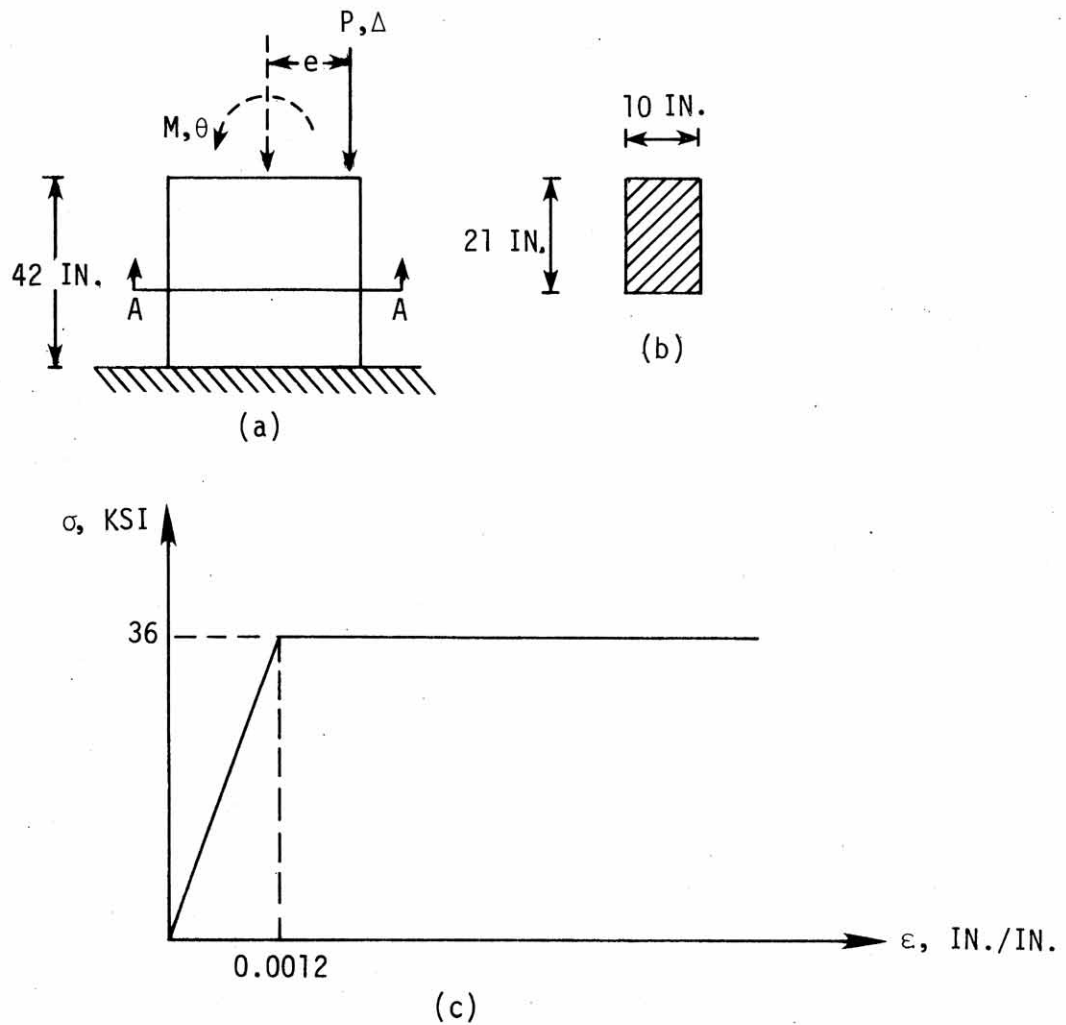


Figure 23. Load-displacement curves for beam-column problem (with 2 and 8 finite elements).



DATA: $A = 210 \text{ in.}^2$	$P_y = 7560 \text{ kips}$
$I_{x-x} = 7717.5 \text{ in.}^4$	$M_y = 2205 \text{ ft-kips}$
$Z_{x-x} = 1102.5 \text{ in.}^3$	$M_p = 3307.5 \text{ ft-kips}$
$C = 5.1667 \text{ ft}$	$\Delta_y = 0.0042 \text{ (pure axial load)}$
$\epsilon_y = 0.0012 \text{ in./in.}$	$\theta_y = 0.0048 \text{ (pure moment)}$
$\sigma_y = 36 \text{ KSI}$	$\theta_p = 0.0072 \text{ (pure moment)}$

Figure 24. (a) A short column subjected to applied load.
 (b) Cross section A-A.
 (c) Stress-strain relation.

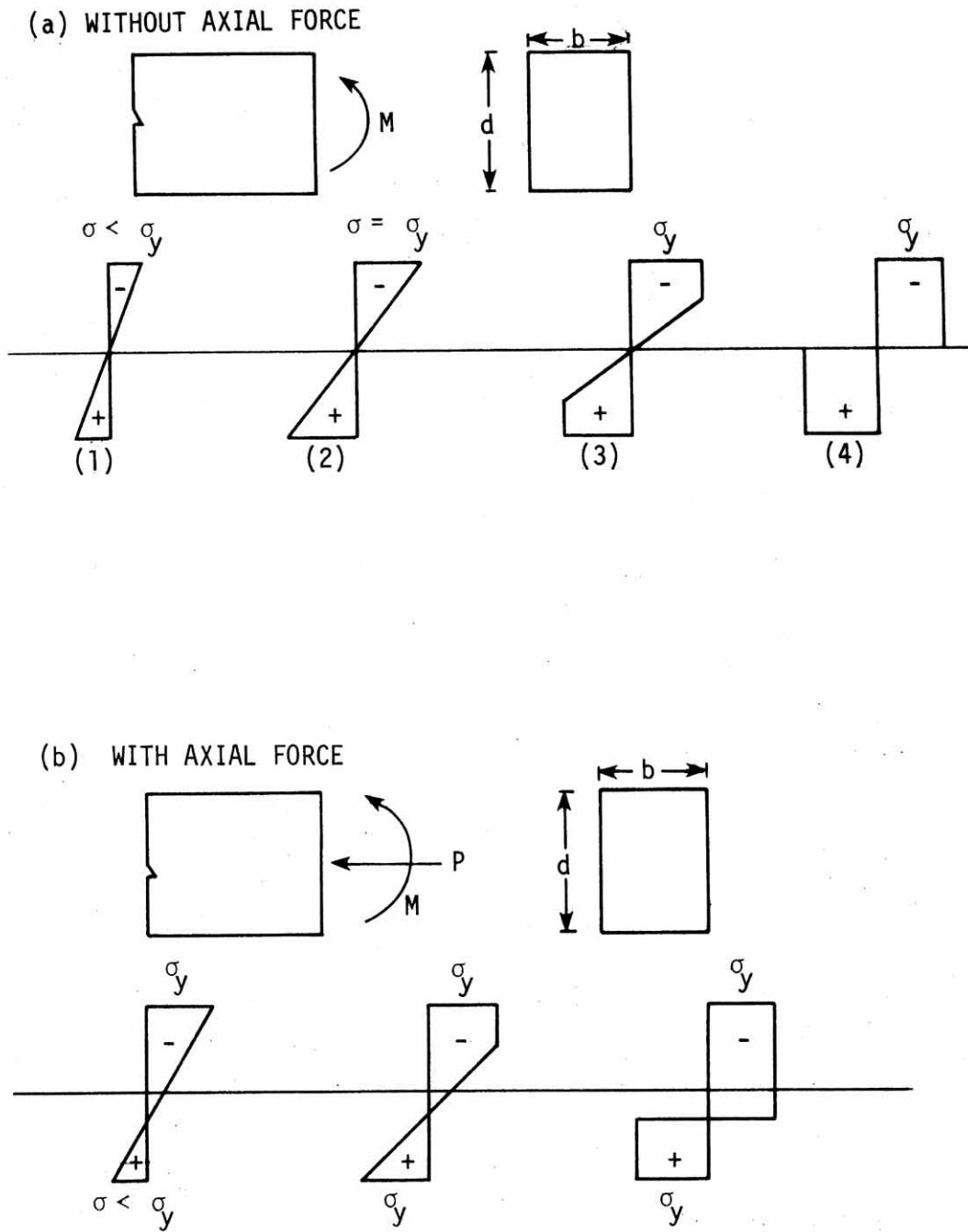


Figure 25. Stress patterns on a cross section as the moment increases.

In this example problem, a rectangular cross section is used. The corresponding formula for M_{pc} can be derived as

$$\frac{M_{pc}}{M_p} = 1 - \left(\frac{P}{P_y}\right)^2 \quad (83)$$

where

$$P_y = \sigma_y bd = \sigma_y A \quad (84)$$

and

$$M_p = \sigma_y bd^2/4 \quad (85)$$

As the material goes into the plastic range, the tangent stiffness of the element will be reduced.

Five different applied load cases are analyzed in this example (see Fig. 24 for the definition of the variables):

Proportional Loading

- | | |
|----------|--|
| Case (1) | $e = \frac{M}{P} = \infty$ (pure moment) |
| Case (2) | $e = 1.327'$ |
| Case (3) | $e = 0.467'$ |
| Case (4) | $e = 0$ (pure axial load) |

Nonproportional Loading

- | | |
|----------|---|
| Case (5) | Displacement increased to θ_p and Δ held equal to zero, then Δ increased as θ is held constant. |
|----------|---|

The results obtained from the above load cases are plotted in Fig. 26. Theoretical values of M_{pc} from Eq. (83) are shown. The computer

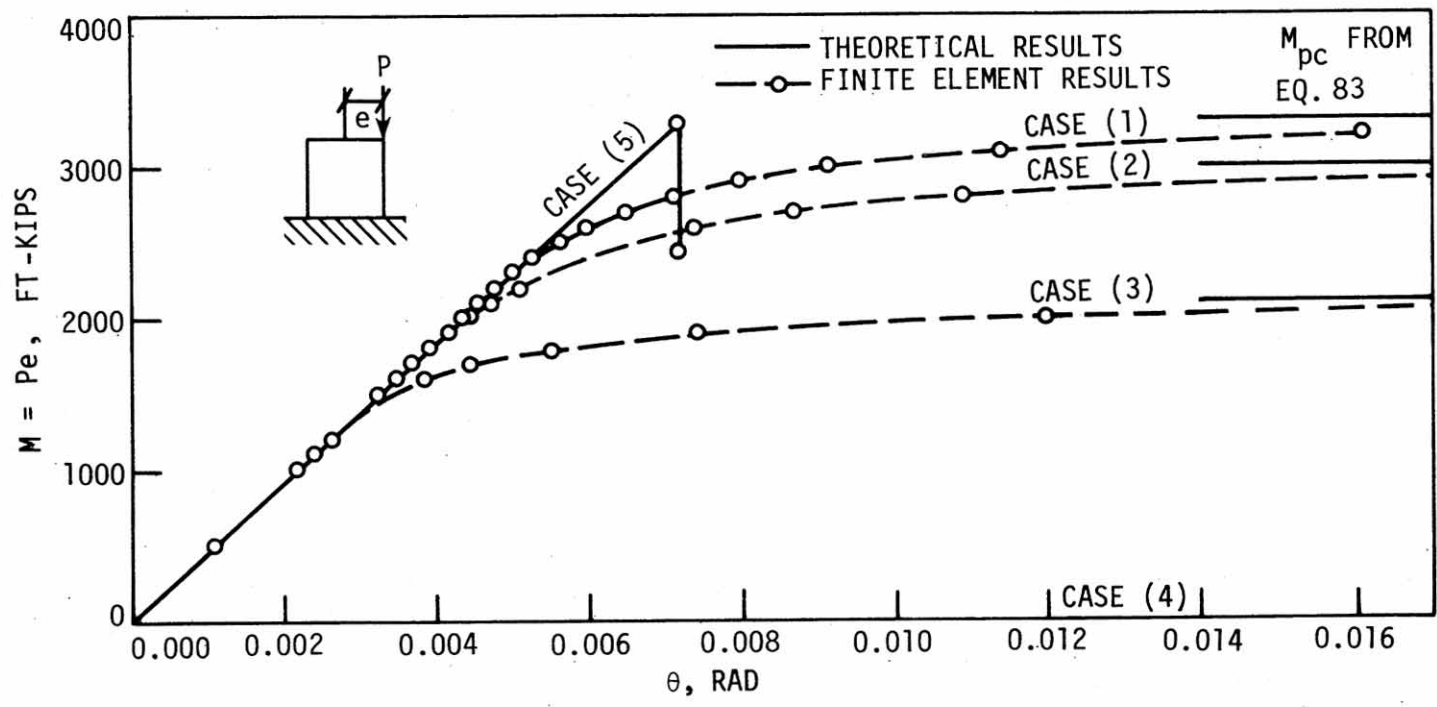


Figure 26. $M-\theta$ characteristics for the example in Figure 24.

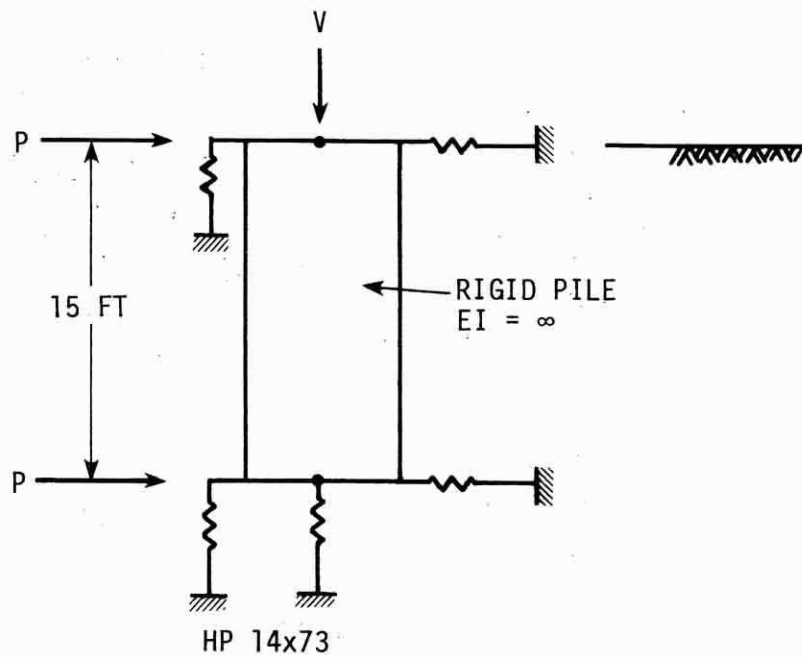
program gives satisfactory agreement with theoretical values. Case (5) illustrates that the moment decreases as the rotation is held constant and the axial deformation is increased.

4.4.3. Soil Problems

Three soil problems were used to check the soil material nonlinearity analysis in three different parts: (a) lateral spring element, (b) vertical spring element, (c) point spring element. For example, suppose an HP 14 × 73 pile was embedded below the ground as shown in Fig. 27. The soil response can then be observed by taking the pile to be rigid. Theoretical displacements and soil resistance follow the p-y curve path. For a specified load, the displacement will be obtained from the Newton-Raphson solution algorithm. Figure 28 shows the iteration path which the computer solution followed for a horizontal load of 1000 kips. Several loading cases have been studied. Results for the vertical springs are presented in Fig. 29 for a vertical load of 3000 kips and in Fig. 30 for the point spring with a vertical load of 10 kips. Results obtained from Yang 5 are consistent with the expected theoretical results as shown in Table 7. The theoretical results were obtained by considering a rigid pile with applied load acting, for example, for the lateral springs, $p = 2P/L$ (kpf) (see Fig. 27).

4.4.4. Experimentally Loaded Piles

Two pile tests are given in [33,63]. The first is a vertical load test on end-bearing steel H-piles driven about 40 ft through sand and gravel. The second is a full-scale lateral load test on drilled piers in hard overconsolidated clay. The observed values from those full-scale load tests will be compared to values predicted by the Yang 5 program.



$b = 1.216 \text{ ft}$
 $c = 4.7 \text{ ft}$
 $L = 15 \text{ ft}$
 $A = 0.1469 \text{ ft}$

SOIL PROPERTIES:

(a) p-y CURVE:

$$E_{si} = 200 \text{ KSF}$$

$$E_{sf} = 40 \text{ KSF}$$

$$n = 5.0$$

$$p_u = 35.0 \text{ KPF}$$

(b) f-Z CURVE

$$E_{si} = 100 \text{ KCF}$$

$$E_{sf} = 20 \text{ KCF}$$

$$n = 5.0$$

$$f_{\max} = 20.0 \text{ KSF}$$

(c) q-Z CURVE

$$E_{si} = 100 \text{ KCF}$$

$$E_{sf} = 20 \text{ KCF}$$

$$n = 5.0$$

$$q_{\max} = 20.0 \text{ KSF}$$

Figure 27. HP 14 x 73 pile used to check soil spring response.

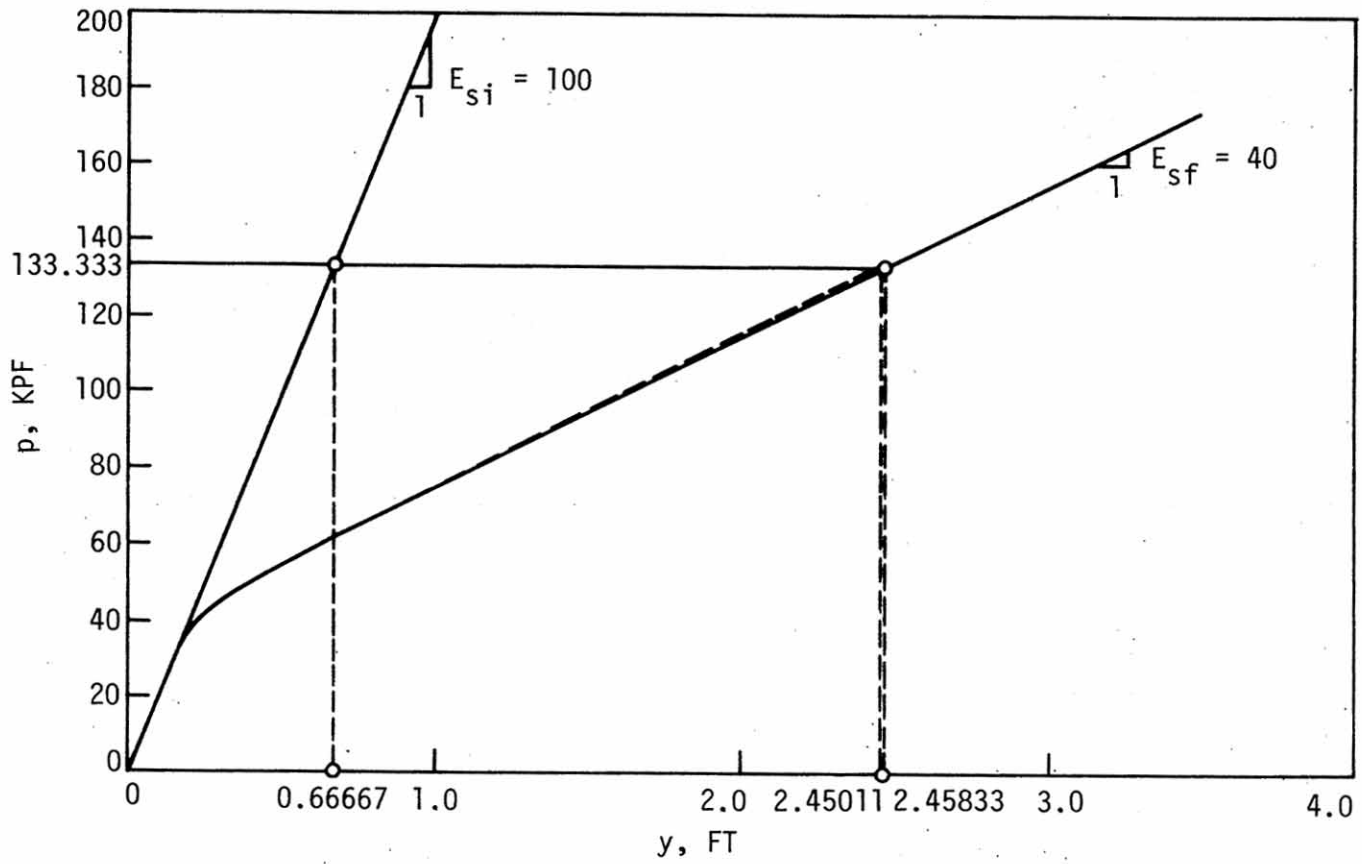


Figure 28. Iteration path for the example in Figure 27 with applied load, $P = 1000$ kips.

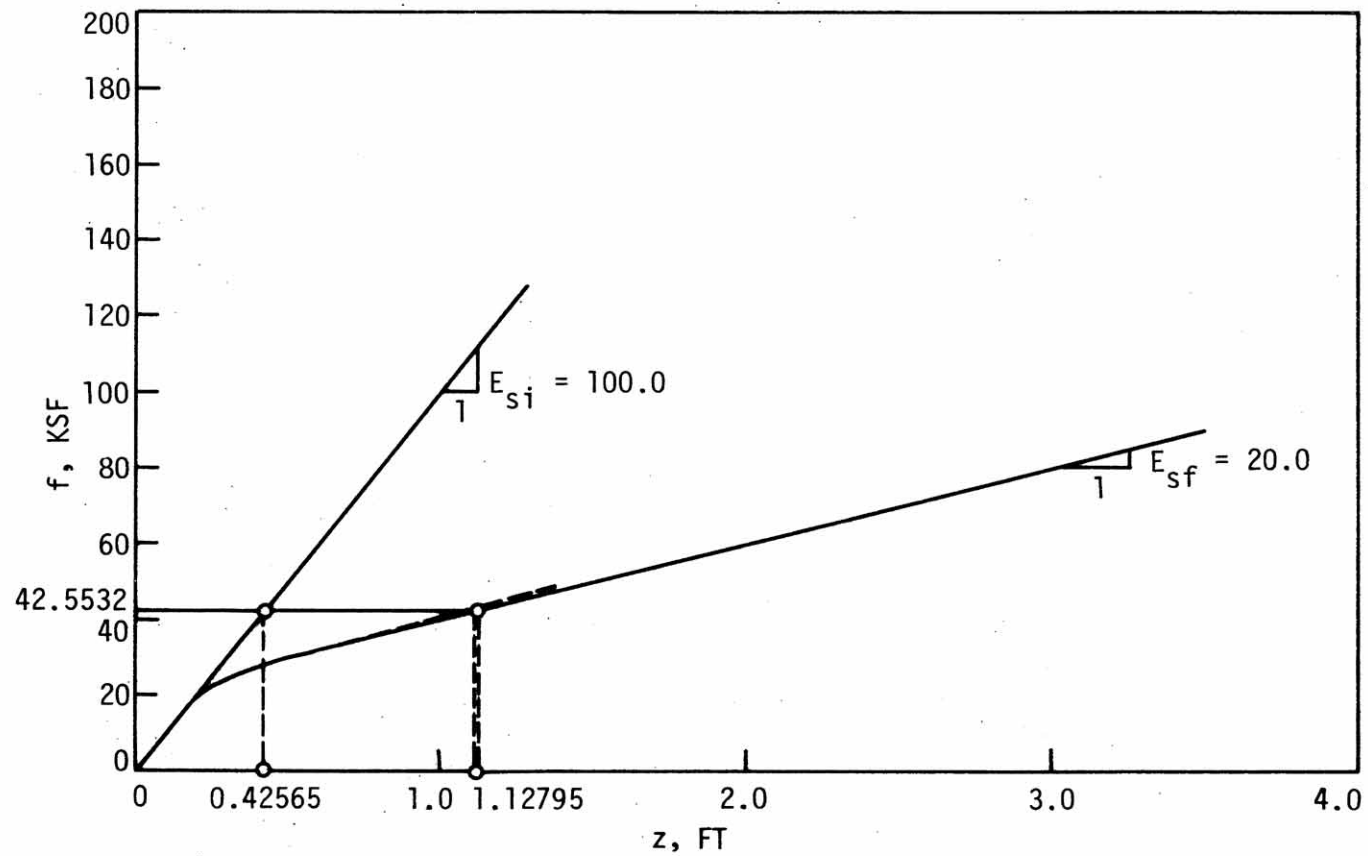


Figure 29. Iteration path for the example in Figure 27 with applied load, $V = 3000$ kips (no point spring).

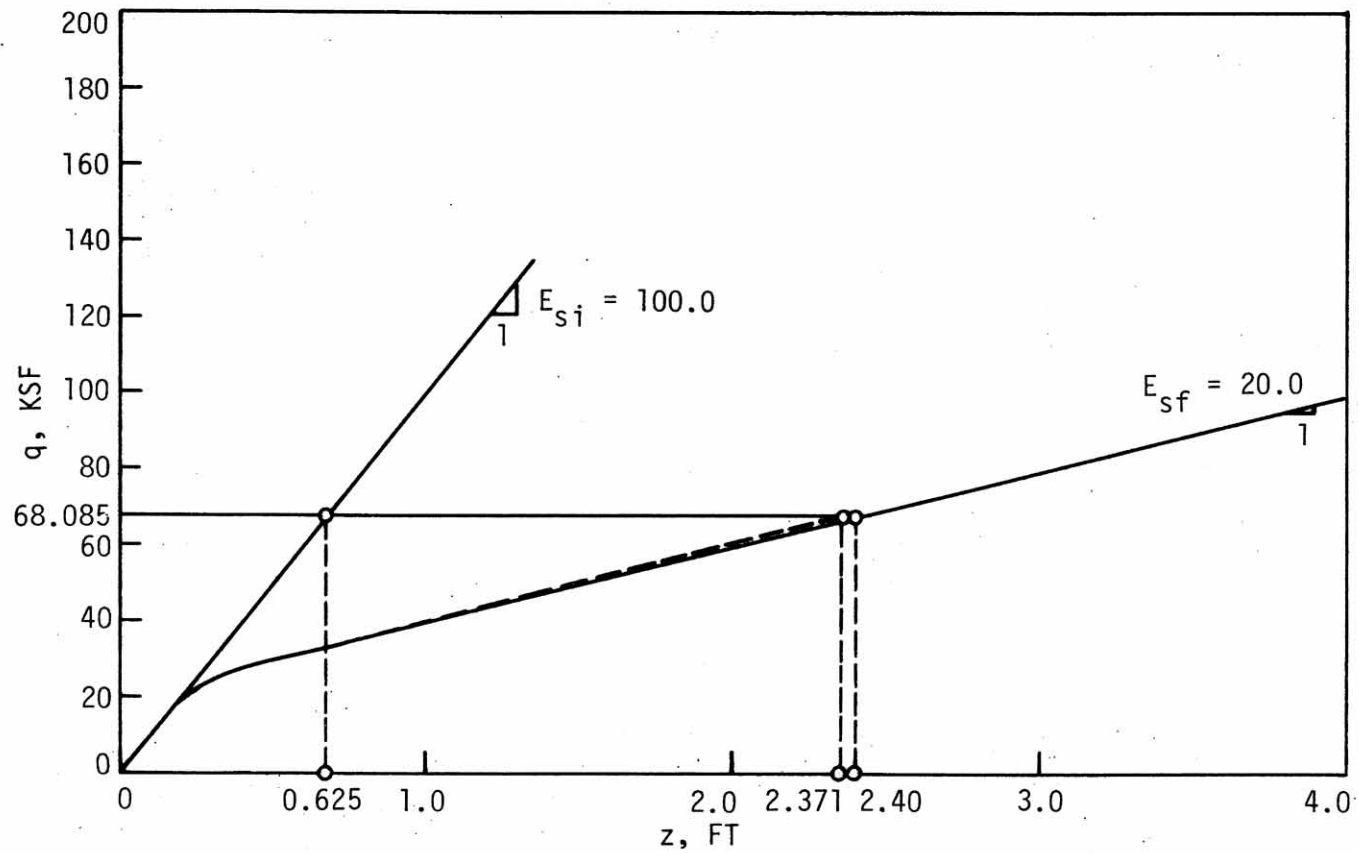


Figure 30. Iteration path for the example in Figure 27 with applied load, $V = 10$ kips (no vertical springs).

Table 7. Comparison between theoretical and numerical results.

Case	Spring	Specified Load/ Displacement	Soil Resistance (p, f or q)	
			Theoretical	Numerical
1	Lateral	1000 k	133.33333 kpf	133.33331 kpf
	Lateral	2000 k	266.66667 kpf	266.66663 kpf
	Lateral	3000 k	400.00 kpf	400.00 kpf
2	Vertical	1000 k	14.18440 ksf	14.18497 ksf
	Vertical	2000 k	28.36879 ksf	28.36912 ksf
	Vertical	3000 k	42.55319 ksf	42.55364 ksf
3	Point	10 k	68.08510 ksf	68.08180 ksf
	Point	20 k	136.17021 ksf	136.16797 ksf
4	Lateral	3 ft	154.99999 kpf	154.99998 kpf

4.4.4.1. Load Transfer in End-Bearing Steel H Piles

In Ref. [63], the increase in the load-carrying capacity of an end-bearing pile due to load transferred to the surrounding soil by friction was experimentally studied. Site conditions, pile driving, and instrumentation were examined. The strain-gauge readings were analyzed to determine the distribution of the load transferred along the piles. The piles were loaded and unloaded in increments to 150 kips, 300 kips, 450 kips, and 600 kips. A plot of pile load as a function of depth is shown in Fig. 31. From curves of the type shown there, the true elastic shortening can be obtained and the tip displacement calculated by subtracting the elastic shortening from the observed butt displacement. Curves of tip displacement as a function of load for HP 14 × 89 and HP 14 × 117 test piles are duplicated in Fig. 32. From these two figures (31 and 32) two sets of f - z curves and q - z curves (one set for each pile) can be constructed by the following procedures:

- (1) From Fig. 31, measure the load transferred to the pile at each specified depth (refer to Fig. 33)
- (2) Calculate the elastic shortening of each pile segment:

$$\varepsilon = \frac{P_{ave}}{AE} \quad (86)$$

where

$$P_{ave} = \frac{P_i + P_{i-1}}{2} \quad (87)$$

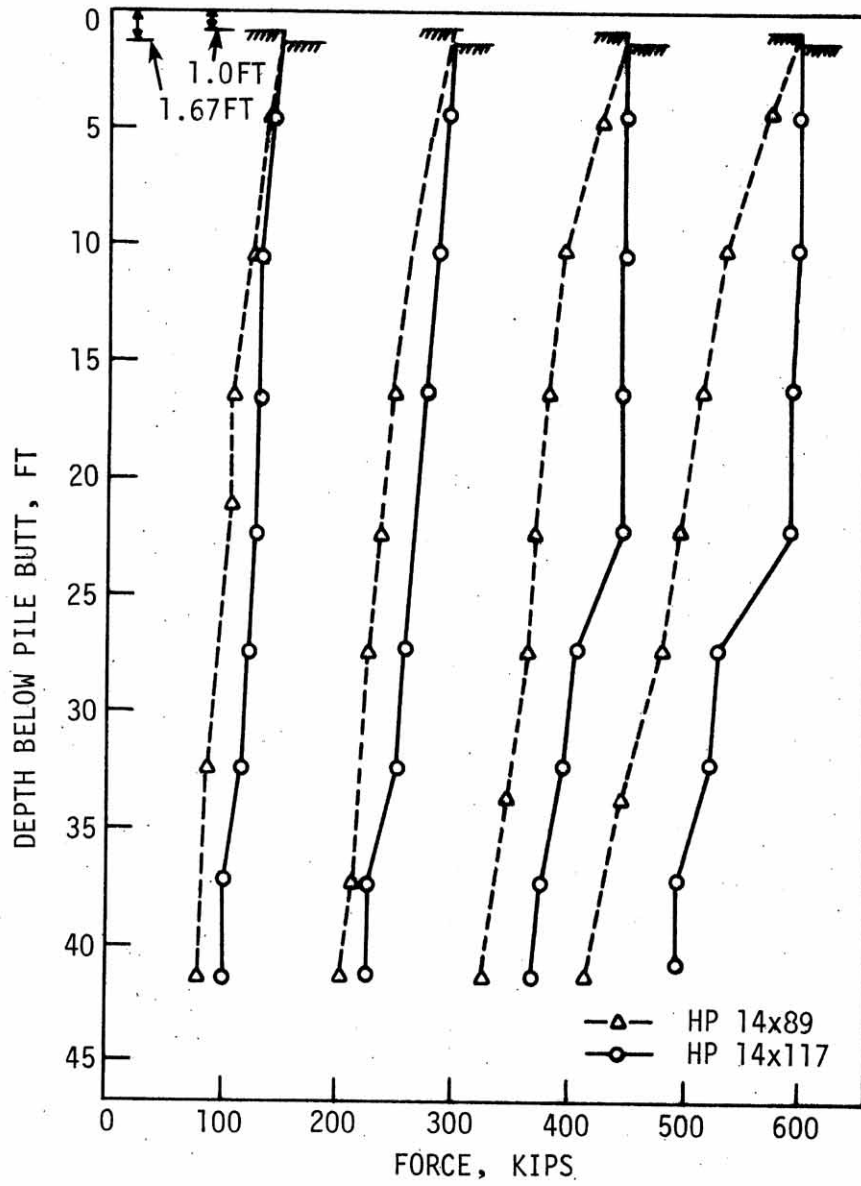


Figure 31. Force in a pile as a function of depth.

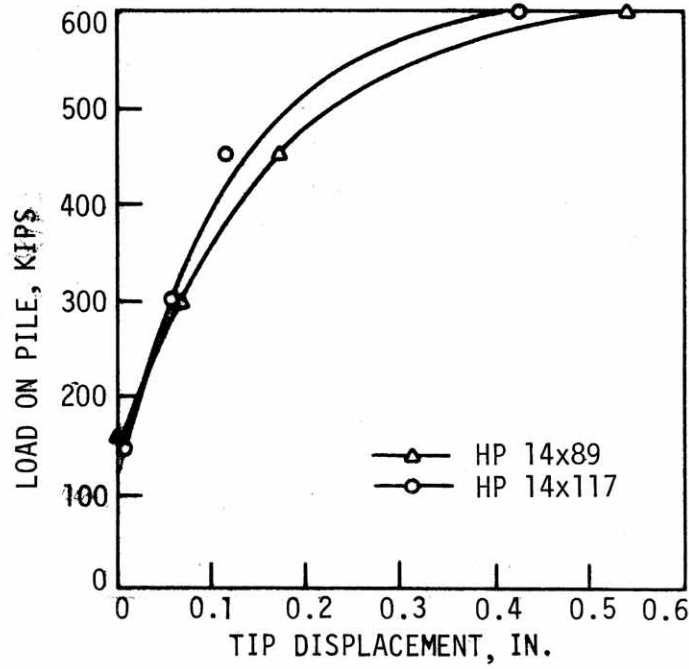


Figure 32. Relationship between tip displacement and load.

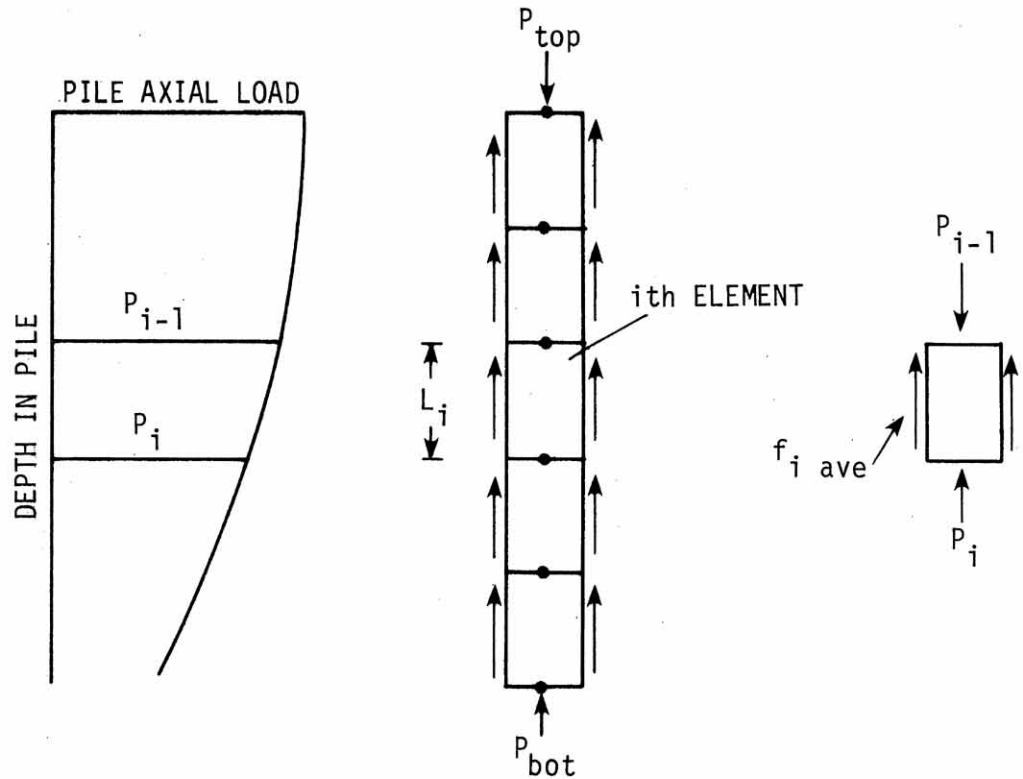


Figure 33. Pile with axial load variation with depth.

E = modulus of elasticity of the pile

A = pile cross section area

P_{i-1} = axial load on the top node of the element i

P_i = axial load on the bottom node of the element i

- (3) Calculate the relative pile displacement at the center of each segment with respect to the soil:

$$z_i = \sum \int_0^{L_i} \epsilon dl + \text{tip displacement} \quad (88)$$

where \sum means the elastic shortening was calculated first at the bottom element and then accumulated to the i th element.

- (4) Find average shear resistance ($f_{i \text{ ave}}$) at each pile segment:

$$f_{i \text{ ave}} = \frac{P_{i-1} - P_i}{C_i L_i} \quad (89)$$

where

C_i = pile perimeter

L_i = pile segment length

- (5) From these $f_{i \text{ ave}}$ and z_i values at pile segment i , plot a set of f - z curves.
- (6) From Fig. 32, the q - z curve can be produced by dividing the load on the tip by an effective tip area to get q :

$$q = \frac{P_{\text{bottom}}}{A_B} \quad (90)$$

where

A_B = effective tip area. For an H pile a rectangular cross section is used.

Since all the pile load tests were held at the same site, the final set of f-z curves was taken as the average of the f-z curves from the HP 14 × 89 and HP 14 × 117. Pile lengths were 44 ft (HP 14 × 89) and 44.5 ft (HP 14 × 117). Soil parameters of the modified Ramberg-Osgood curves are obtained by approximately fitting the irregular shape of the average f-z curves and q-z curves. The load-settlement curves, both observed and predicted values, are plotted in Fig. 34 (HP 14 × 89) and Fig. 35 (HP 14 × 117), respectively. The results calculated from the computer solution (Yang 5) are a fairly good approximation of the results obtained in the experiment.

4.4.4.2. Lateral Load Tests on Drilled Piers in Stiff Clay

Two drilled piers were selected from the laterally loaded pile tests conducted by Bhushan et al. [33]. Measurements of horizontal ground line displacements were made for two piers. Soil properties were determined by drilling two borings at each test site and testing the soil samples in the laboratory. The piers were reinforced with No. 11 reinforcing bars providing about 3% steel area and having a diameter of 4 ft and an embedded length of 15 ft. The soil condition is summarized in Table 8.

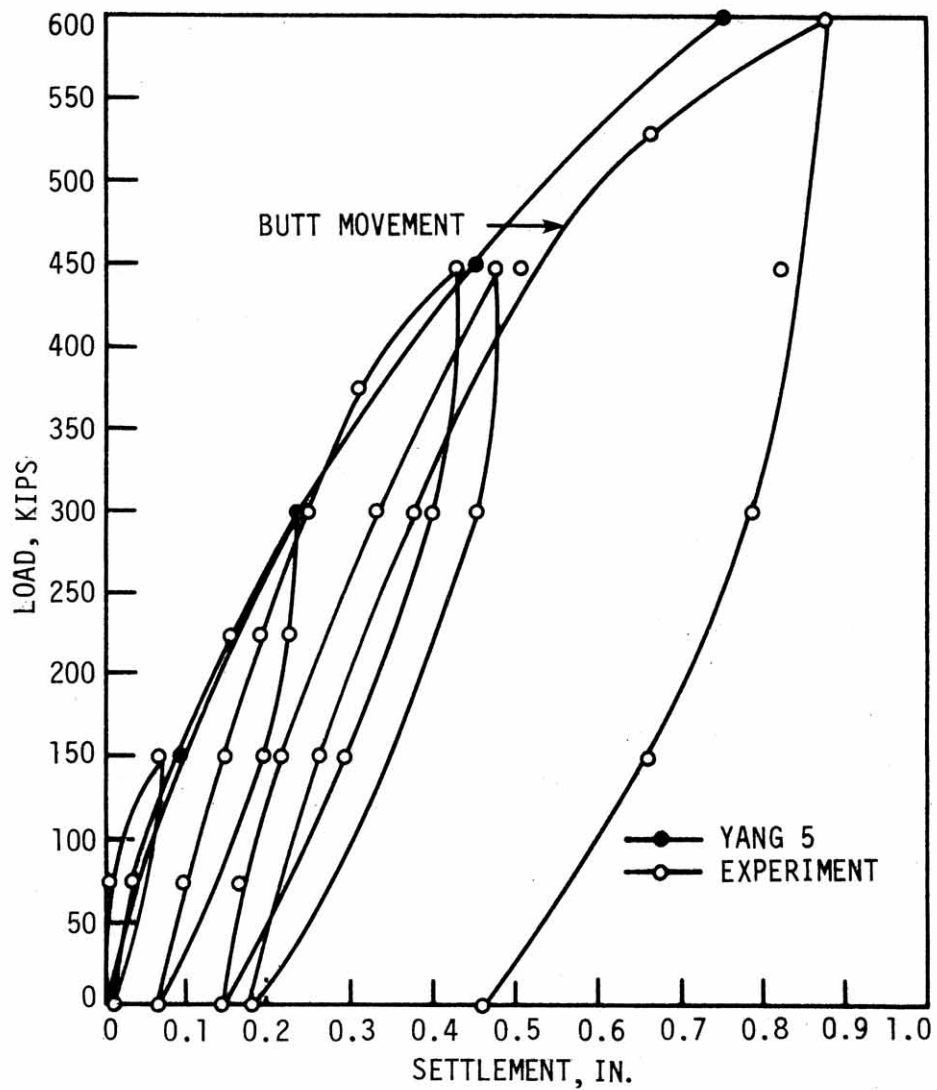


Figure 34. Load settlement curve for HP 14 x 89 test pile.

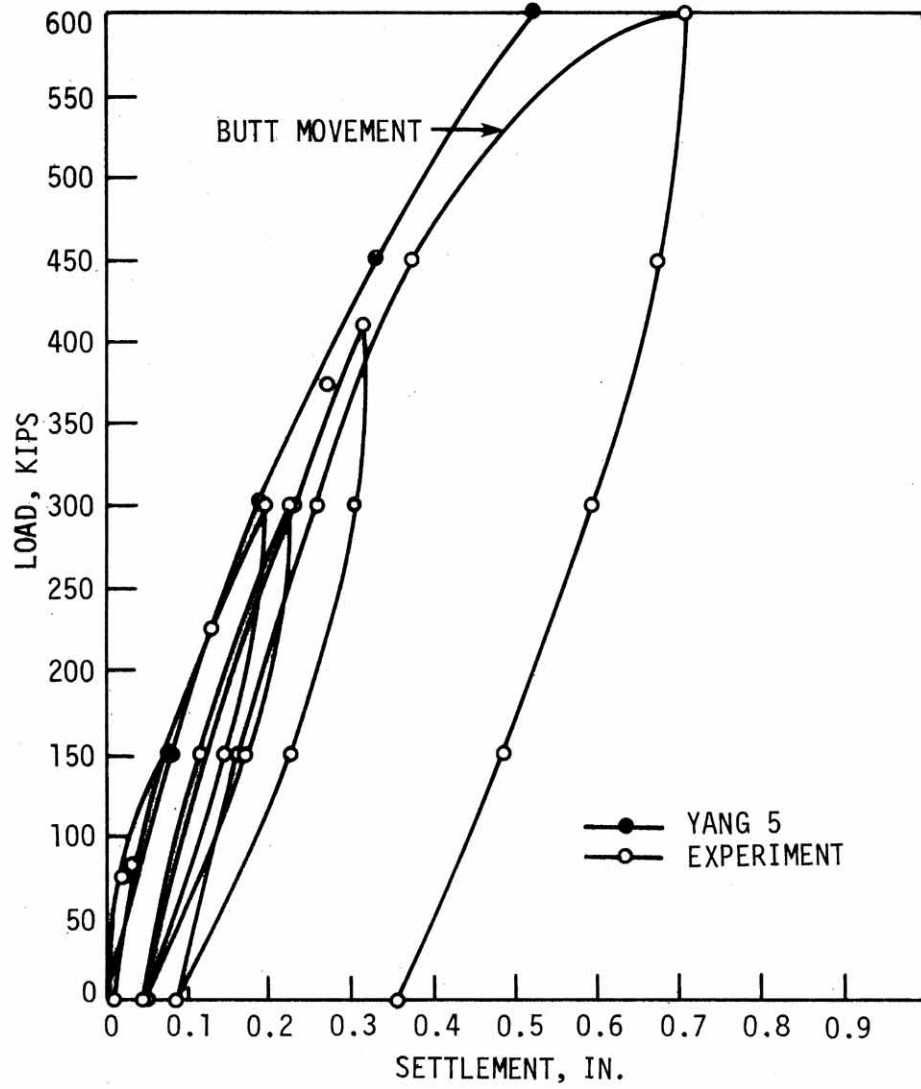


Figure 35. Load settlement curve for HP 14 x 117 test pile.

Table 8. Soil characteristics.

Pier No.	Site No.	Soil Type	Total Unit ₃ Wt. lbs/ft ³	Avg. undrained shear strength lbs/ft ²	ϵ_{50} %	Depth ft
1	A	Sandy Clay (CL - CH)	130	5500	0.96	0 ~ 9
2	B	Sandy Clay (CL)	130	4750	0.72	0 ~ 16

Two two piers (Piers 1 and 2 in Table 8) were constructed with a spacing of about 20 ft and were loaded by jacking between them. A diagram of both test arrangements is shown in Fig. 36. The load was applied to the piers through a circular collar, and the point of application of the load was assumed to be the midheight of the collar, 9 in. above the ground surface. Displacements of the piers were measured by the dial gauges located 1 ft above ground surface. Loads were applied by a 600-kip hydraulic jack in 20-50 kip increments [33].

The soil properties are characterized by lateral soil resistance-displacement (p-y) curves. A set of p-y curves can be generated by using the criteria for constructing the p-y curves in very stiff clay following the procedure outlined in Section 3.2.1. Based on theoretical considerations and parametric study, values of $C_1 = 2.0$, $J = 2.0$ and $n = 0.5$ were selected for computing the p-y curves [33].

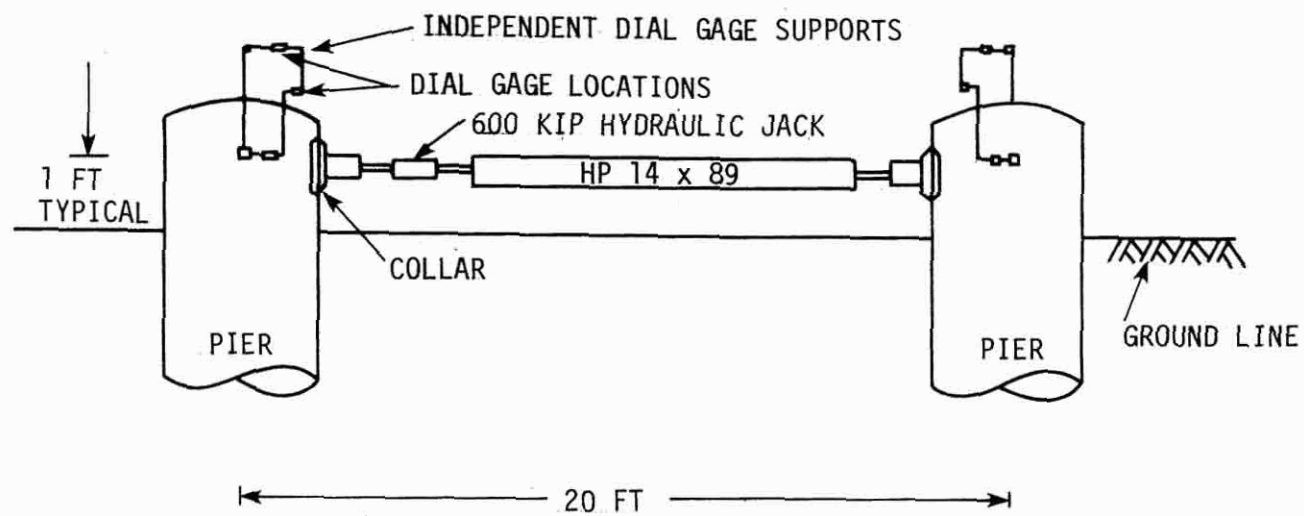


Figure 36. Schematic test setup.

The above results must be approximated by a modified Ramberg-Osgood model. A set of p - y curves was constructed and plotted in non-dimensional form as shown in Fig. 37. From this curve, the initial tangent modulus is infinite, and p is equal to p_u when $y \geq 4y_{50}$. A set of modified Ramberg-Osgood curves is also plotted in Fig. 37 to compare with the Reese p - y curves. Among these modified Ramberg-Osgood curves, the $n = 1$ curve was selected to approximate the Reese p - y curves.

The predicted displacements at the top of the pier are obtained by running the Yang 5 program. The results are plotted in Fig. 38 (Pier No. 1) and Fig. 39 (Pier No. 2). Comparison between the predicted values obtained from Yang 5 and another computer program, COM 622 [65], show that the results are certainly adequate and quite close to the observed values.

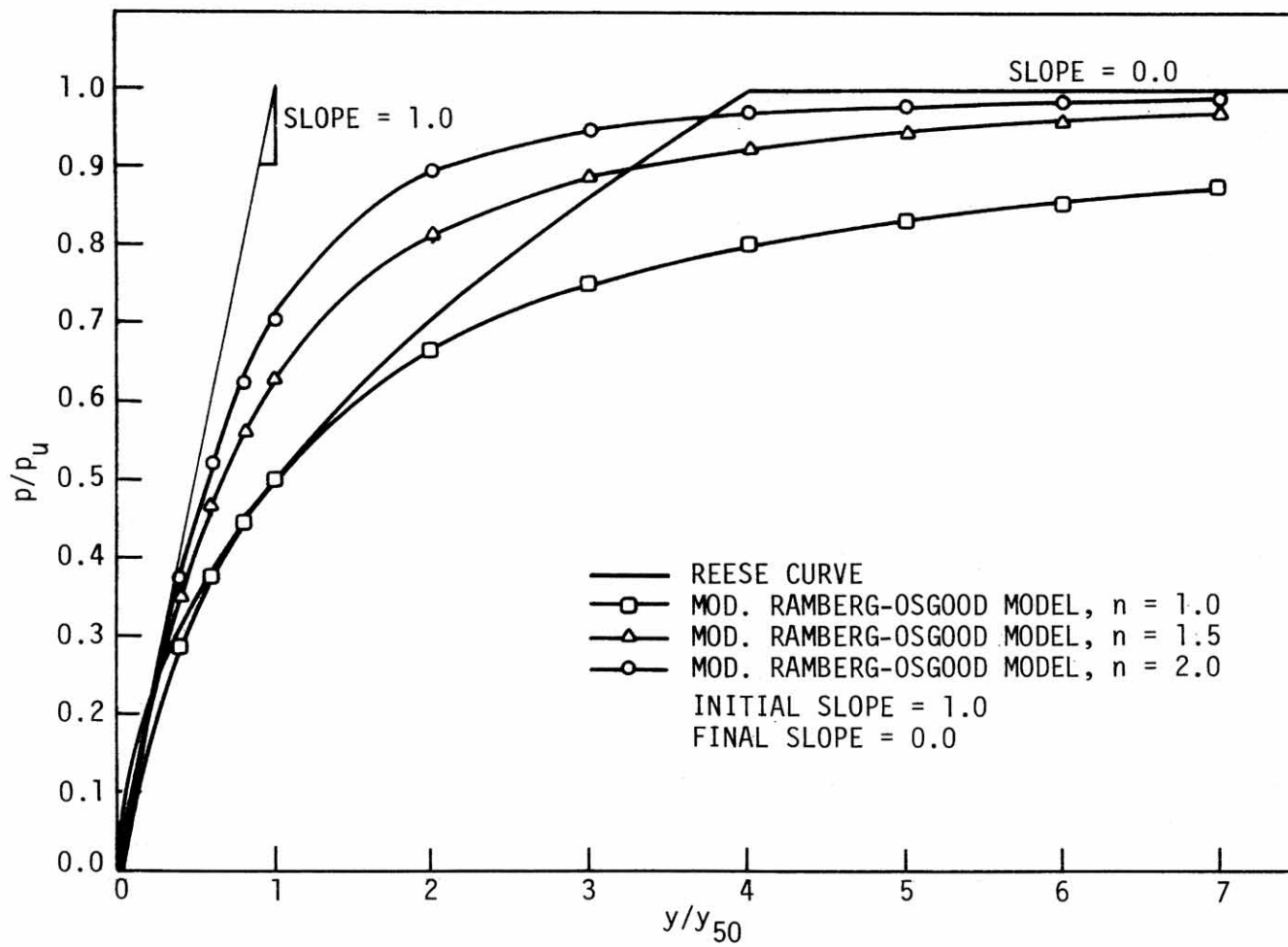


Figure 37. Comparison between the Reese (p-y) curve and modified Ramberg-Osgood model (nondimensional).

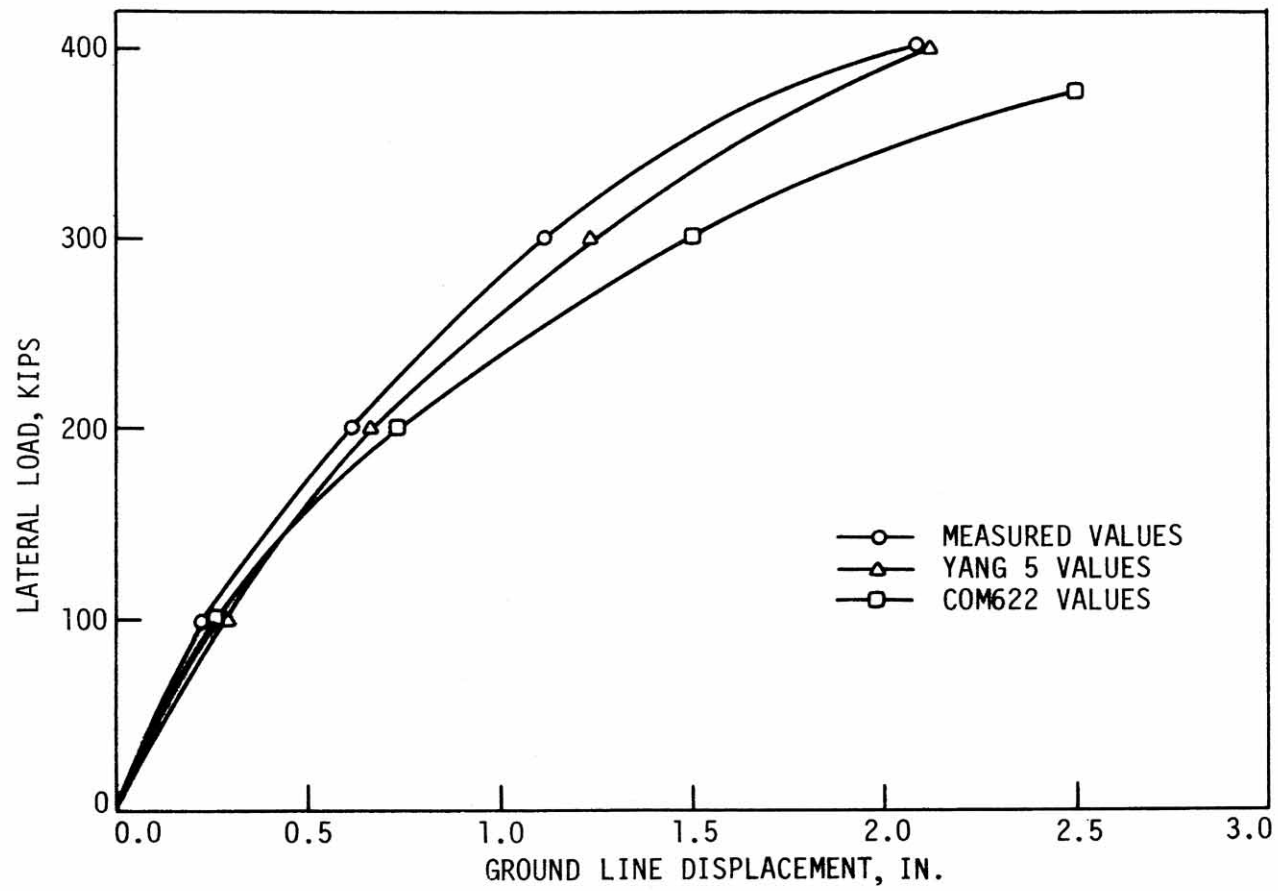


Figure 38. Load-displacement curves, pier 1.

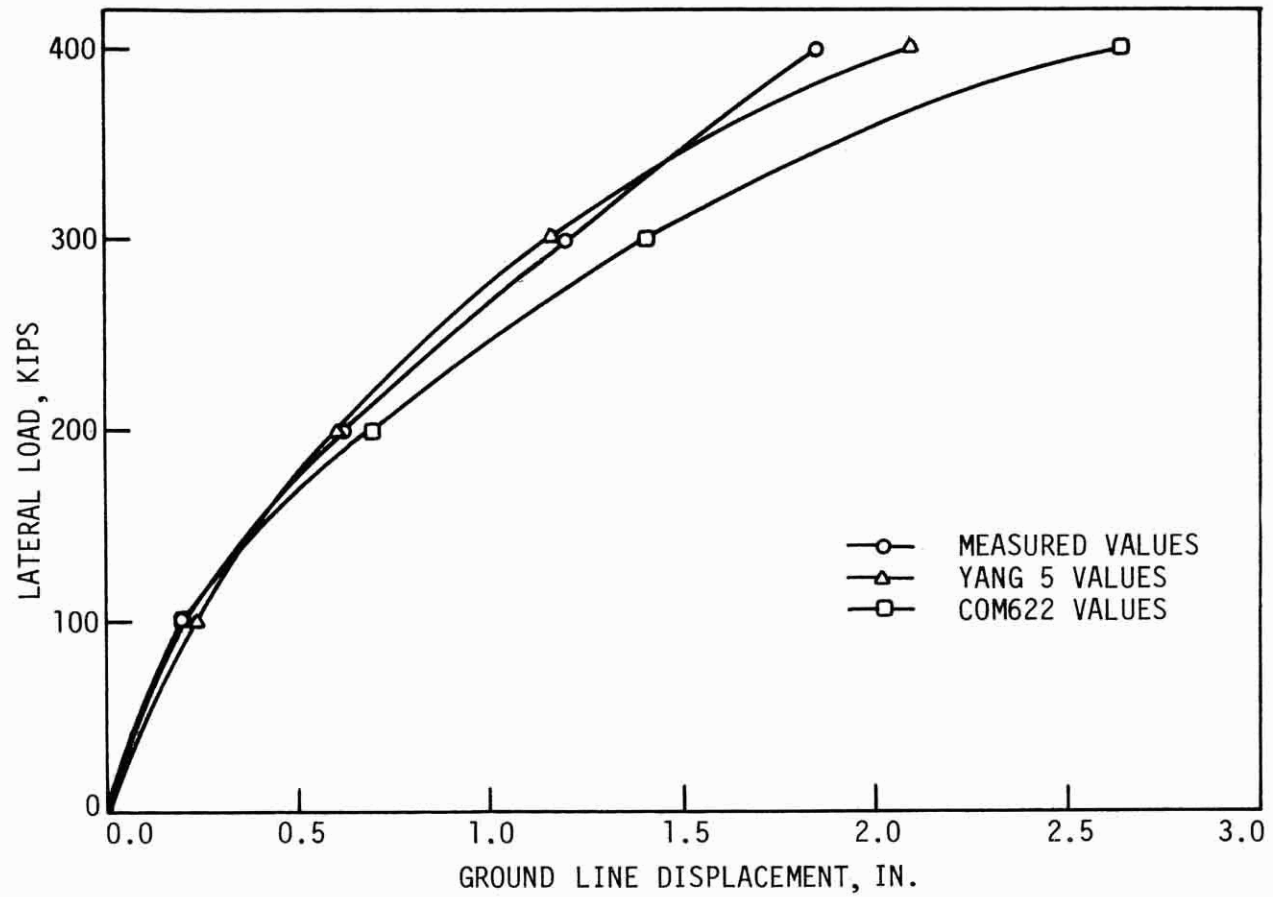


Figure 39. Load-displacement curves, pier 2.

5. NUMERICAL RESULTS

An idealized mathematical model of an integral abutment bridge is shown in Fig. 12. The left part of the model, shown in Fig. 40, with pile embedded in Iowa type soils, will be analyzed in this section.

5.1. Pile Description

Steel H piles are used extensively to carry both live and dead loads either as end-bearing or friction piles in foundations of bridges, piers, buildings, and other major structures. In Iowa, the most common type of H pile used in bridges according to engineers at the Iowa D.O.T. is HP 10 × 42 with an embedded length of about 40 feet. This type of pile will be used to evaluate the ultimate vertical load after lateral pile displacement has occurred.

5.2. Soil Description

Soil properties should be investigated first by test boring at the bridge site, by measuring penetration resistance, and by laboratory testing on intact samples. If a complete investigation of the soil properties is not feasible, empirical relationships may be useful. These empirical data which are obtained by numerous test results and long-term observations are expected to provide reasonable and conservative values.

In consultation with Iowa Department of Transportation engineers, several typical Iowa soils were selected by studying the information in

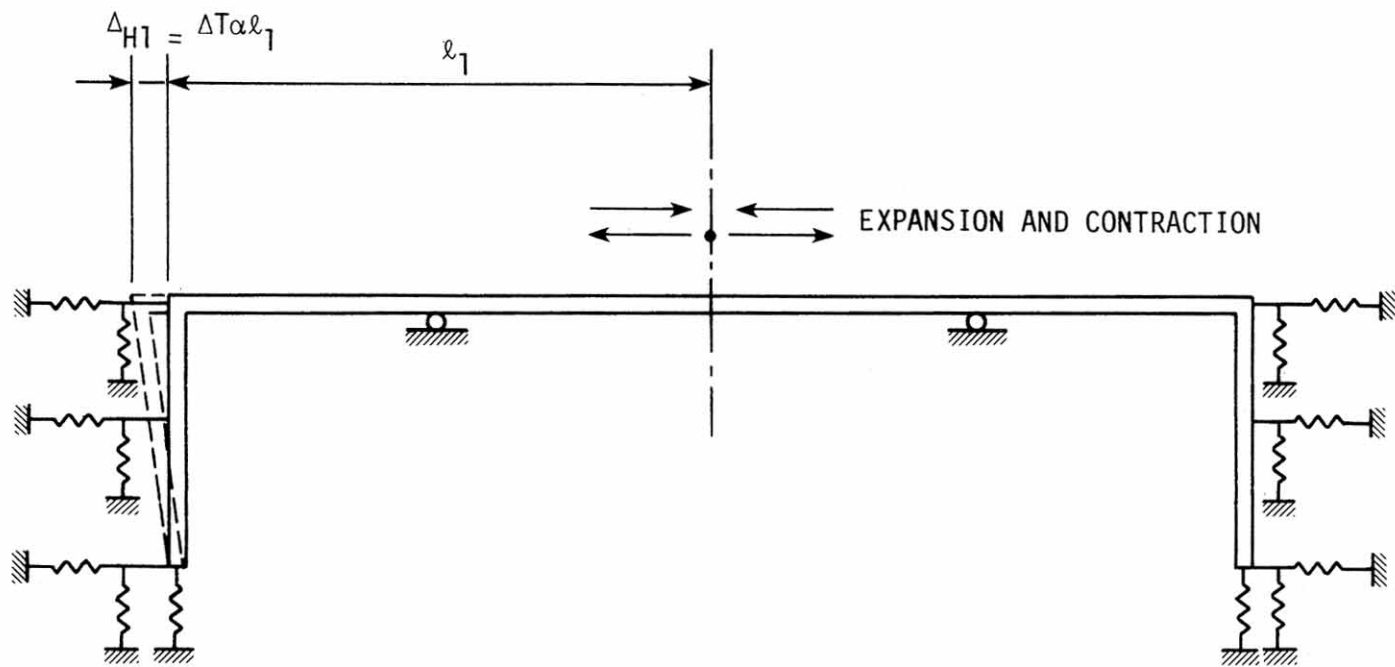


Figure 40. Mathematical model of an integral abutment bridge.

Appendix 9.3 and Tables 9 and 10 [65]. These typical Iowa soils and their significant strength characteristics are shown in Table 11.

For each type of soil, p-y, f-z and q-z curves will be generated by following the procedures listed in Section 3.2. Examples of p-y, f-z and q-z curves corresponding to Iowa soils are given in Tables 12 and 13 for clay soil and sand respectively (refer to Section 3.2 for notations).

For the present work, since the Reese p-y, f-z, and q-z curves have infinite initial tangent modulus and zero final tangent modulus, a modified Ramberg-Osgood equation is used to model the soil resistance-displacement curves. A correspondence should be made between the Reese p-y, f-z, and q-z curves which were obtained above and a set of modified Ramberg-Osgood models. Nondimensional curves of the Reese equations and the modified Ramberg-Osgood equations are presented in Figs. 41-46. For example, the nondimensional Reese curve in Fig. 41 has infinite initial tangent modulus and zero final tangent modulus with ultimate soil resistance equal to f_{\max} . Knowing the above three parameters, a set of modified Ramberg-Osgood models has been plotted with different initial slopes. Decisions could be made immediately to pick up a modified Ramberg-Osgood model with slope = 10 and $n = 1.0$ which fits the Reese curve closely. The soil parameters are represented by nondimensional modified Ramberg-Osgood models in different types of soils, for clays and sands, and are given in Table 14.

Table 9. Cohesionless soils - typical values.

Sands and Gravels	Natural Unit Weight, γ , lb/ft ³	Submerged Unit Weight, γ' , lb/ft ³	Angle of friction, ϕ
Loose	90 ~ 125	55 ~ 65	30°
Medium	110 ~ 130	60 ~ 70	35°
Dense	110 ~ 140	65 ~ 80	40°

Table 10. Cohesive soils - typical values.

Clay	Cohesion, c_u , lb/ft ²	Natural Unit Weight, γ , lb/ft ³	Submerged Unit Weight, γ' , lb/ft ³
Very stiff	Over 3000	120 ~ 140	60 ~ 80
Stiff	1500 ~ 3000	115 ~ 135	55 ~ 75
Firm	750 ~ 1500	105 ~ 125	45 ~ 65
Soft	375 ~ 750	90 ~ 110	30 ~ 50
Very soft	Under 375	90 ~ 100	30 ~ 40

Table 11. Typical Iowa soils.

Soil Type	Mean Values of Blow Count, N	Natural Unit Weight, γ , lb/ft ³	Undrained Cohesion, Cu, lb/ft ²	Angle of Friction, ϕ
Soft clay	3	100	405	--
Stiff clay	15	120	1569	--
Very stiff clay	50	130	5000	--
Loose sand	5	110	--	30°
Medium sand	15	120	--	35°
Dense sand	30	130	--	40°

Table 12. f-z, q-z and p-y curves for clays.

Soil Type	Soft Clay	Stiff Clay	Very Stiff Clay
Reduction factor, α	1.0	0.5	0.5
$f_{\max} = \alpha C_u$ ksf	0.405	0.785	0.25
Mean value of z_c , ft	0.021	0.021	0.021
q_{\max} , ksf	3.645	3.645	3.645
ϵ_{50}	0.02	0.01	0.005
C_1	2.5	2.5	2.0
b, ft	0.81	0.81	0.81
$y_{50} = C_1 b \epsilon_{50}$, ft	0.0405	0.0203	0.0081
p_u at $x = 0 \sim 2$ ft	1.5512	5.5761	32.3606
p_u at $x = 2 \sim 4$ ft	2.1182	7.3355	36.45
p_u at $x = 4 \sim 6$ ft	2.6852	9.1029	36.45
p_u at $x = 6 \sim 8$ ft	2.9525	10.8663	36.45
p_u at $x = 8 \sim 40$ ft	2.9525	11.4380	36.45

Table 13. f - z , q - z and p - y curves for sand.

Soil Type	Loose Sand	Medium Sand	Dense Sand
$f_{\max} = 0.04N$, ksf	0.20	0.60	1.20
Mean value of z_c , ft	0.033	0.033	0.033
q_{\max} , ksf	40.0	120.0	180.0
J	200	600	1500
$k_p = \tan^2(45^\circ + \phi/2)$	3.0	3.69	4.60
$k_a = \tan^2(45^\circ - \phi/2)$	0.33	0.27	0.22
$k_o = 1 - \sin\phi$	0.5	0.43	0.36
α	10°	17.5°	20°
β	60°	62.5°	65°
p_u at $x = 0 \sim 2$ ft	1.032	1.891	2.980
p_u at $x = 2 \sim 4$ ft	3.175	6.231	10.076

(Note: p_u will be different at different depths. Only two values of p_u are presented here.)

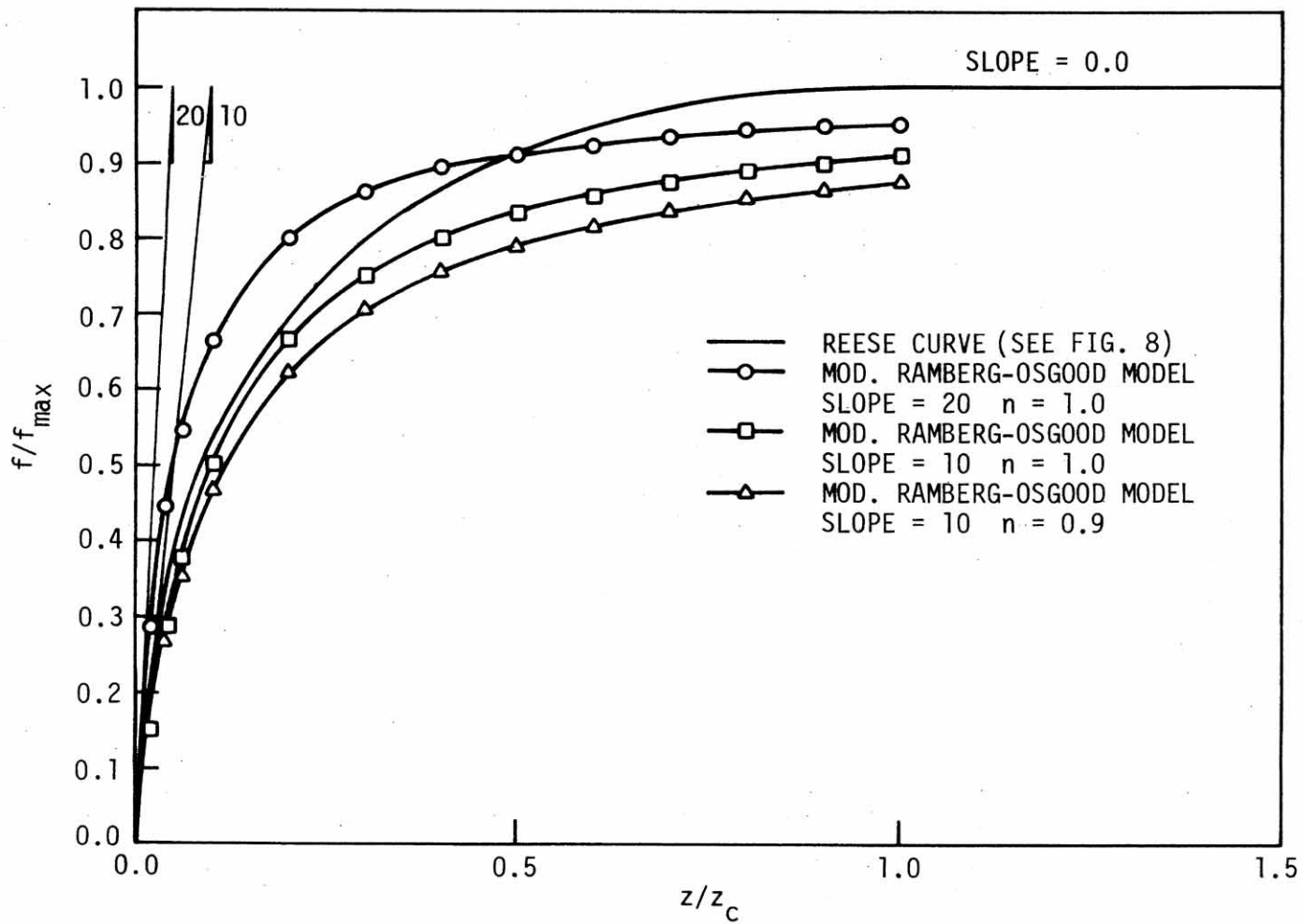


Figure 41. Comparison between the Reese ($f-z$) curve and modified Ramberg-Osgood model (nondimensional).

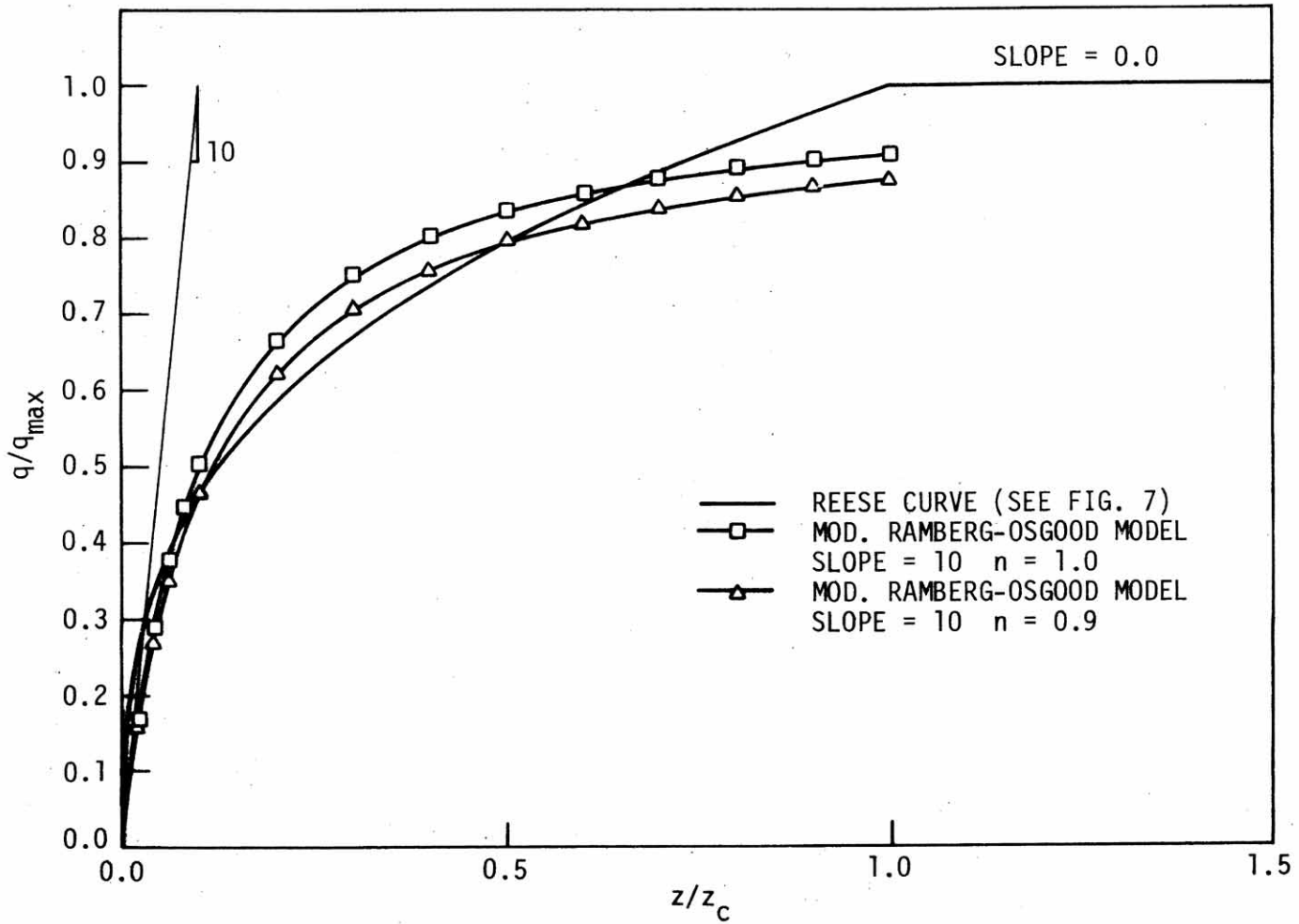


Figure 42. Comparison between the Reese ($q-z$) curve and modified Ramberg-Osgood model (nondimensional).

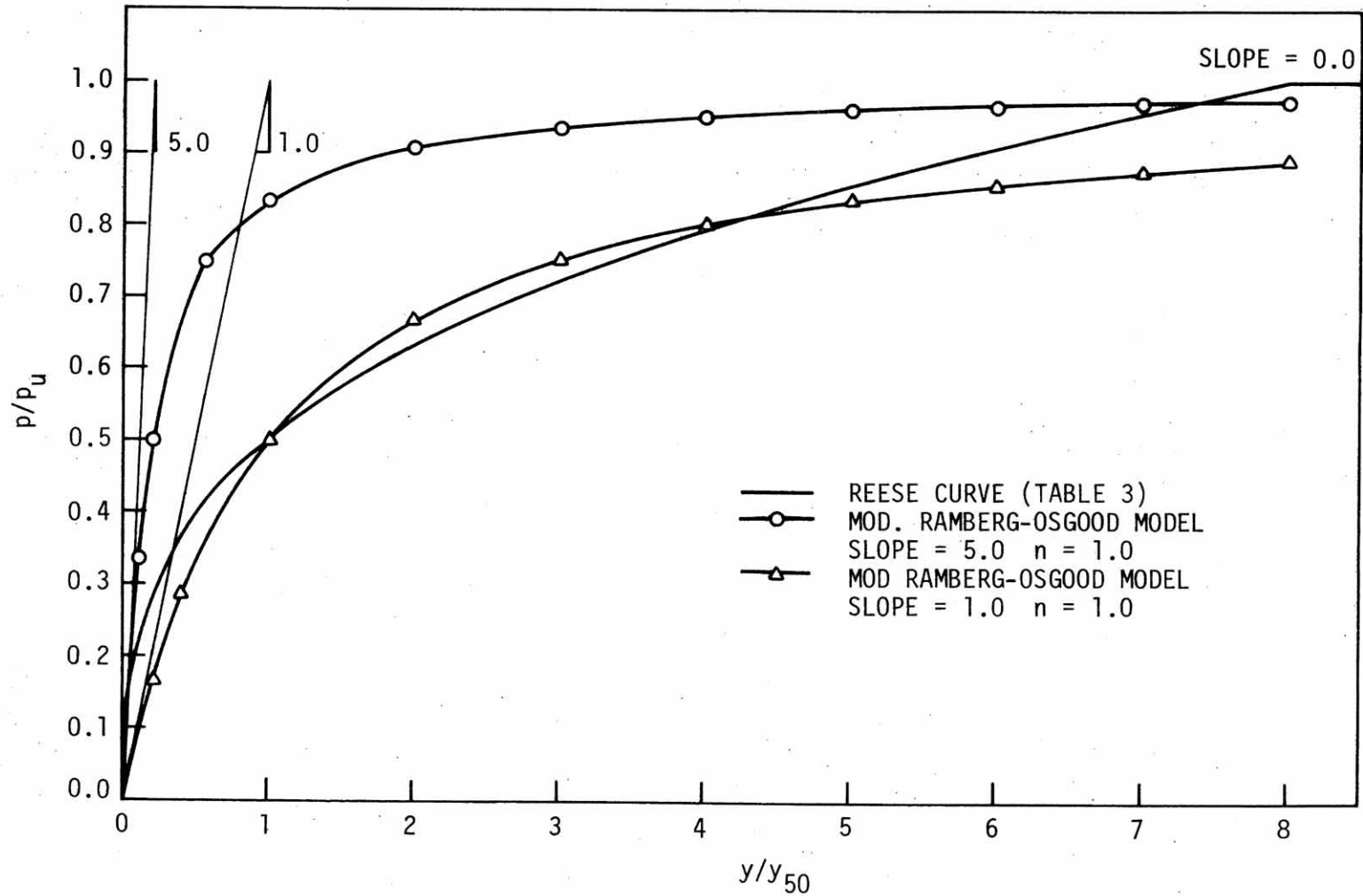


Figure 43. Comparison between the Reese (p - y) curve and modified Ramberg-Osgood Model (nondimensional, soft clay).

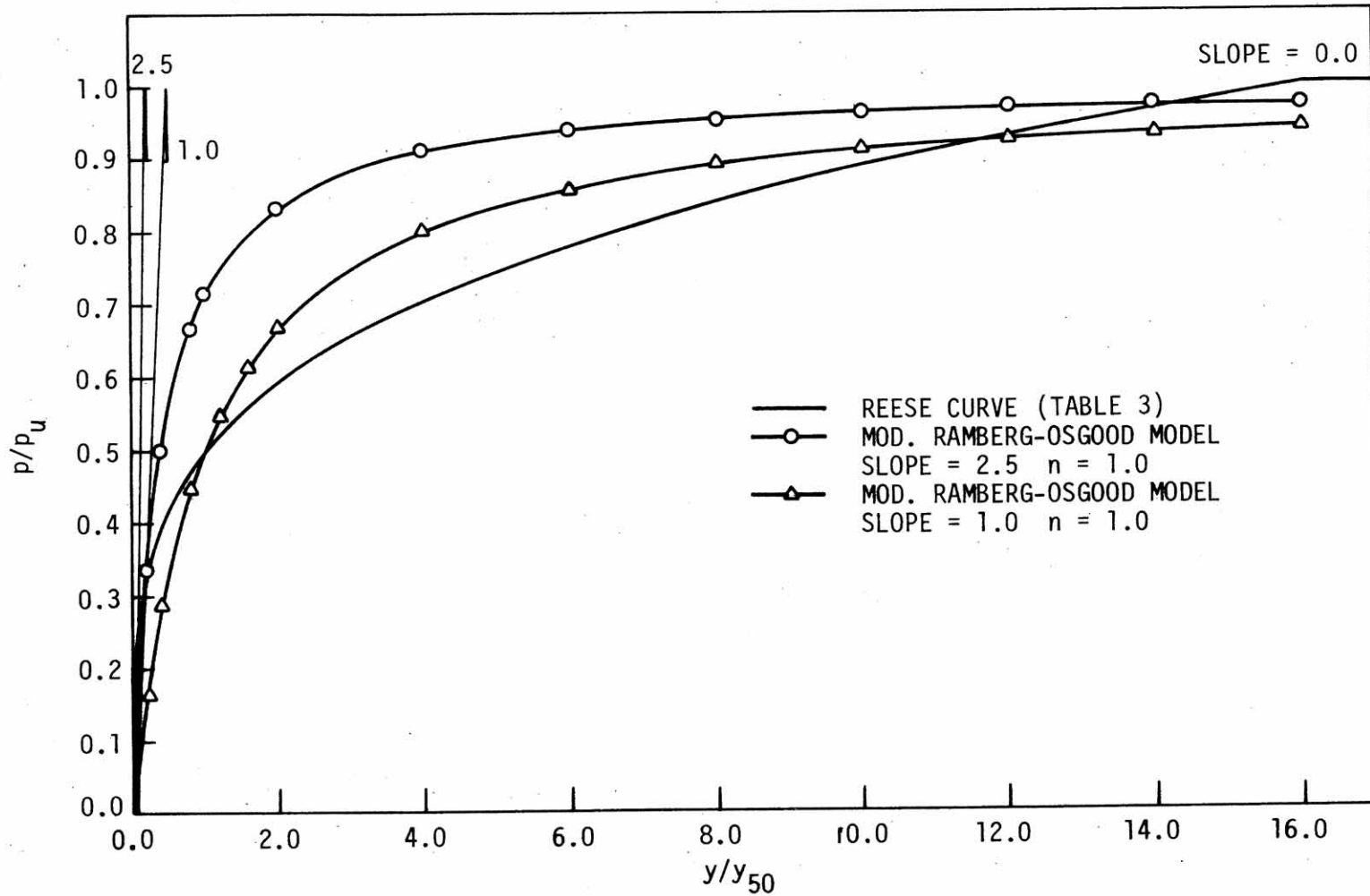


Figure 44. Comparison between the Reese (p-y) curve and modified Ramberg-Osgood model (nondimensional, stiff clay).

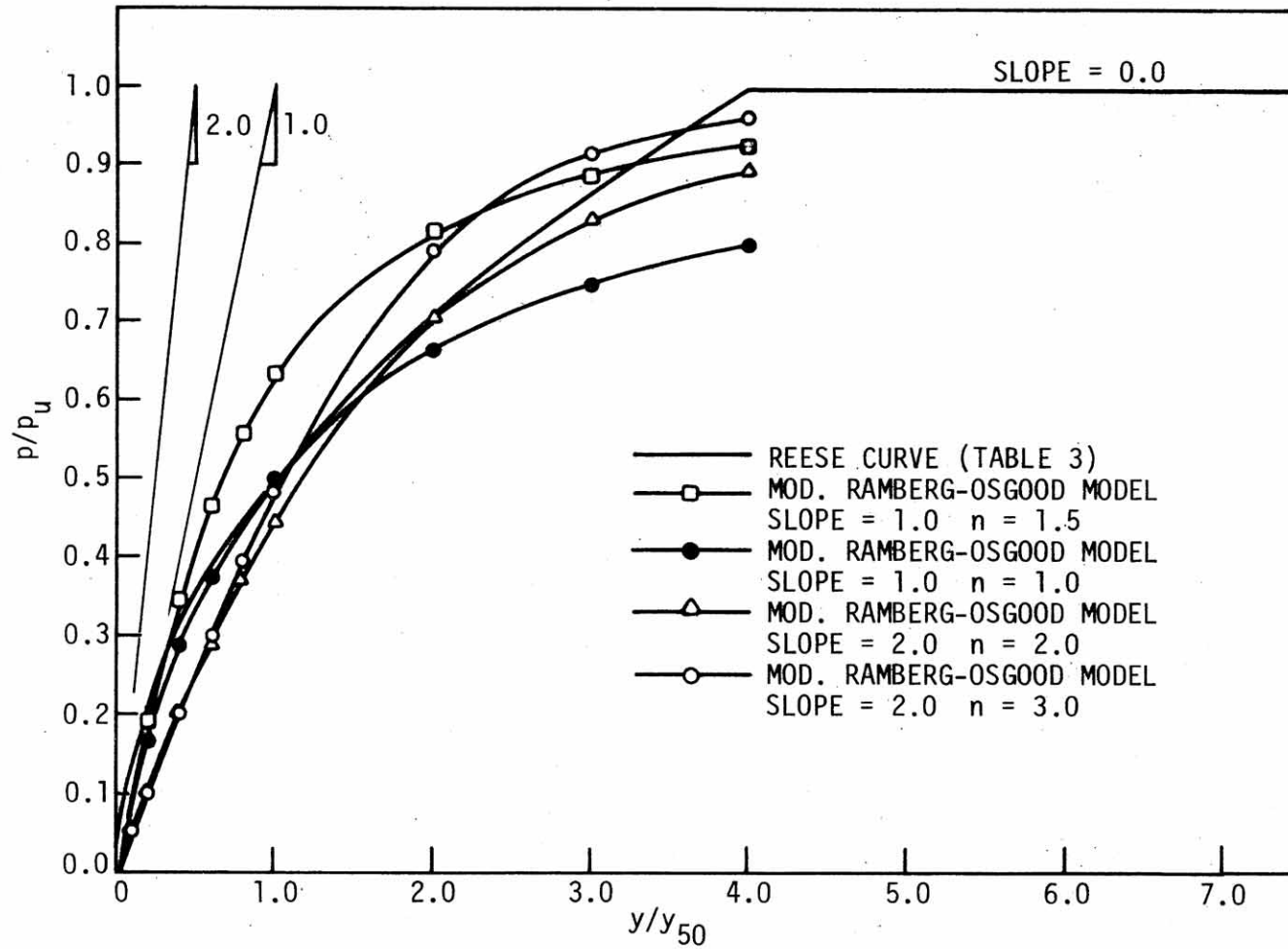


Figure 45. Comparison between the Reese (p-y) curve and modified Ramberg-Osgood model (nondimensional, very stiff clay).

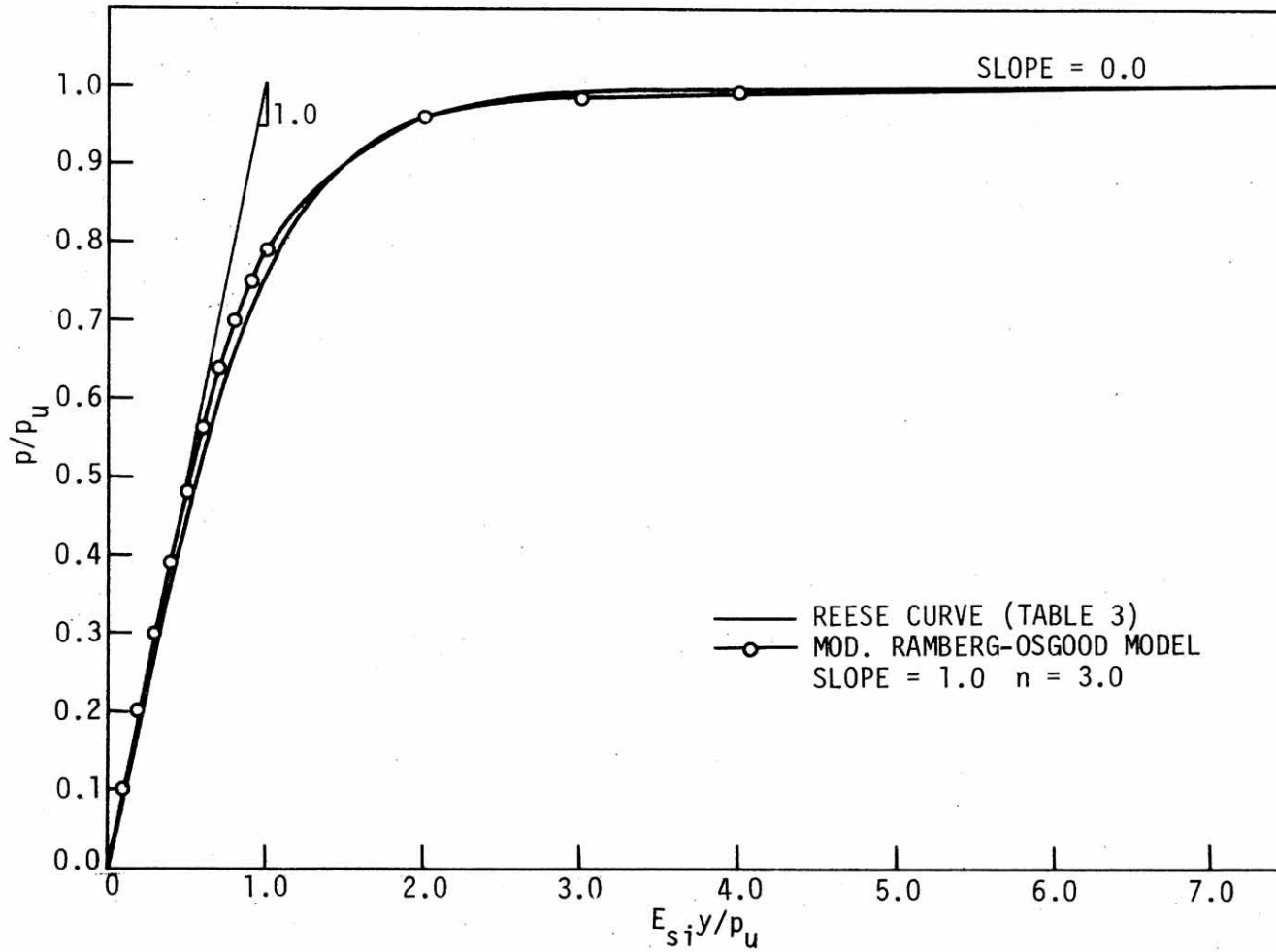


Figure 46. Comparison between Reese (p-y) curve and modified Ramberg-Osgood model (nondimensional, sand).

Table 14. Soil parameters in Iowa soils.

Model	Parameters	Soft Clay	Stiff Clay	Very stiff Clay	Loose Sand	Medium Sand	Dense Sand
f-z	f_{max} , ksf	0.405	0.785	2.5	0.2	0.6	1.20
	E_{si} , kcf	192.86	373.81	1190.48	60.61	181.82	363.64
	E_{sf} , kcf	0.0	0.0	0.0	0.0	0.0	0.0
	n	1.0	1.0	1.0	1.0	1.0	1.0
q-z	q_{max} , ksf	3.645	14.121	45.0	40.0	120.0	180.0
	E_{si} , kcf	1736	6767	21429	12121.21	36363.64	54545.45
	E_{sf} , kcf	0.0	0.0	0.0	0.0	0.0	0.0
	n	1.0	1.0	1.0	1.0	1.0	1.0
p-y x = 0 ~ 2 ft	p_u , kpf	1.5512	5.5761	32.3606	1.032	1.891	2.980
	E_{si} , ksf	38.30	274.68	1997.57	32.593	106.667	288.889
	E_{sf} , ksf	0.0	0.0	0.0	0.0	0.0	0.0
	n	1.0	1.0	2.0	3.0	3.0	3.0
p-y x = 2 ~ 4 ft	p_u , kpf	2.1182	7.3395	36.45	3.175	6.231	10.076
	E_{si} , ksf	52.30	361.55	2250	65.185	213.333	577.778
	E_{sf} , ksf	0.0	0.0	0.0	0.0	0.0	0.0
	n	1.0	1.0	2.0	3.0	3.0	3.0

5.3. Loading Pattern

The bridge with integral abutment is subjected to dead and live loads during and after thermal expansion or contraction. The worst situation is assumed to occur after thermal expansion or contraction has occurred and the bridge is subsequently loaded to its maximum vertical load. A typical pile in an integral abutment bridge will be analyzed by first applying a horizontal displacement Δ_H (to simulate the induced thermal expansion or contraction) and no rotation (since the bridge is much stiffer than the pile) at the top and then applying a vertical load V (to simulate the bridge load) until failure occurs (see Fig. 47). In this manner, the effect of the horizontal pile top displacement on the pile capacity can be observed. In the Yang 5 program, the total ΔH is applied in increments of 0.25 in. while V is held equal to zero. Once the total Δ_H is achieved (0, 1, 2, or 4 in.), V is increased in increments of 5^K until the vertical load capacity of the pile is reached.

The heat transfer analysis is similar for both concrete and steel bridges. Steel bridges have higher temperature changes for a number of reasons, including the thermal mass of concrete reducing fluctuations and the darker color and steel absorbing more heat than concrete does.

5.4. Results

Results obtained by running the Yang 5 program will be presented here to show the behavior of steel pile embedded in Iowa soils. A set of vertical load-settlement curves with specified lateral displacements,

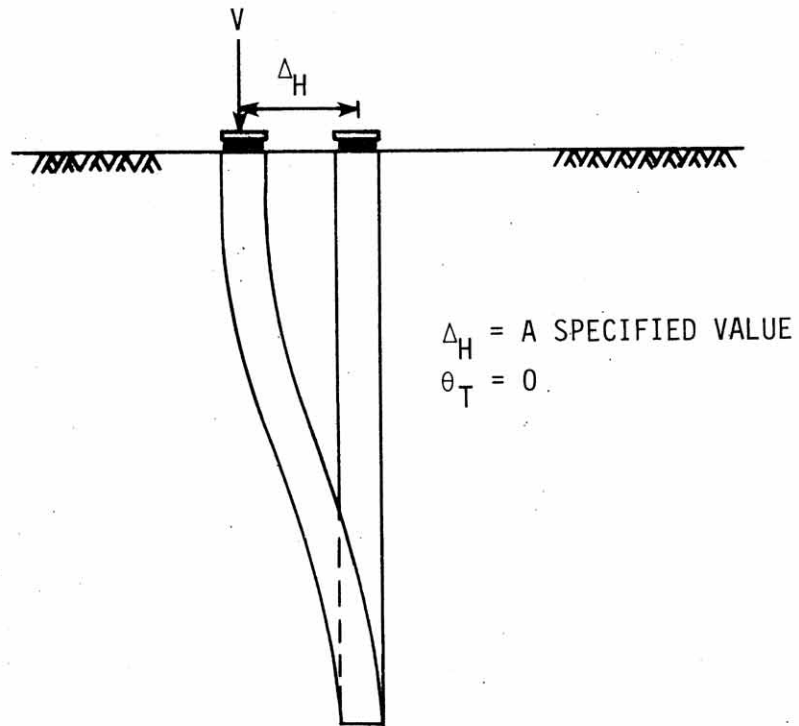


Figure 47. Loading pattern on a single vertical H pile.

Δ_H (0, 1, 2, 4 in., see Fig. 47), are shown in Figs. 48-53 in which the total load is plotted as a function of the settlement of the pile head. In these figures, the vertical load-settlement curve for Δ_H (1, 2, or 4 in.) has been shifted to the origin in an amount Δ_{VH} , a second order vertical displacement, which is caused by the specified lateral displacement Δ_H before loading. The determination of the ultimate pile load is, to some degree, a matter of interpretation. In many of the pile load tests conducted by the Iowa Department of Transportation the ultimate pile load was taken as a vertical settlement of 0.2 inches [16]. This seems to be a reasonable approach based on many pile load tests. Another reasonable procedure [66] that takes account of the significant variables is illustrated in Fig. 54 for typical load-settlement curves. Curve (a) represents a pile that slipped or plunged suddenly when the load reached a definite value termed the ultimate pile load or pile capacity. Curves (b) and (c), on the other hand, show no well-defined breaks. The procedure which determines the ultimate pile load for curves (b) and (c) is illustrated in the figure. The elastic shortening of the pile is computed by means of the expression VL/EA and plotted on the load-settlement diagram as line OO' . The line CC' is drawn parallel to line OO' with an intercept on the settlement axis equal to $(0.0125 + 0.0083b)$ ft., where b is diameter of the pile in feet. The intercept is a measure of the tip settlement required to develop the capacity. The ultimate load is defined as the load at which the line CC' intersects the load settlement curve. Based on the above procedure, the ultimate pile load V_{ult} was obtained from each of the previous curves for the various specified lateral displacements (bridge

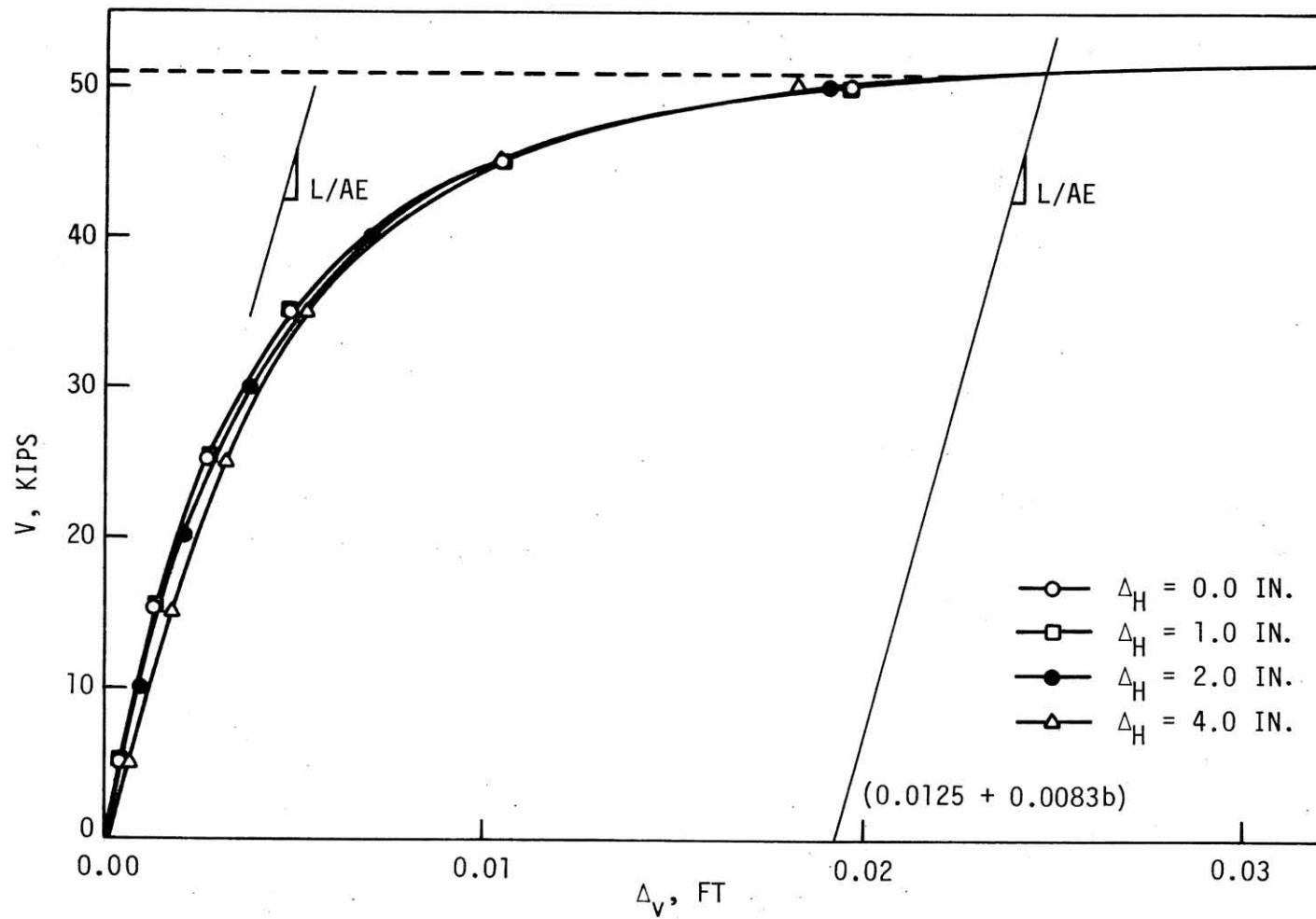


Figure 48. Vertical load-settlement curves with specified lateral displacements, Δ_H (0, 1, 2, 3, 4 in.) for soft clay.

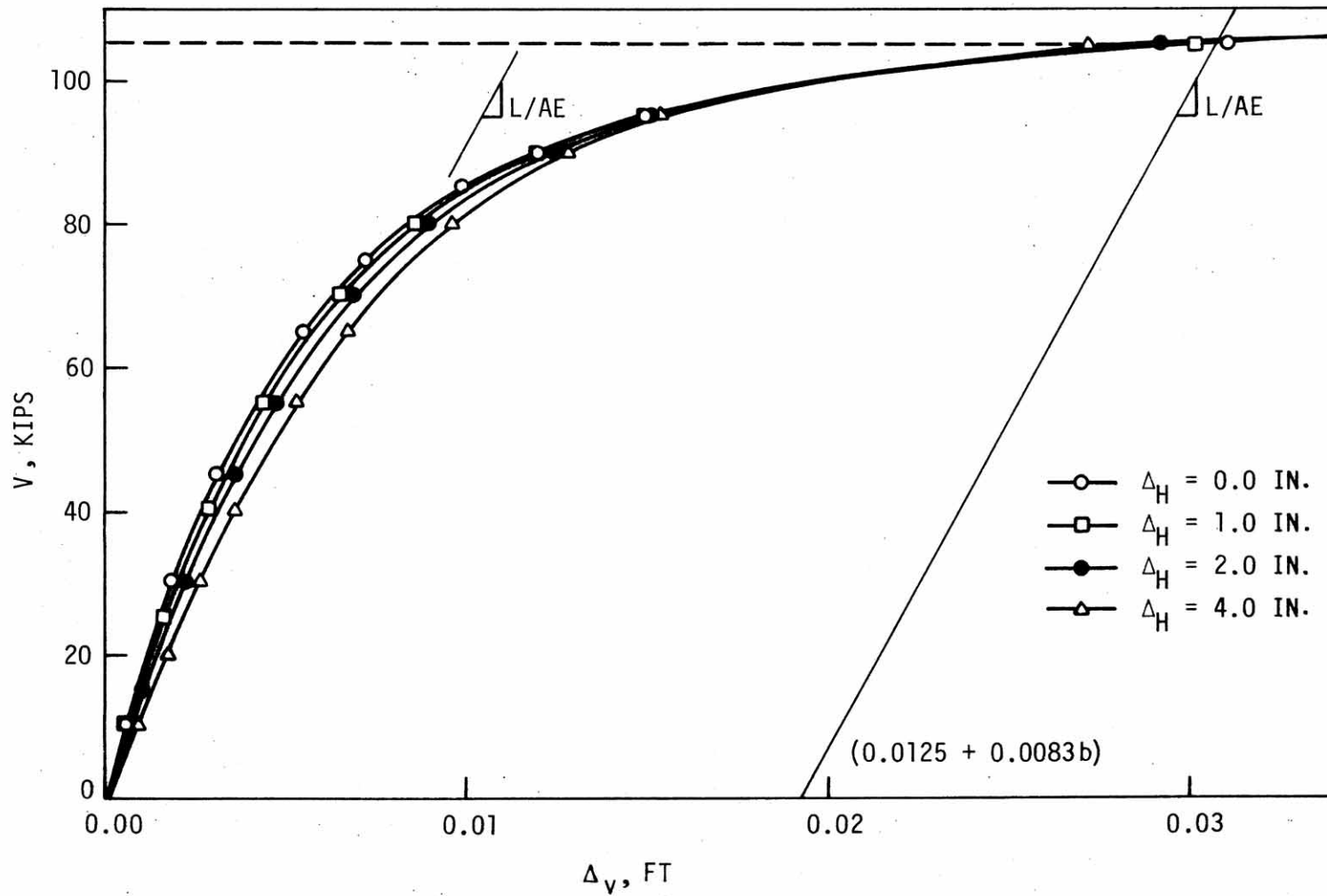


Figure 49. Vertical load-settlement curves with specified lateral displacements, Δ_H (0, 1, 2, 4 in.) for stiff clay.

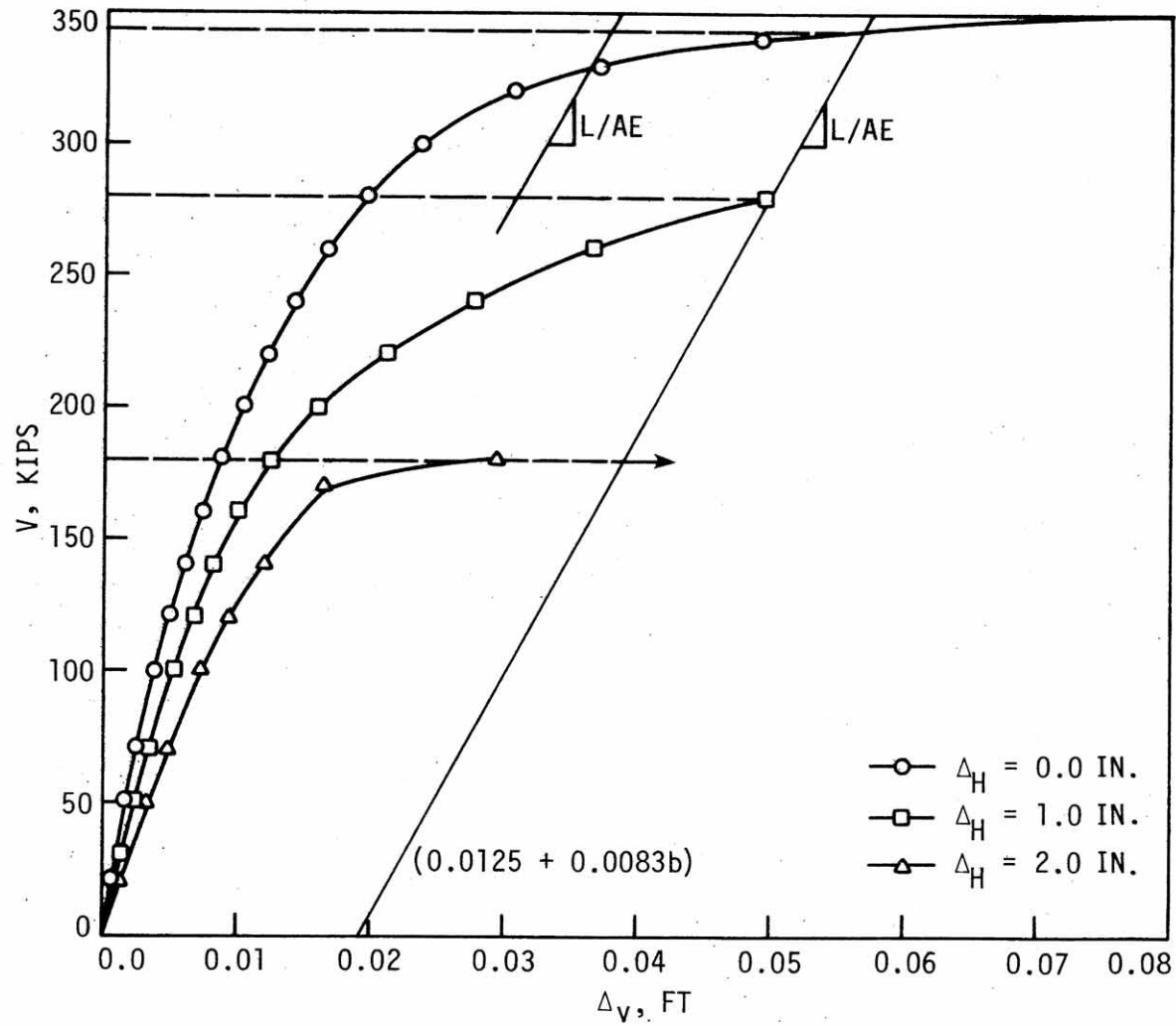


Figure 50. Vertical load-settlement curves with specified lateral displacements, Δ_H (0, 1, 2 in.) for very stiff clay.

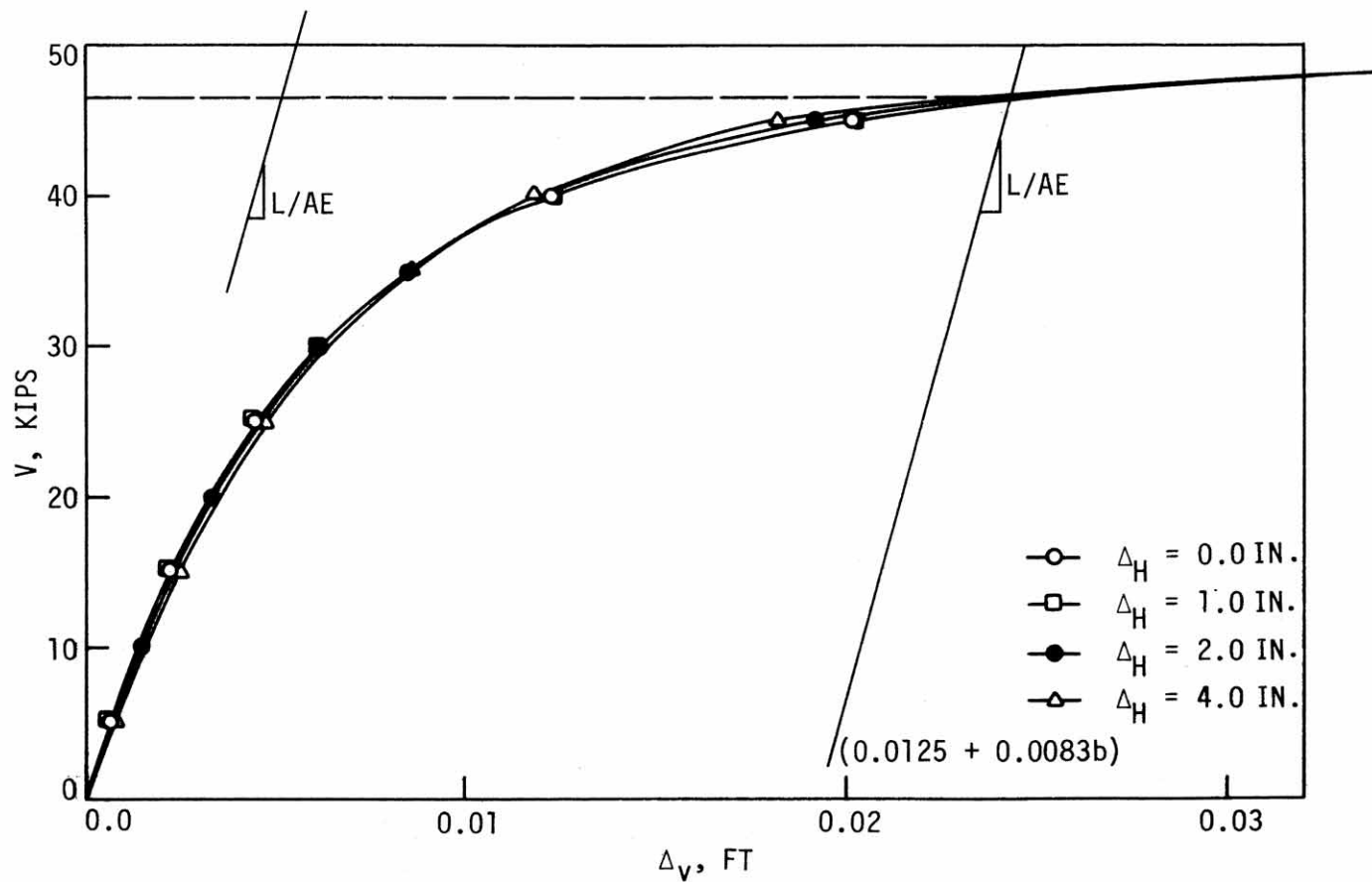


Figure 51. Vertical load-settlement curves with specified lateral displacements, Δ_H (0, 1, 2, 4 in.) for loose sand.

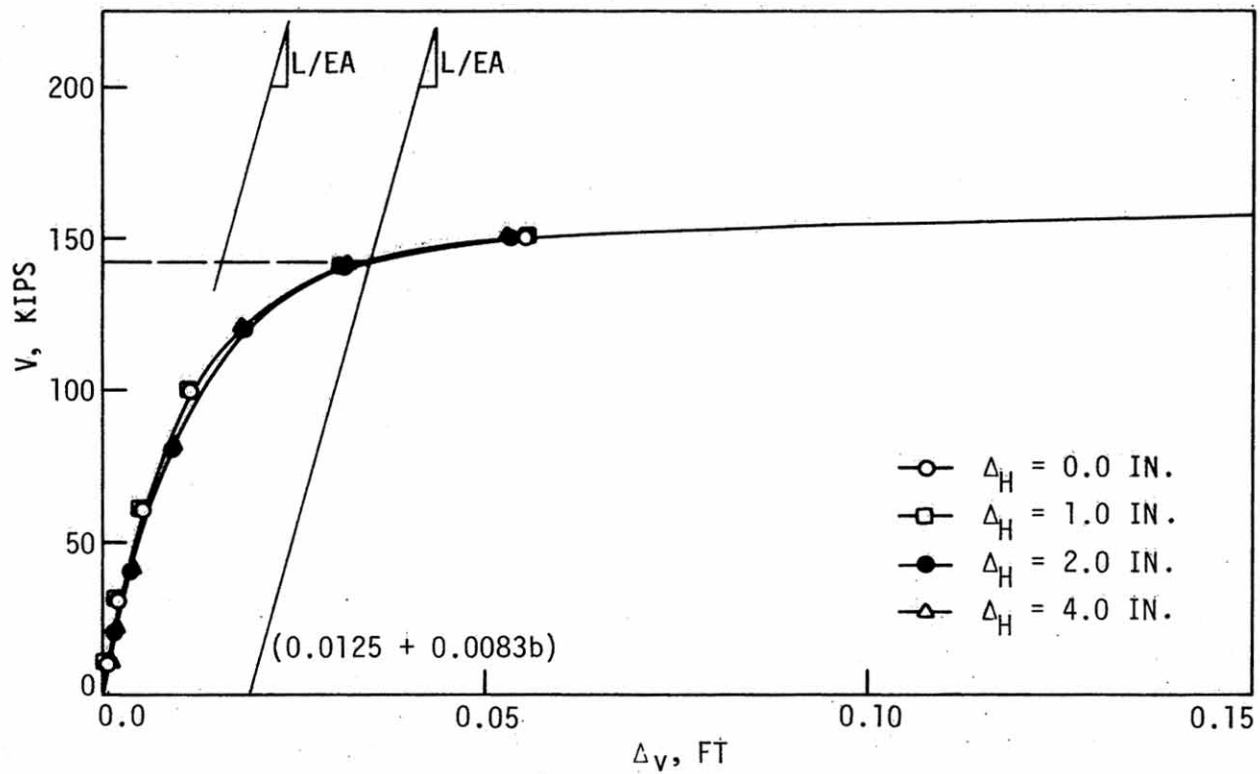


Figure 52. Vertical load-settlement curves with specified displacements, Δ_H (0, 1, 2, 4 in.) for medium sand.

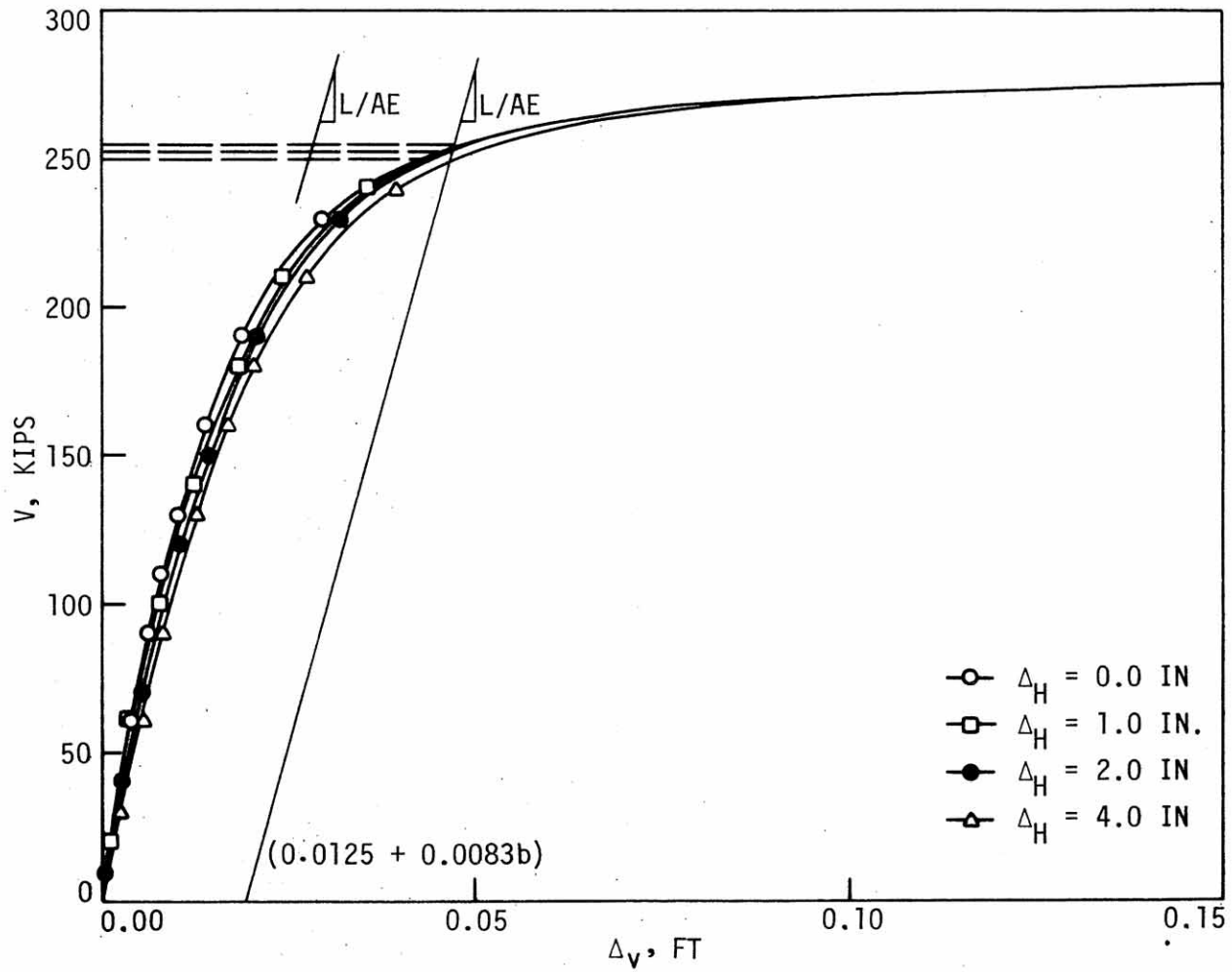


Figure 53. Vertical load-settlement curves with specified lateral displacements, Δ_H (0, 1, 2, 4 in.) for dense sand.

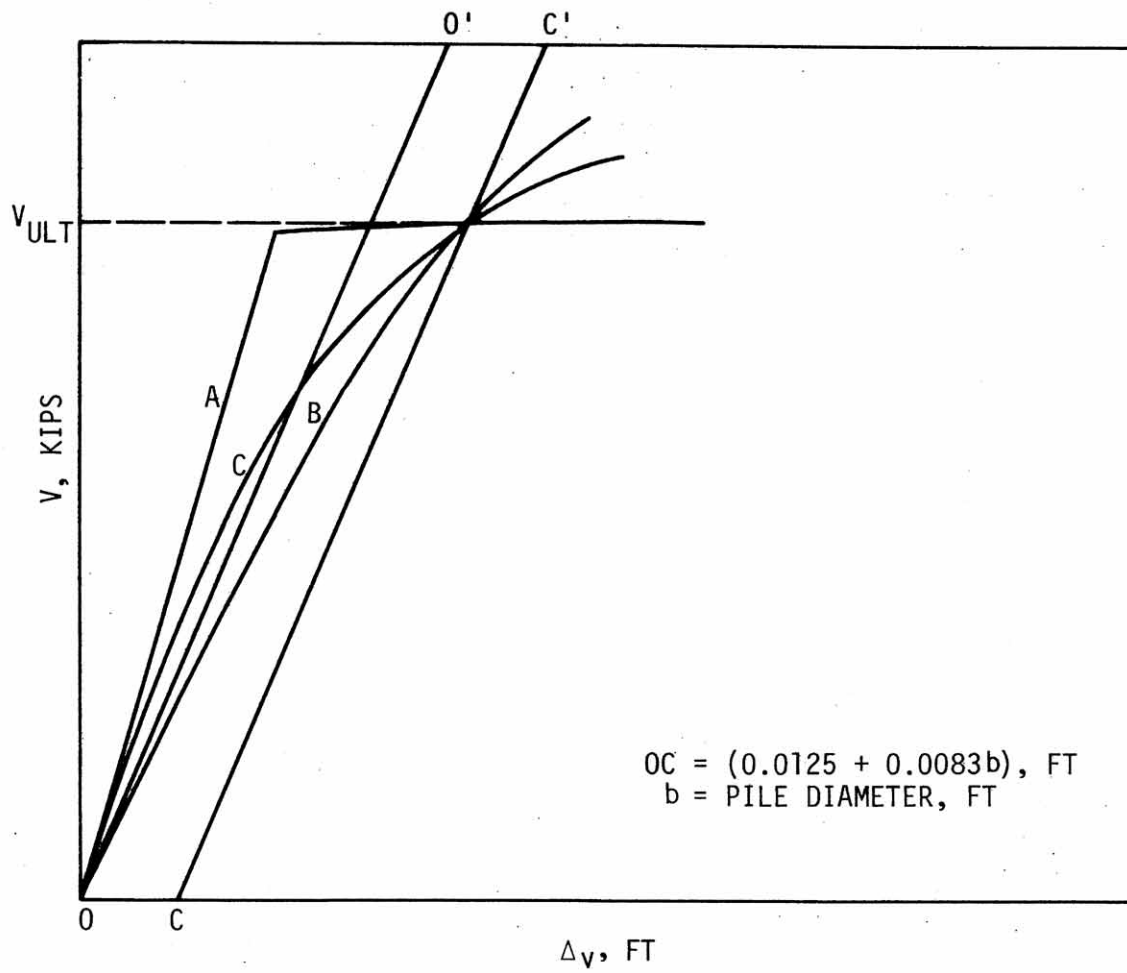


Figure 54. Typical load-settlement curves for (A) friction pile, (B) bearing pile, (C) friction-bearing pile.

motions). A set of curves showing ultimate pile load (V_{ult}) versus specified lateral displacements, Δ_H , for the different Iowa soils is shown in Figs. 55 to 56. Nondimensional forms are given in Fig. 57.

The deflected shapes of the H pile with specified lateral displacement $\Delta_H = 1.0$ in. and vertical loads of zero and after ultimate load are shown in Figs. 58-63.

5.5. Behavior of Pile and Soil

In spite of the extensive research on the resistance of piles to lateral and vertical loading, a simple design method that can be universally applied to any soil or type of pile has not been established. There are many interrelated factors. The dominant one is the pile stiffness relative to soil stiffness and strength. This influences the deflected shape and determines whether the failure mechanism is one of the rotation and/or vertical translation of a rigid element or is due to flexure followed by the failure in bending of a flexible pile.

In this investigation, failure mechanisms can be generalized in two types: (a) lateral type failure and (b) vertical type failure. Lateral type failure can occur in several modes: (1) buckling failure of the pile due to large displacement, (2) plastic hinge formation in the pile, and (3) lateral soil failure. Usually, lateral failure is a combination of all three: large lateral displacement of the pile due to inelastic pile buckling and lateral soil failure. Vertical type failure can occur with: (1) plastic deformation of the pile caused by large pile stresses and (2) soil friction or point bearing failure as the pile moves down through the soil as a rigid body.

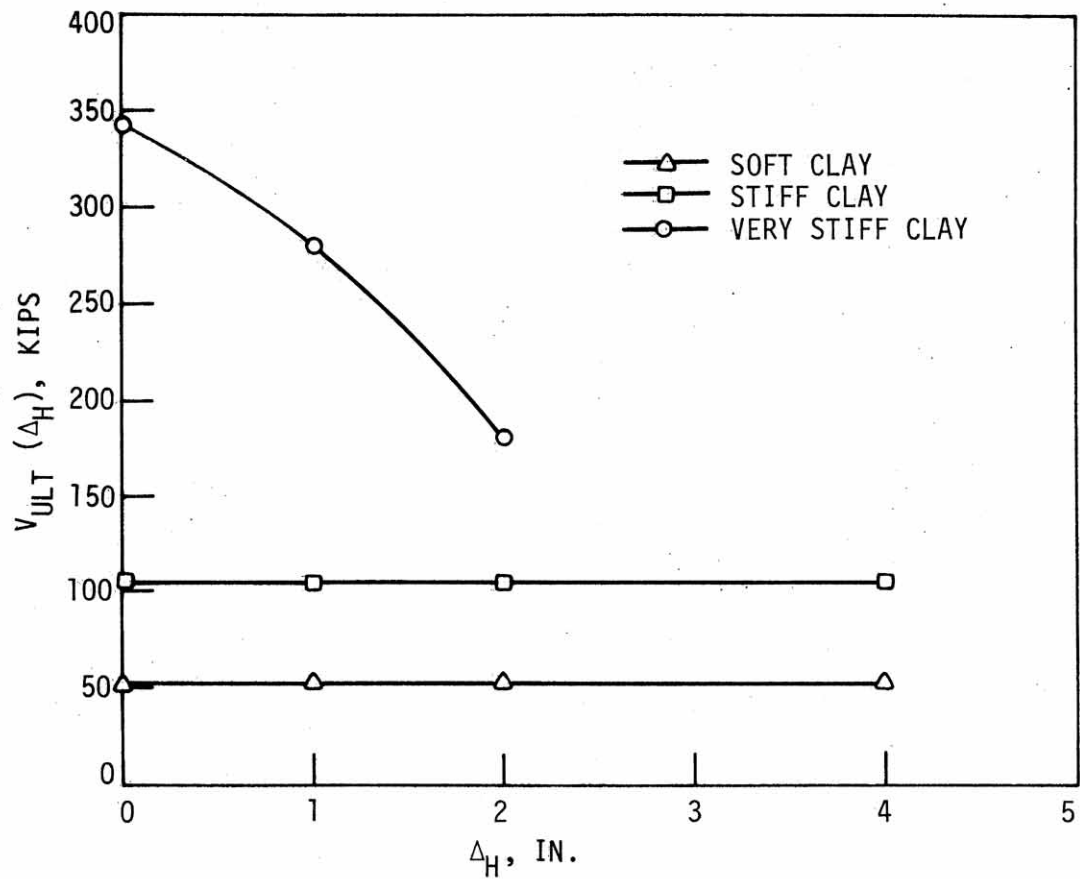


Figure 55. Ultimate vertical load versus lateral specified displacements (clay).

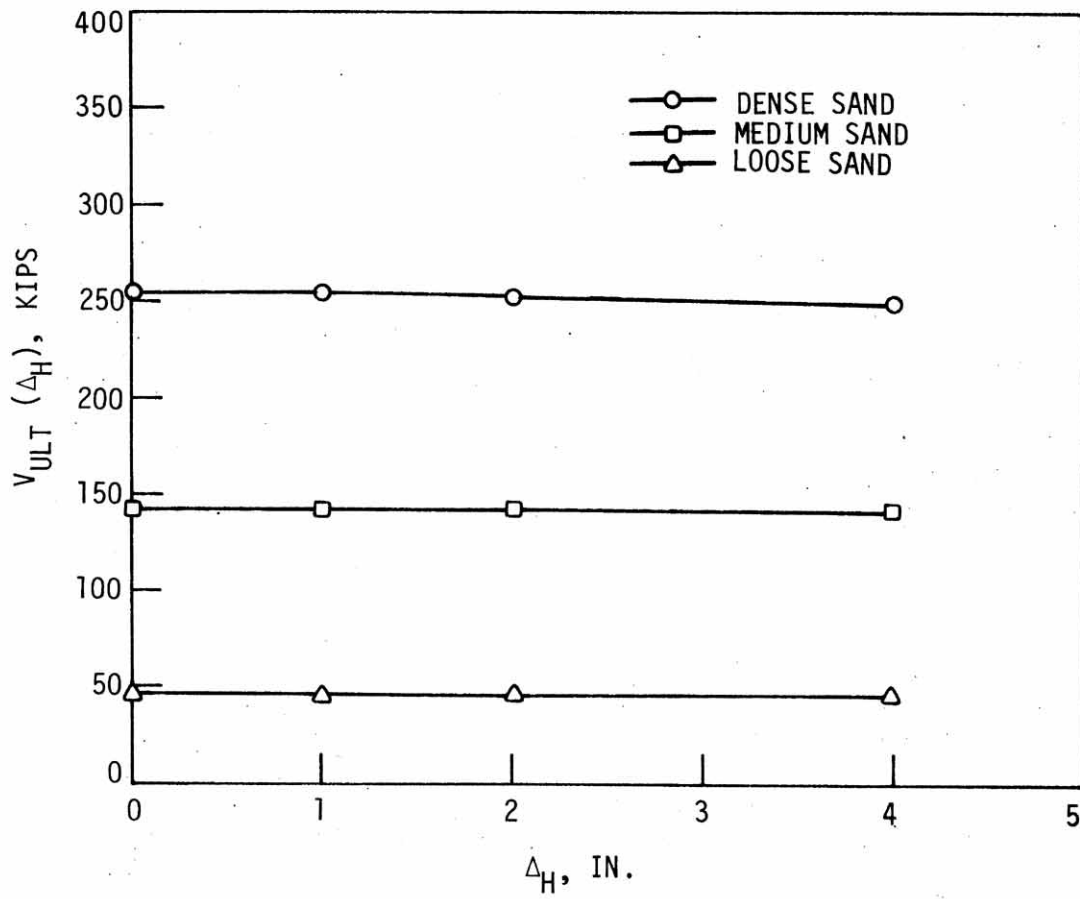


Figure 56. Ultimate vertical load versus lateral specified displacements (sand).

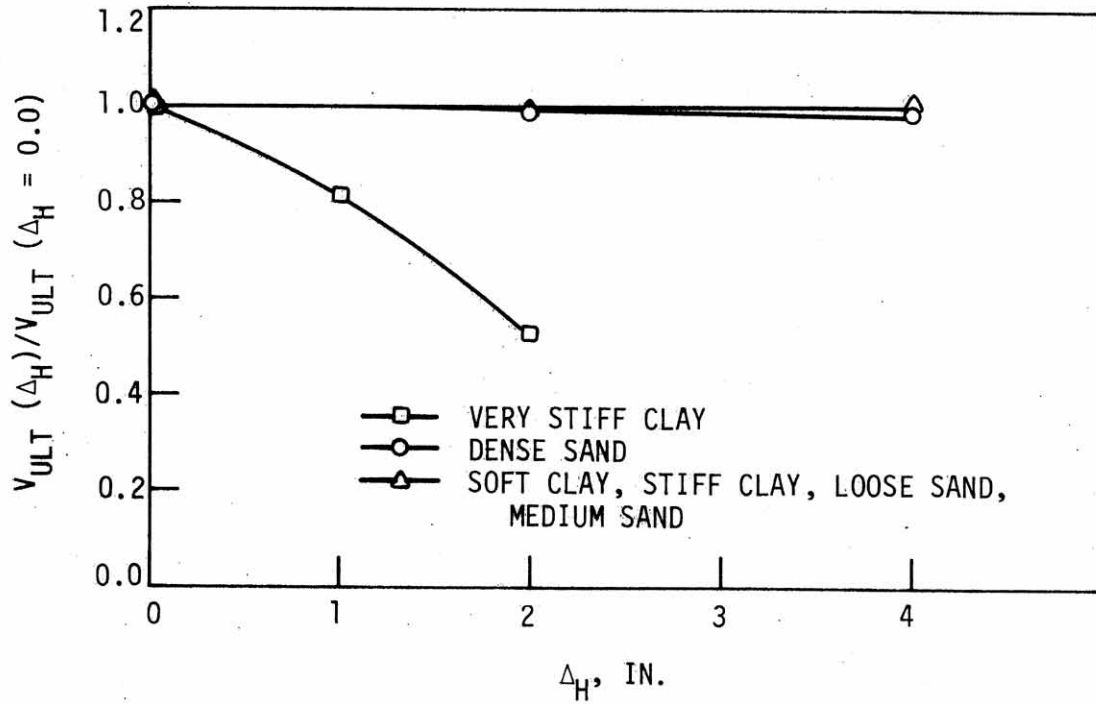


Figure 57. Nondimensional forms of ultimate vertical load versus lateral specified displacements, Δ_H in Iowa soils.

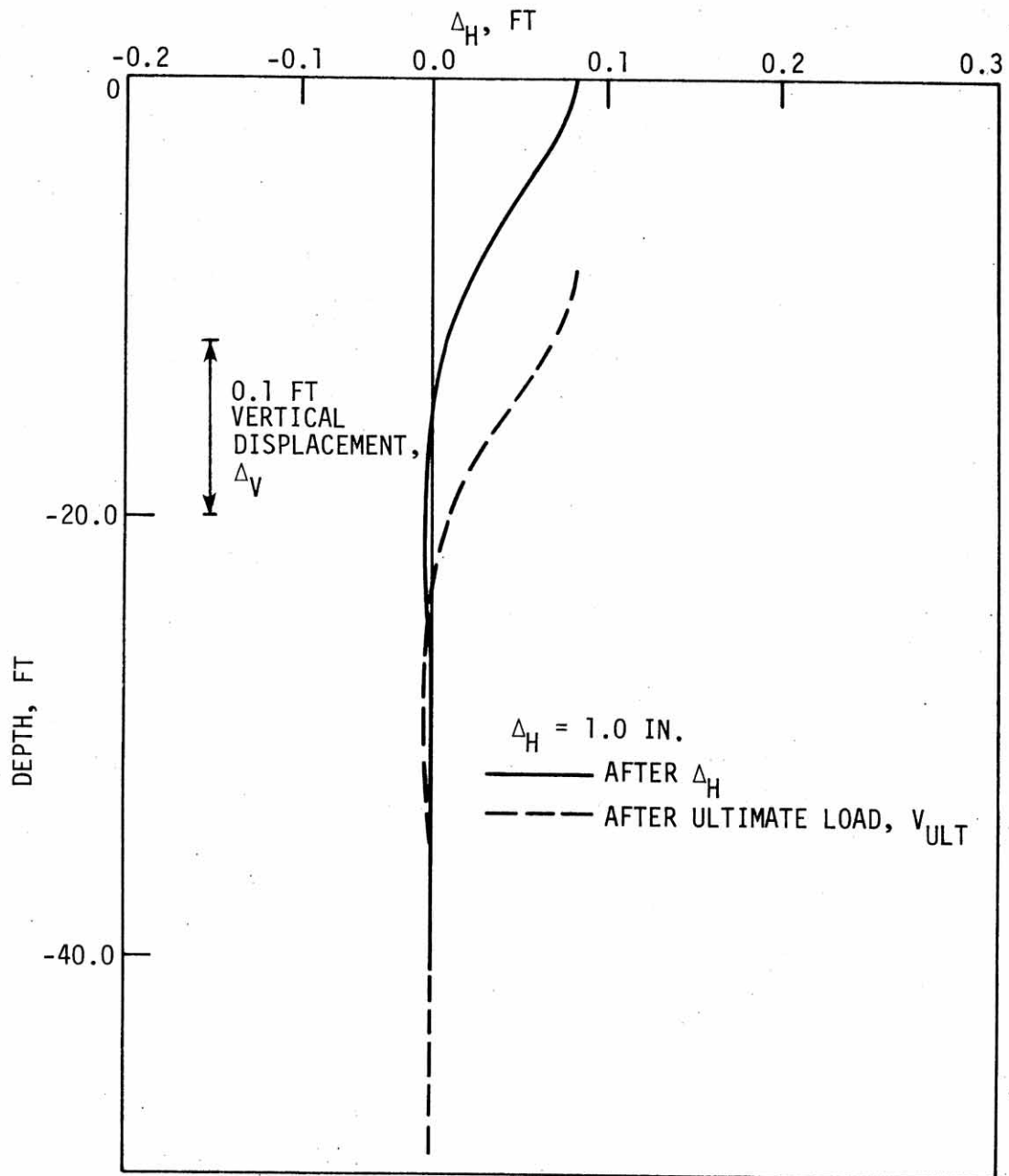


Figure 58. Deflected shapes in soft clay (a) after Δ_H ,
(b) after ultimate load, V_{ULT} .

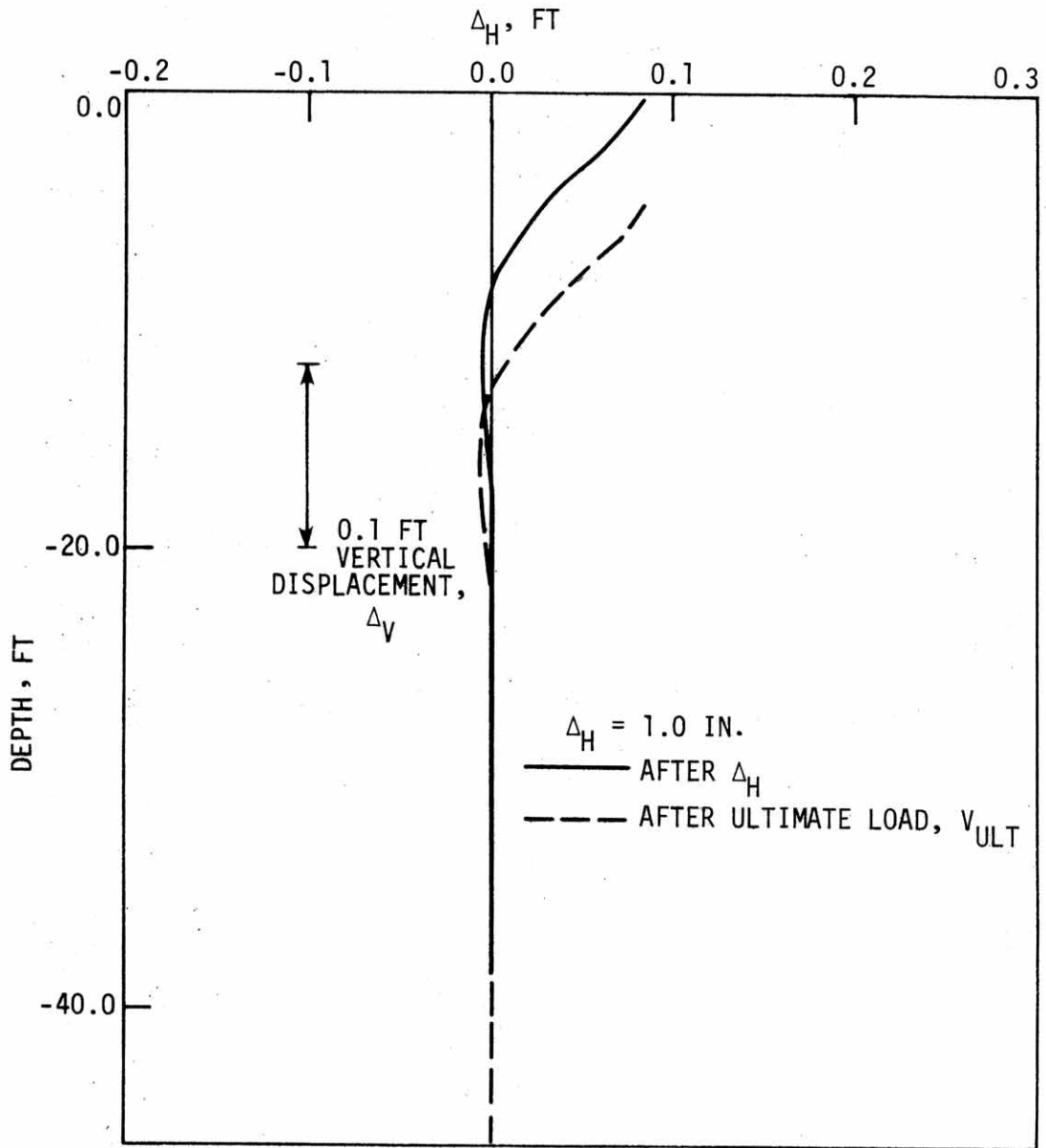


Figure 59. Deflected shapes in stiff clay (a) after Δ_H ,
(b) after ultimate load, V_{ULT} .

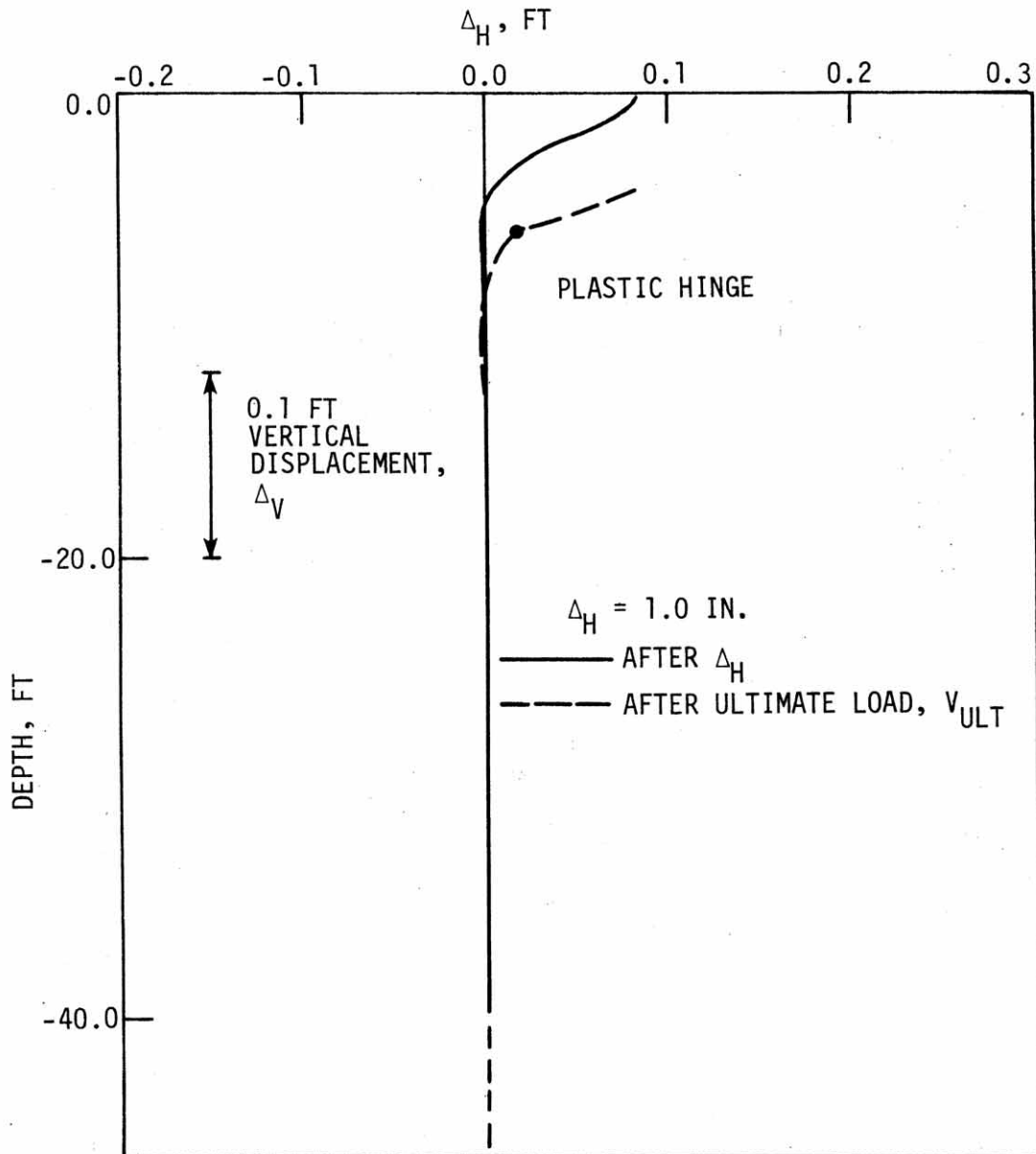


Figure 60. Deflected shapes in very stiff clay (a) after Δ_H ,
(b) after ultimate load, V_{ULT} .

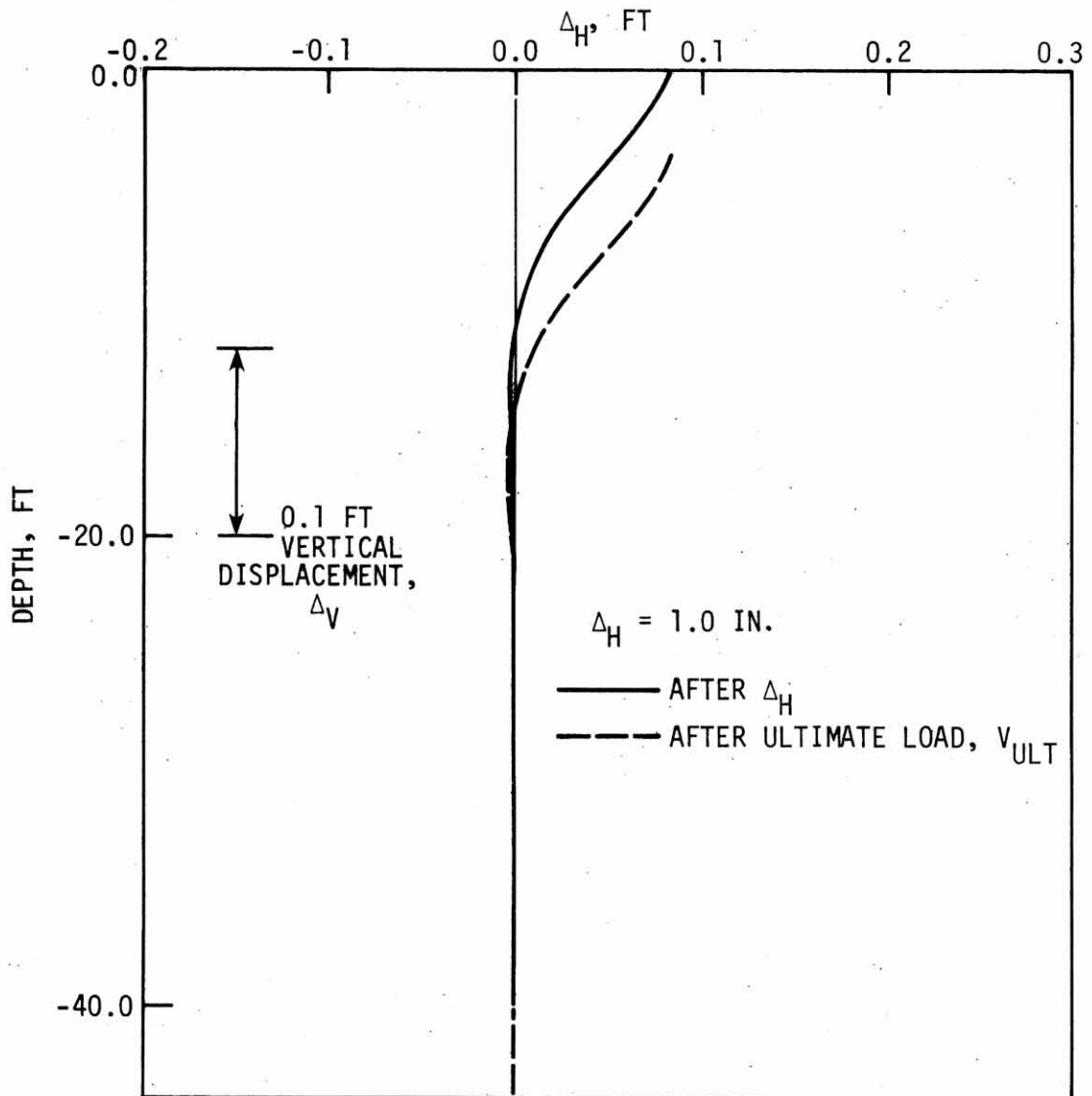


Figure 61. Deflected shapes in loose sand (a) after Δ_H , (b) after ultimate load, V_{ULT} .

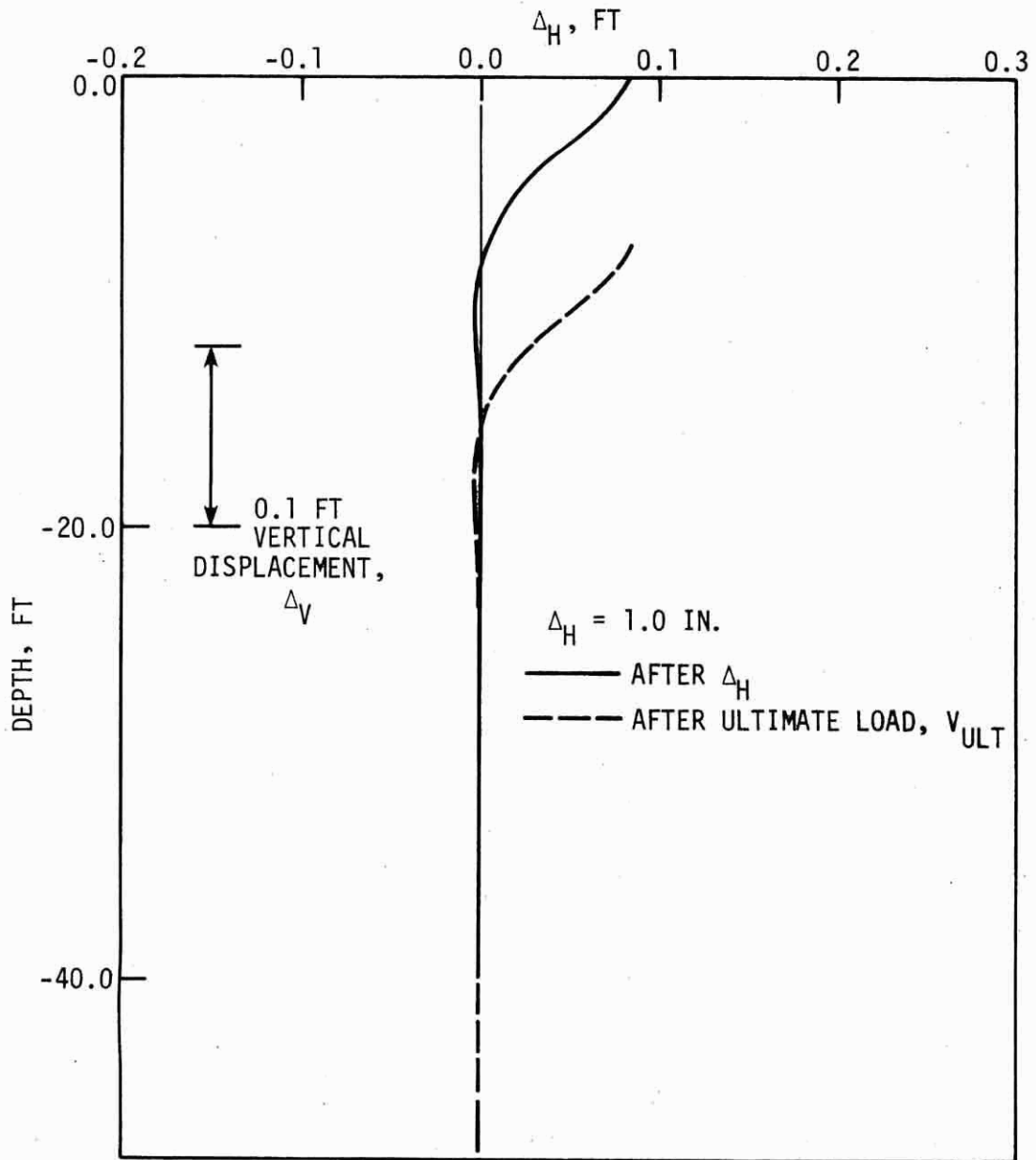


Figure 62. Deflected shapes in medium sand (a) after Δ_H , (b) after ultimate load, V_{ULT} .

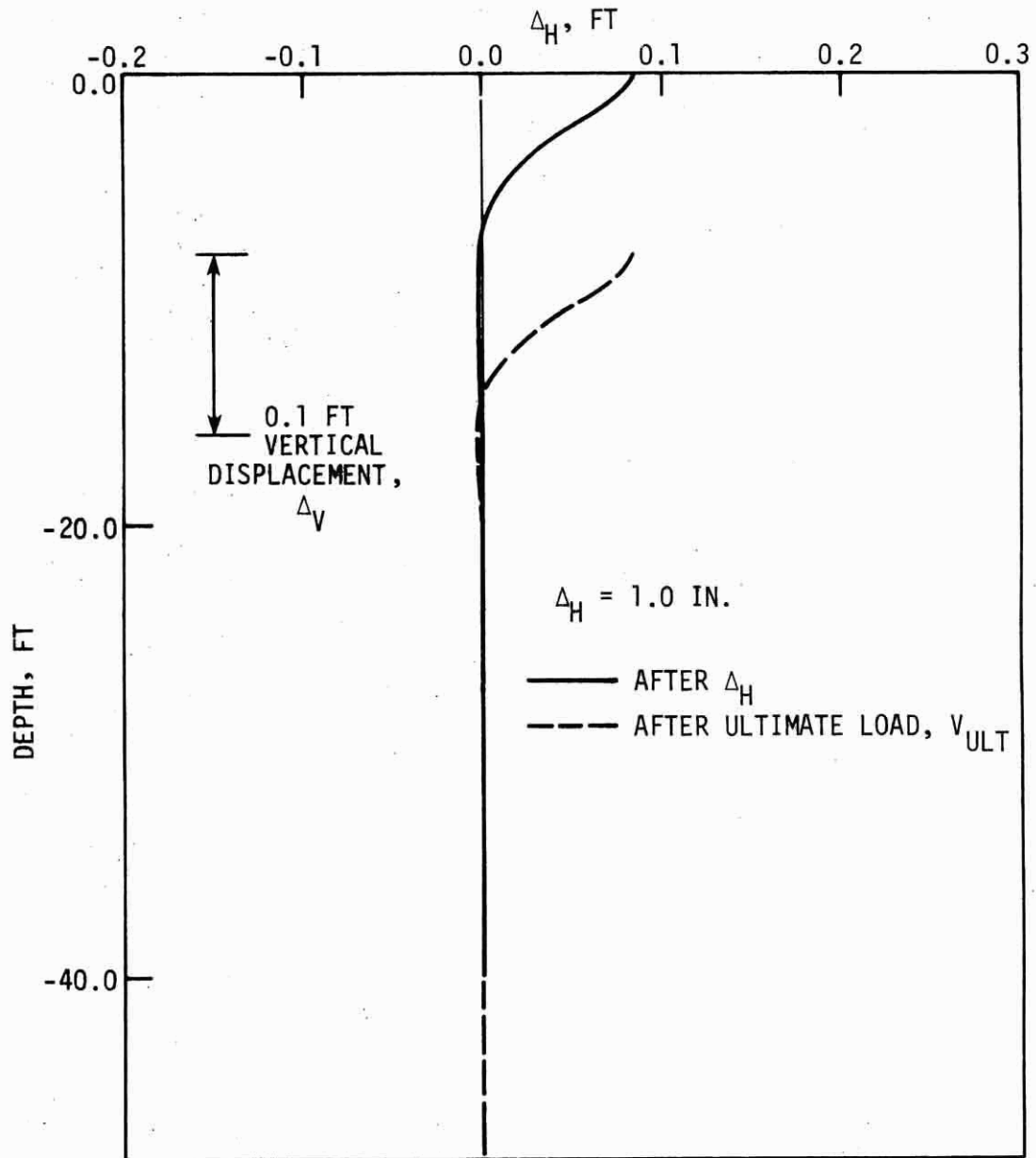


Figure 63. Deflected shapes in dense sand (a) after Δ_H , (b) after ultimate load, V_{ULT} .

From observing the load-settlement curves (Figs. 48-53), it appears that most of the analyzed piles failed by the second type (vertical type failure). That is, the applied load reached the ultimate soil frictional resistance (for sands, soft clay and stiff clay). The load-settlement curves became horizontal as the load reached the ultimate pile load for all prescribed lateral displacements. Comparing the deflected shapes of the pile before loading and after loading (Figs. 58-59 and 61-63) shows that the lateral displaced shapes do not change significantly as the vertical displacements increase. This implies that plastic hinge does not form or lateral strength is not exceeded before the vertical soil failure occurs. The ultimate load capacity determined by the procedures of Section 5.4 and shown in Figs. 55 and 56 are not affected by the lateral displacement Δ_H or caused by thermal expansion or contraction of the integral abutment bridge.

For the soils examined here very stiff clay is the only case in which the lateral failure occurs before vertical failure. From Fig. 50, the load-settlement curve shows that when $\Delta_H = 0.0$ in. the failure is similar to the pile in other soil types (sands, soft clay, stiff clay). For $\Delta_H = 2.0$ in. the applied load was terminated at $V = 180$ Kips because the solution was converging very slowly. A plastic hinge which forms in the pile for this case significantly increases the number of iterations required for convergence. The deflected shapes of the pile before vertical loading and after loading (Fig. 60) show the position of the plastic hinge. For this case, the last converged solution was taken as the ultimate load. Figure 50 illustrates that this is reasonable. The ultimate load capacity for the pile in very stiff clay is affected by

the lateral displacement induced by thermal expansion or contraction of the bridge.

Lateral type failure did not occur in dense sand. For a pile embedded in soil, the critical location for lateral soil failure is 0 to 10 ft from the ground line (refer to pile deflected shapes from Figs. 58-63). The lateral soil stiffness for very stiff clay is much higher than dense sand so that the pile stress induced by the specified lateral displacement (Δ_H) in very stiff clay is larger than dense sand and reaches the yield stress and plastic hinge forms. Since the stiffness of the very stiff clay is greater than the stiffness of other soils in the top portion of the pile, the deflected shapes of other soils have deeper deflected "S" shapes than the very stiff clay.

6. SUMMARY, CONCLUSIONS AND RECOMMENDATIONS

FOR FURTHER STUDY

6.1. Summary

The highway departments of all fifty states were contacted to find the extent of application of integral abutment bridges, to survey the different guidelines used for analysis and design of integral abutment bridges, and to assess the performance of such bridges through the years. The survey showed a wide variation in design assumptions and limitations among the various states in their approach to the use of integral abutments. The survey also showed that the variations among the different states are due largely to the empirical basis for development of current design criteria, thereby underscoring the need for a simple, rational method of accurately predicting pile stresses.

The states that use integral abutments indicated that they were generally satisfied with the performance of the bridges and that they were economical. Some problems have been reported, however, concerning secondary effects of inevitable lateral displacements at the abutment. These include abutment, wingwall and pavement distress and backfill erosion. Only a few states noted that any difficulty had been encountered. Other states reported that solutions have been developed for most of the ill effects of abutment movements. They include:

- additional reinforcing and concrete cover in the abutment;
- more effective pavement joints which allow thermal movements to occur; and
- positive control of bridge deck and roadway drainage.

The length limitations on integral abutment bridges used by the different states in 1980 are summarized in Appendix 9.1. Many of the states have been progressively increasing length limitations for the use of integral abutments over the last thirty years. Improvements in details have also taken place which generally can eliminate the possibility of serious distress occurring with abutment movements of up to 1 inch. These progressive steps in the state of the art of integral abutment bridge engineering have occurred over the past thirty years primarily as the result of the observance of satisfactory performance in actual installations. Very little work, however, has been done to monitor the actual behavior of integral abutments except in checking for obvious signs of distress in visible elements of the bridge.

An algorithm based on a state-of-the-art nonlinear finite element procedure was developed and used to study piling stresses and pile-soil interaction in integral abutment bridges. The finite element idealization consists of a one-dimensional idealization for the pile and nonlinear springs for the soil. Important parameters for analysis are the pile and soil characteristics. On the basis of review of the literature, it was decided to represent pile characteristics by beam-column elements with geometric and material nonlinearities and soil characteristics by p - y , f - z , and q - z curves (see Section 3.2). An idealized soil model (modified Ramberg-Osgood model) was introduced in this investigation to obtain the tangent stiffness of the nonlinear spring elements.

Incremental finite element updated Lagrangian formulation including material and geometric nonlinearities is used. The scope of the geometric and material nonlinear effects is discussed (see Section 4). Explicit

forms of the small displacement stiffness matrix and initial stress matrix are presented. Several numerical techniques available for the solutions of the nonlinear equations are reviewed and the incremental and iterative techniques used in the study are discussed in detail. The procedure used in the calculation of residual loads and residual displacements to satisfy the convergence criteria is also discussed. A computer program (Yang 5) has been written based on the finite element procedure described.

Several numerical examples are presented in order to establish the reliability of the finite element model and the computer software developed. Three problems with analytical solutions were first solved and compared with theoretical solutions: (a) a beam-column problem was used to check the geometric nonlinearity feature; (b) a short, thick column problem was used to check material nonlinearity; and (c) a simple soil problem was used to check soil nonlinearity. Finally, the results obtained from two experimentally field-loaded piles were compared with the numerical results from the model.

After verification of the model, a 40 ft H pile (HP 10 × 42) in six typical Iowa soils was analyzed by first applying a horizontal displacement Δ_H (to simulate bridge motion) and no rotation at the top and then applying a vertical load V incrementally until failure occurred. Based on the numerical results, the failure mechanisms were generalized to be of two types: (a) lateral type failure and (b) vertical type failure. It appears that most piles in Iowa soils (sand, soft clay and stiff clay) failed when the applied vertical load reached the ultimate soil frictional resistance (vertical type failure). In very

stiff clays, however, the lateral type failure occurs before vertical type failure because the soil is sufficiently stiff to force a plastic hinge to form in the pile as the specified lateral displacement is applied.

6.2. Conclusions

From comments received from state highway departments on integral abutment bridges, the writers infer that the benefits from using integral abutments are sufficient to justify the additional care in detailing to make them function properly.

The results obtained from analyses of piles in different Iowa soils show that two types of failure mechanisms are possible: (a) lateral type failure and (b) vertical type failure. For sand, soft clay and stiff clay, vertical type failure usually occurs when the applied vertical load exceeds the ultimate soil frictional resistance. For very stiff clays, lateral type failure occurs because of plastic hinge formation in the pile.

Preliminary results from this investigation showed that the vertical load-carrying capacity of H piles is not significantly affected by lateral displacements of 2 inches in soft clay, stiff clay, loose sand, medium sand and dense sand. However, in very stiff clay (average blow count of 50 from standard penetration tests), it was found that the vertical load carrying capacity of the H pile is reduced by about 50 percent for 2 inches of lateral displacement and by about 20 percent for lateral displacement of 1 inch. The average AASHTO (American

Association of State Highway and Transportation Officials) temperature change for Iowa is 40 °F for concrete bridges and 75 °F for steel bridges. If a lateral displacement of 1 inch was to be permitted, this would translate into allowable lengths of 700 feet for concrete bridges and 350 feet for steel bridges without expansion joints.

On the basis of the preliminary results of this investigation, the 265-foot length limitation in Iowa for integral abutment concrete bridges appears to be very conservative. The writers feel that further numerical studies and monitoring of piling stresses in integral abutment bridges should be performed before a reliable length limitation can be set. Since the upper layer soils in integral abutment bridges are frequently compacted, further investigation of the very stiff clay and soils with higher blow counts from standard penetration tests will be helpful in the effort to set reliable length limitations for concrete and steel integral abutment bridges.

6.3. Recommendations for Further Study

1. Only six typical Iowa soils have been brought into this investigation. More study should be done of other representative Iowa soils and layered soils with different combinations.
2. The properties of Iowa soils should be determined by standard laboratory tests to enable better representation of soil characteristics in the model so that piling stresses and soil-pile interaction could be predicted more accurately.

3. The investigation should be expanded to include skewed bridges with integral abutments.
4. An actual bridge should be instrumented and pile stresses monitored through several cycles of temperature change. (A model bridge or a portion of a bridge may also provide adequate data.) Some research in this area has been performed in North and South Dakota (see Section 3.3).
5. Complete documentation of the Yang 5 computer program should be provided. This aspect will be covered in a supplemental report to be issued in August 1982.

7. ACKNOWLEDGMENTS

The study presented in this report was conducted by the Engineering Research Institute of Iowa State University and was sponsored by the Iowa Department of Transportation, Highway Division, through the Iowa Highway Research Board.

The authors wish to extend sincere appreciation to the engineers of Iowa DOT for their support, cooperation, and counseling. A special thanks is extended to Charles A. Pestotnik, Henry Gee, Vernon Marks and Kermit L. Dirks.

Appreciation is also extended to Bruce Johnson, graduate student in structural engineering and Assistant Bridge Engineer - Federal Highway Administration, for his contributions in various phases of the project. In particular, his contribution in conducting the survey of the fifty states on current practice in analysis and design of integral abutment bridges is gratefully acknowledged. Special thanks also go to Professors W. W. Sanders, Jr. and J. E. Bowles for their contributions to this investigation.

8. REFERENCES

1. Lee, H. W. and Sarsam, M. B., "Analysis of Integral Abutment Bridges," South Dakota Department of Highways, Pierre, South Dakota, March 1973.
2. Pestotnik, C. A., Gee, H. and Marks, V., Engineers, Iowa Department of Transportation, Ames, Personal communications, 1980.
3. "State Highway No. 44 Over Pine Creek, Mellette County, South Dakota," United States Steel Bridge Report, ADUSS 88-7126-01, March 1977.
4. "Bridge Planning and Design Manual," Vol. IV, Detailing, California Department of Transportation, Sacramento, June 1979.
5. "Design Manual," Section 3.72, Sheet 4.3.1, Bridge Division, Missouri State Highway and Transportation Commission, Jefferson City, October 1977.
6. Gee, H., "Length Limit of a Bridge Using Integral Abutments," Office of Bridge Design, Iowa Department of Transportation, Ames, February 13, 1969.
7. Emanuel, J. H., et al., "An Investigation of Design Criteria for Stresses Induced by Semi-Integral End Bents," Report, University of Missouri, Rolla, 1972.
8. "Integral, No-Joint Structures and Required Provisions for Movement," Federal Highway Administration, U.S. Department of Transportation, T5140.13, January 28, 1980.
9. Johnson, B., "State-of-the-Art Methods for Design of Integral Bridge Abutments," Research Report, M.S. (Structural Engineering), Iowa State University, Ames, August 1981.
10. Wasserman, E., Engineer, Office of Structures, Tennessee Department of Transportation, Nashville, Telephone Conversation, May 1981.
11. Wilkinson, E., Bridge Engineer, Kansas State Highway Commission, Topeka, Telephone Conversation, May 1981.
12. Moberly, J., Structural Engineer, Bridge Division, Missouri State Highway and Transportation Commission, Jefferson City, Telephone Conversation, May 1981.
13. Durrow, F., Assistant Bridge Engineer, North Dakota State Highway Department, Bismarck, Telephone Conversation, May 1981.

14. Jorgenson, J., Chairman of the Civil Engineering Department, North Dakota State University, Fargo, Telephone Conversations, June 1981.
15. Cassano, R. C., Chief, Office of Structures Design, California Department of Transportation, Sacramento, Correspondence, 900.05, June 10, 1981, and telephone conversations, June 1.
16. Gee, H., Structural Engineer; Lundquist, W., Bridge Design Engineer; and Miller, G., Geotechnical Engineer; Iowa Department of Transportation, Ames, Conversations, June 1981.
17. McNulty, J. F., "Thrust Loading on Piles," Journal of the Soil Mechanics and Foundations Division, ASCE, Vol. 82, No. SM4, Paper 1081, 1956.
18. Poulos, H. G. and Davis, E. H., Pile Foundation Analysis and Design, John Wiley and Sons, Inc., New York, 1980.
19. Madhav, M. R., Rao, N. S. V. K., and Madhavan, K., "Laterally Loaded Pile in Elasto-Plastic Soil," Soils and Foundations, Vol. 11, No. 2: 1-15, 1971.
20. Kubo, J., "Experimental Study of the Behavior of Laterally Loaded Piles," Proceedings, 6th International Conference on Soil Mechanics and Foundation Engineering, Vol. 2: 275-279, 1965.
21. Welch, R. C., and Reese, L. C., "Lateral Load Behavior of Drilled Shafts," Research Report 89-10, Center for Highway Research, The University of Texas at Austin, May 1972.
22. Douglas, D. J. and David, E. H., "The Movement of Buried Footings Due to Moment and Horizontal Load and the Movement of Anchor Plates," Geotechnique, Vol. 14: 115-132, 1964.
23. Poulos, H. G., "Behavior of Laterally-Loaded Piles: I--Single Piles," Journal of the Soil Mechanics and Foundations Division, ASCE, Vol. 97, No. SM5: 711-731, 1971.
24. Banerjee, P. K. and Davies, T. G., "Analysis of Pile Groups Embedded in Gibson Soil," Proceedings, 9th International Conference on Soil Mechanics and Foundations Engineering, Tokyo, Vol. 1: 381-386, 1977.
25. Matlock, H. and Reese, L. C., "Foundation Analysis of Offshore Pile Supported Structures," Proceedings, 5th International Conference on Soil Mechanics and Foundations Engineering, Vol. 2: 91-97, 1961.
26. Bowles, J. E., Analytical and Computer Methods in Foundation Engineering, McGraw-Hill Book Co., New York, 1974.

27. Reese, L. C., Hudson, B. S. and Vijayvergiya, B. S., "An Investigation of the Interaction Between Bored Piles and Soil," Proceedings, 7th International Conference on Soil Mechanics and Foundations Engineering, Vol. 2: 211-215, 1969.
28. Reese, L. C., Cox, W. R., and Koop, F. D., "Analysis of Laterally Loaded Piles in Sand," Proceedings of the Offshore Technology Conference, Houston, Texas, 1974.
29. Reese, L. C. and Matlock, H., "Non-Dimensional Solutions for Laterally Loaded Piles with Soil Modulus Assumed Proportional to Depth," Proceedings, 8th Texas Conference on Soil Mechanics and Foundations Engineering, 1956.
30. Reese, L. C. and Cox, W., "Soil Behavior from Analysis of Tests of Uninstrumented Piles Under Lateral Loading," ASTM STP 444, 1969.
31. Matlock, H., "Correlations for Design of Laterally Loaded Piles in Soft Clay," Proceedings of the Offshore Technology Conference, Houston, Texas, 1970.
32. Reese, L. C., and Welch, R. C., "Lateral Loading of Deep Foundations in Stiff Clay," Journal of the Geotechnical Engineering Division, ASCE, Vol. 101, No. GT7: 633-649, July 1975.
33. Bhushan, K., Haley, S. C., and Fong, P. T., "Lateral Load Tests on Drilled Piers in Stiff Clays," Journal of the Geotechnical Engineering Division, ASCE, Vol. 105, No. GT8: 969-985, August, 1979.
34. Reese, L. C., "Laterally Loaded Piles," Proceedings of the Seminar Series, Design, Construction and Performance of Deep Foundations, ASCE, Univ. of California, Berkeley, 1975.
35. Alizadeh, M. and Davisson, M. T., "Lateral Load Tests on Piles--Arkansas River Project," Journal of the Soil Mechanics and Foundations Division, ASCE, Vol. 96: 1583-1603, September 1970.
36. Paduana, J. A. and Yee, W. S., "Lateral Load Tests on Piles in Bridge Embankments," Transportation Research Record 517, 1974.
37. Ha, N. B. and O'Neill, M. W., "Field Study of Pile Group Action," Federal Highway Administration, Technical Report No. FHWA/RD-81/003, 1981.
38. Vijayvergiya, V. N., "Load-Movement Characteristics of Piles," Proceedings, Ports '77 Conference, ASCE, Long Beach, California, March 1977.
39. Yee, W. S., "Lateral Resistance and Deflection of Vertical Piles, Final Report - Phase 1," Bridge Department, California Division of Highways, Sacramento, 1973.

40. Vesic, A. S., "Design of Pile Foundations," N.C.H.R.P. Synthesis of Highway Practice No. 42, Transportation Research Board, Washington, D.C., 1977.
41. Meyerhof, G. G., "Bearing Capacity and Settlement of Pile Foundations," Journal of the Geotechnical Engineering Division, ASCE, Vol. 102, No. GT3: 197-228, March 1976.
42. "Memo to Designers," Office of Structures Design, California Department of Transportation, Sacramento, November 15, 1973.
43. "Long Structures Without Expansion Joints," Bridge Department, California Division of Highways, Sacramento, June 1967.
44. Davisson, M. T., "Lateral Load Capacity of Piles," Transportation Research Record 333, 1970.
45. Parker, F., Jr., and Reese, L. C., "Experimental and Analytical Studies of Behavior of Single Piles in Sand Under Lateral and Axial Loading," Research Report 117-2, Center for Highway Research, The University of Texas at Austin, Nov. 1970.
46. Desai, C. S. and Abel, J. F., Introduction to the Finite Element Method, Van Nostrand Reinhold Co., New York, 1972.
47. Martin, H. C. and Carey, G. F., Introduction to Finite Element Analysis: Theory and Application, McGraw-Hill Book Company, New York, 1973.
48. Gallagher, R. H., Finite Element Analysis Fundamentals, Prentice-Hall Inc., Englewood Cliffs, N.J., 1975.
49. Oden, J. T., Finite Elements of Nonlinear Continua, McGraw-Hill Book Company, New York, 1972.
50. Cook, R. D., Concepts and Applications of Finite Element Analysis, 2nd Edition, John Wiley & Sons Co., New York, 1981.
51. Belytschko, T., and Hsieh, B. J., "Non-Linear Transient Finite Element Analysis with Convected Coordinates," International Journal for Numerical Methods in Engineering, Vol. 7, No. 3: 255-271, 1973.
52. Zienkiewicz, O. C., The Finite Element Method, 3rd Edition, McGraw-Hill Book Company, New York, 1977.
53. Desai, C. S., "Nonlinear Analysis Using Spline Functions," Journal of the Soil Mechanics and Foundations Division, ASCE, Vol. 97, No. SM10: 1461-1481, Sept. 1971.

54. Drnevich, V. P., "Constrained and Shear Moduli for Finite Elements," *Journal of the Geotechnical Engineering Division, ASCE*, Vol. 101, No. GT5, Nov. 1975.
55. Duncan, J. M., and Chang, C. Y., "Nonlinear Analysis of Stress and Strain in Soils," *Journal of the Soil Mechanics and Foundations Division, ASCE*, Vol. 96, SM5: 1629-1653, Sept. 1970.
56. Ramberg, W., and Osgood, W. R., "Description of Stress-Strain Curves by Three Parameters," Technical Note No. 802, National Advisory Committee for Aeronautics, Washington, D.C., 1943.
57. Richard, R. M., and Abbott, B. J., "Versatile Elastic-Plastic Stress-Strain Formula," Technical Note, *Journal of the Engineering Mechanics Division, ASCE*, Vol. 101, No. EM4, Aug. 1975.
58. Desai, C. S., and Wu, T. H., "A General Function for Stress-Strain Curves," in Numerical Methods in Geomechanics, ASCE, 1976.
59. Timoshenko, S. P., and Gerc, J. M., Theory of Elastic Stability, 2nd Edition, McGraw-Hill Book Company, New York, 1961.
60. "Commentary on Plastic Design in Steel," *ASCE Manuals of Engineering Practices*, No. 41, 1961.
61. Beedle, L. S., Plastic Design of Steel Frame, 2nd Edition, John Wiley & Sons, Inc., New York, 1961.
62. Neal, B. G., The Plastic Methods of Structural Analysis, 3rd Edition, A Halsted Press Book, New York, 1977.
63. D'Appolonia, Z., and Romualdi, J. P., "Load Transfer in End-Bearing Steel H-Pile," *Journal of the Soil Mechanics and Foundations Division, ASCE*, SM2: 1-25, March 1963.
64. Reese, L. C., "Laterally Loaded Piles: Program Documentation," *Journal of the Geotechnical Engineering Division, ASCE*, Vol. 103, No. G74, Proc. Paper 12862: 287-305, April 1977.
65. Winklerhorn, H. F., and Fang, H. Y., Editors, Foundation Engineering Handbook, Van Nostrand Reinhold Co., New York, 1975.
66. Peck, R. B., Hanson, W. E., and Thornburn, T. H., Foundation Engineering, John Wiley & Sons, Inc., New York, 1974.

9. APPENDICES

9.1. Questionnaire for Bridges with Integral Abutments
and Summary of Responses

Part 1. Questionnaire

Part 2. Responses to all questions except number 4

Part 3. Responses to question 4

Part 4. Additional comments made by some of the states

Note: States not listed in Part 2 answered "no" to question 1 and, therefore, did not complete the remainder of the questionnaire.

6. What type of structural assumption is made for the top of the pile?

pinned (moment equal zero) _____ Is the joint detailed as a pin? _____
 fixed (rotation equal zero) _____
 partially restrained _____ { restrained by girder _____
 other assumptions _____ { restrained by soil on abut. _____

7. What loads do you include when calculating pile stress?

thermal _____ temperature range _____
 shrinkage _____
 soil pressure on abutment face _____

8. How is bending accounted for in the pile?

Neglect or assume bending stresses do not affect pile performance _____
 Assume location of pile inflection point and analyze pile as
 bending member _____
 Reduce bending by prebored hole _____
 Other _____

9. What type of backfill material do you specify on the backside of the abutment?

10. Does the approach pavement rest directly on the abutment?

yes _____ no _____

11. Briefly evaluate the performance of integral abutment bridges in your state. (Compare to bridges with expansion devices.)

Construction

relative cost more _____ same _____ less _____
 special problems _____

Maintenance

relative costs more _____ same _____ less _____
 special problems _____

Please return to: Lowell Greimann
 420 Town Engineering
 Iowa State University
 Ames, Iowa 50011

Part 2. Summary of responses to Questions 1, 2, 3, 5, 6, and 7.

State	Reason	Steel			Concrete			Prestressed			Girder End Fixity	Pile Top Fixity	Pile Loads		
		Use	Length		Use	Length		Use	Length				Thermal	Shrinkage	Soil Pressure
			<30*	>30*		<30*	>30*		<30*	>30*					
AL	Cost	Y	300	---	Y	---	115	Y	416	104	Pin	Pin	Y	N	Y
AZ	Maint	Y	253	N	Y	330	N	Y	404	N	Pin	Pin	Y	Y	Y
CA	Cost	Y	---	---	Y	320	320	Y	230	230	Pin	R. Res	N	N	N
CO	Cost	Y	200	---	Y	400	---	Y	400	---	Pin	Pin	N	N	Y
CT	---	Y	200	---	N	---	---	N	---	---	Pin	Fix	Y	N	N
GA	El. Jt	Y	300	---	Y	300	---	Y	300	---	Pin	---	N	N	N
IA	Cost	N	---	---	Y	265	---	Y	265	---	Pin	Fix	Y	N	N
ID	Cost	Y	200	N	Y	400	N	Y	400	N	Pin	Pin	N	N	N
IN	Cost	N	---	---	Y	---	100	N	---	---	---	---	N	N	N
KS	El. Jt	Y	300	300	Y	350	350	Y	300	300	Pin	Pin	Y	Y	N
KY	Cost	N	N	N	Y	300	N	Y	300	N	Fix	Fix	Y	N	Y
MO	El. Jt	Y	400	---	Y	400	400	Y	500	500	Pin	Pin	N	N	N
MT	Cost	Y	300	N	Y	100	N	Y	300	N	Pin	Pin	N	N	Y
ND	Maint	Y	350	---	Y	350	---	Y	450	---	Pin	Fix	N	N	N
NE	El. Jt	Y	300	---	N	300	---	Y	N	---	Pin	Pin	Y	N	N
NM	El. Jt	Y	---	---	Y	---	---	Y	---	---	P. Res.	P. Res.	Y	Y	Y
NY	Cost	Y	305	---	---	---	---	---	---	---	Pin	---	Y	N	N
OH	Cost	Y	300	300	Y	300	300	Y	300	300	Pin	Pin	N	N	N
OK	---	Y	200	N	Y	200	N	Y	200	N	P. Res.	P. Res.	N	N	N
OR	El. Jt	Y	N	N	Y	350	300	Y	350	300	Pin	Pin	N	N	N
SD	Cost	Y	320	---	Y	450	---	Y	450	---	Pin	Fix	N	N	N
TN	El. Jt	Y	400	400	Y	800	800	Y	800	800	Pin	Pin	N	N	N
UT	El. Jt	Y	300	250	N	---	---	Y	300	250	Pin	Pin	N	N	N
VA	Simp.	Y	242	---	N	---	---	Y	454	---	Pin	Pin	N	N	Y
VT	Cost	Y	150	100	N	N	N	N	N	N	P. Res.	P. Res.	Y	N	N
WA	Cost	N	---	---	Y	350	---	N	---	---	Pin	Pin	N	N	N
WS	Cost	Y	200	200	Y	300	N	Y	300	300	P. Res.	Fix	N	N	N
WY	Simp.	Y	300	300	Y	500	500	Y	500	500	Pin	Pin	N	N	N
R15	El. Jt	N	N	N	Y	270	160	Y	300	240	P. Res.	Pin	N	N	N

Y Yes
 N No
 --- No Response
 * Bridge skew in degrees

Part 2. Summary of responses to Questions 8, 9, 10, and 11.

State	Neglect	Pile Bending		Backfill	Approach Pavmt. on Abutment	Construction Cost			Maintenance Cost		
		Infl. Pt.	Prebore			More	Same	Less	More	Same	Less
AL	Y	Y	N	Gran.	N	N	N	Y	N	N	Y
AZ	Y	N	N	Cohes.	Y	N	N	Y	N	N	Y
CA	Y	N	N	Perv.	Y	N	N	Y	N	N	Y
CO	Y	N	Y	Gran.	Y	N	N	Y	N	N	Y
CT	Y	N	N	Perv.	Y	N	N	Y	N	N	Y
GA	Y	N	N	Rd. Fill	Y	N	N	Y	N	N	Y
IA	N	N	Y	Gran.	Y	N	N	Y	N	N	Y
ID	Y	N	N	Rd. Fill	Y	N	N	Y	N	N	Y
IN	Y	N	N	Gran.	Y	N	N	Y	N	N	Y
KS	Y	N	N	Rd. Fill	Y	N	N	Y	N	N	Y
KY	N	Y	Y	Gran.	N	N	N	Y	N	N	Y
MO	Y	N	N	Rd. Fill	Y	N	N	Y	N	N	Y
MT	Y	N	N	Gran.	Y	N	N	Y	N	N	Y
ND	Y	N	N	Gran.	Y	N	N	Y	N	N	Y
NE	Y	N	N	Rd. Fill	Y	N	Y	N	N	N	Y
NM	N	Y	N	Rd. Fill	Y-N	N	N	N	N	N	N
NY	Y	N	N	Gran.	Y	N	N	Y	N	N	Y
OH	Y	N	N	Gran.	Y	N	N	Y	N	N	Y
OK	Y	N	N	---	Y	N	N	Y	N	N	Y
OR	Y	N	N	Gran.	Y	N	N	Y	N	N	Y
SD	N	N	Y	Gran.	Y	N	N	Y	N	N	Y
TN	Y	N	N	Gran.	Y	N	N	Y	N	N	Y
UT	Y	N	N	Gran.	Y	N	N	Y	N	N	Y
VA	Y	N	N	Gran.	N	N	N	N	N	N	N
VT	Y	N	N	---	N	N	N	Y	N	N	Y
WA	N	N	N	Gran.	Y	N	N	Y	N	N	Y
WS	Y	N	N	Gran.	N	N	N	Y	N	N	Y
WY	Y	N	N	Gran.	Y	N	N	Y	N	N	Y
R15	Y	N	N	Perv.	Y	N	N	Y	N	Y	N

Y Yes
 N No
 --- No Response

Part 3. Summary of responses to Question 4.

State	Steel	Timber	Concrete
AL	*	*	*
AZ	9 ksi in Brg., <9 ksi in Fric.	Not used	In friction only
CA	Assume 5 kips Lat. Resis./pile	Same as steel	13 k. Lat. R./pile
CO	*	Not used	Not used
CT	Use in bearing	---	---
GA	Use in weak axis	Not used	Not used
IA	Use in weak axis, Fric. only	Use of Br. Length < 150'	Not used
ID	*	Not used	Not used
IN	Use H-pile or shell	---	---
KS	Mostly used in bearing	Mostly used in bearing	Mostly used in Brg.
KY	Use in Brg. or friction	---	Used in friction
MO	10' minimum length	Not used	Used in friction
MT	9 ksi in bearing	Used in friction	Not used
ND	*	*	*
NE	Used in weak axis	---	---
NM	Use steel only	Not used	Not used
NY	*	Not used	*
OH	*	Not used	*
OK	Use in bearing	Not used	Not used
OR	*	Not used	*
SD	*	*	*
TN	*	Not used	*
UT	Use in single row	Use in single row	Use in single row
VA	Upper portion allowed to flex	---	---
VT	15' minimum length	Not used	Not used
WA	Use in bearing or friction	Use in Brg. or Fric.	Use in Brg. or Fric.
WS	Use in bearing or friction	Use in friction	Use in Brg. or Fric.
WY	Use in bearing or friction	Not used	Not used
R15	Use in weak axis	Not used	Not used

* No limitations.

---No response.

Part 4. Summary of Additional Comments Made by Some of the States

Alaska

No special construction or maintenance problems were noted.

Arizona

The additional lateral movement associated with this system, particularly with cast-in-place, post-tensioned concrete box girders, dictates longer wingwalls for backfill containment and the careful compaction of backfill material. Also, an adequate drainage system must be provided to prevent surface runoff from entering voids created at the ends of the wings and approach slabs; otherwise, progressive erosion of the approach embankment and under the approach slab occurs.

California

The abutment is not stable when standing alone during construction if the backwall height is too great. Wingwalls must be cast after stressing of cast-in-place prestress construction to avoid rotation and translation of walls. If soils don't yield, piling absorbs a large amount of prestressing force resulting in a large rotation at abutments and a large downward deflection in the span. This has been a particular problem with simple span cast-in-place prestress construction.

Colorado

We do have some problems with settlement of backfill behind the abutment and cracks in the asphalt pavement, but the problems are much less than the problems associated with snowplows and bridge expansion devices and bearing devices.

Connecticut

We have constructed one bridge to date and are very satisfied with it.

Georgia

Have had a problem with cracks in the wingwalls.

Idaho

Some problems have resulted from failing to provide adequate expansion joints in concrete approach pavements, but such problems are not peculiar to design concept under consideration. Problems are to be expected if the bridge is long, has no expansion joints anywhere, is a steel bridge, is on a substantial skew, or a combination of the foregoing. If used with discretion, the design concept is good in that it saves initial and maintenance costs of expansion joints.

Kentucky

No special construction or maintenance problems have been reported.

Missouri

We limit integral abutment bridges to a 40 degree skew.

Montana

No special construction problems noted. Integral abutment bridges probably require a little more maintenance due to embankment settlement.

Nebraska

Maintenance can be a problem if no concrete approach slab is provided.

New York

We assume that construction costs are lower because of simpler abutment-forming details and fewer piles. Setting the girders directly on

the piles created some alignment difficulty for the contractor. In the future we plan to use a detail similar to the detail shown in No. 1 of your questionnaire.

The continuous approach slab on a 125 foot single-span steel bridge built in 1980 has cracked at the rear face of the backwall. It is a tight crack that runs the full width of the slab but does not appear to be detrimental. To date, no detectable cracking has occurred in the backwalls and the abutments seem to be functioning as designed.

Ohio

As yet, no significant construction or maintenance problems have been noted.

Oklahoma

Integral abutments are used only on bridges with zero skew.

South Dakota

With steel bridges and longer concrete, we still utilize an expansion device in the approach slab system. Savings is in bearings and piling. Sill or abutment does not have to be designed for overturning loads.

For most steel bridges and longer concrete, we feel it is necessary to attach the approach slab with integral curb and gutter to the bridge. Without this provision, severe erosion around the wings can result and problems with approach fill settlement are increased.

Utah

No special construction or maintenance problems have been noted.

Vermont

Some minor approach settlement is anticipated.

Washington

Sometimes the piles may not end up in a straight line and at the right location. Some maintenance problems with downdrag and settlement have been noted.

Wisconsin

Cracking of diaphragms has been noted on bridges with large skews (greater than 20 degrees) and/or with long abutments. We limit integral abutment bridges to 40 degree skews.

Wyoming

No special construction or maintenance problems have been noted.

FHWA Region 15

We noted a problem with pavement cracking at bridge ends. This has since been eliminated with the use of approach slabs.

9.2. Memorandum to Designers, Office of Structures Design,
California Department of Transportation

This memorandum was attached to California's response to the integral abutment questionnaire. It describes California's criteria for the use of end diaphragm abutments, which includes both integral and semi-integral types.

Memo to Designers

The end diaphragm is an integral part of the bridge superstructure. Frequently this diaphragm is extended below the soffit of the superstructure to rest directly on piles or on a footing. This type of support is an "End Diaphragm Abutment." The discussion here will be limited to those situations where the diaphragm is fixed at the soffit and in effect is a cantilever beam between the soffit and the base which rests on piles or a footing.

Structure Movement:

Thermal movements are easily absorbed by this abutment. Concrete bridges of 400 feet between abutments, when conventionally reinforced, have shown no evidence of distress even though the end diaphragms rested directly on piles.

Elastic shortening due to post tensioning, however, is rapid and must be provided for in the abutment design when the initial shortening due to stressing exceeds $3/8$ ". When the span adjacent to the abutment exceeds about 160 feet, there could be an additional problem of rotation. To minimize the damage to the abutments of single span post tensioned structures due to earthquake, both abutments should be on sliding supports when that is the recommended treatment (see table below).

Below are listed some guidelines for use in providing for abutment movement. The limits shown are by no means absolute, but illustrate a conservative approach to the problem. Seat-type abutments are advisable where movement ratings are equal to or greater than $1-1/2$ inches.

Restraining Forces:

Listed below are assigned values for resistance offered by various end conditions. This force is applied at the base of the end diaphragm to determine the proper reinforcement. The values shown do not take into account the special situations where very long piles or small timber piles offer little resistance to longitudinal movement. Note that earthquake longitudinal force may govern over those shown below. See Section 2-25 Bridge Planning & Design Manual, Volume I.

Abutment Type	Design Logit. Force
End Diaphragm on CIDH piles	* 25 kips per pile
End Diaphragm on Concrete Driven Piles	* 20 kips per pile
End Diaphragm on 45T Steel Piles	* 15 kips per pile
End Diaphragm on Neoprene Strip or Pads	15% of dead load
End Diaphragm on Rollers	5% of dead load

* These values are intended for use in the design of end diaphragm only. For determining the number of piles required for longitudinal force, see Section 4-15.8(3) of Bridge Planning & Design Manual, Vol. I.

Earthquake Forces:

Shear keys must be added to provide resistance to transverse and longitudinal earthquake forces acting on the structure. These normally will be placed behind and at the ends of the abutment wall on narrow structures. On wide structures, additional keys may be located in the

interior. One half inch expansion joint filler should be specified at the sides of all keys to minimize the danger of binding. For earthquake design forces, see Section 2-25.2, Bridge Planning & Design Manual, Vol. I. For key sizes and key reinforcement, see Section 1, Bridge Planning & Design Manual, Volume III.

Drainage

1. No pervious material collector or weep holes required for flat slab bridges.
2. Continuous pervious backfill material collector and weep holes may be used for abutments in fills or well drained cuts in desert locations and at sites where a 5-ft level berm is specified.

End Slope Treatment	Weep Hole Discharge
Unprotected berm	Directly on unprotected berm
Bib slope paving	On spacer or groove in paved surface
Full slope paving	On spacer on groove in paved surface

3. Continuous permeable material and Perforated Steel Pipe collector discharging into Corrugated Steel Pipe overside drains should be used for all other abutments.
4. Corrugated Steel Pipe overside drains must be coordinated with road plans. If there is no discharge system and no collector

ditch, the outfall must be located away from the toe of slope to prevent erosion of the end slope.

5. Abutment drainage systems should be coordinated with the slope paving. See Memo to Designers 5-10.

Backfill Placement:

Unless there are special soil conditions or unusual structure geometrics, the designer need not specify the method or timing of backfill placement. Passive resistance of soil in front of the end diaphragm offers little restriction to structure movement due to stressing. Nor will the active pressure of backfill behind the end diaphragm materially alter the stress pattern even if the fill is completed at one abutment before being started at the other.

Suggested Details:

Sketches showing suggested abutment details are located in Bridge Planning and Design Manual, Volume IV, Detailer's Guide.

9.3. Iowa Department of Transportation Foundation Soils Information Chart

A majority of the bridge foundations designed by the Highway Division, Iowa Department of Transportation rest upon pilings which derive their support primarily from the shear strength of the surrounding soil rather than from end bearings. Economical and safe design of such foundations requires a knowledge of the bearing capacity of the foundation soils. A chart for pile length determination based upon the available information and experience was first introduced in 1958. This chart provided a feasible method of selecting pile lengths which effectively reduced pile cut-off. As more information becomes available, it is necessary that the "Foundation Soils Information Chart," used for estimating pile lengths, be periodically updated.

A total of 234 pile load tests have been performed since 1950. To evaluate the information properly, the tests were categorized as (a) pile tested to yield, and (b) pile tested to bearing. Of the total, 117 pile load tests were grouped into the "pile tested to yield" category. To evaluate the bearing capacity of foundation soils the piles tested to yield were reviewed, excluding the inconclusive tests. Sufficient numbers of conclusive tests are available for review.

The pile load tests performed on piles founded in only one foundation soil have enabled establishing a definite bearing value for that soil. Pile tests on certain soils have indicated a need for change in the bearing values given in the previous charts.

All available foundation soil information has been evaluated and incorporated in the revised design chart. Blow count values (N-Values^{*})

obtained from standard penetration tests performed on foundation soils and bedrocks have been included in the chart and in the additional recommendations. Statistical analysis was used to determine the mean value and standard deviation for blow counts on all soils.

Evaluation of pile load tests performed upon tapered steel shell piles on the I-129 project at the Missouri River crossing south of Sioux City indicate that the bearing value of the tapered pile in cohesionless foundation soils is greater than the bearing for parallel sided pile. However, the bearing value for tapered piling is not as high as originally indicated by the test loads made at the Council Bluffs viaduct. The additional column for steel shell piles has been left in the revised chart but the values have been reduced. According to Peck[†] the effect of taper pile in unconsolidated cohesive soils does not increase the bearing capacity of the pile.

The attached "Foundation Soils Information Chart" gives the allowable friction bearing per foot length of pile for different types of piles in different foundation soils. The chart and the methods of pile length determination described on subsequent pages will allow the designer to effectively select adequate pile lengths. To make effective use of the chart, the sounding nomenclature should compare with the chart nomenclature. The revised chart and the information contained herein will be subject to change as additional information becomes available.

* N-Value: The number of blows required by a 140-lb hammer with a free fall of 30 in. to drive a 2-in. O.D. by 1-3/8 in. I.D. split tube sampler 1.0 ft into the soil.

† Peck, Ralph B.: A Study of the Comparative Behavior of Friction Piles: Washington, D.C.: Highway Research Board: Special Report #36: 1958.

The hammer formulas used for pile driving during construction shall conform to the Standard Specifications and current Supplemental Specifications unless otherwise specified. The present hammer formulas are used as a check for pile bearing during construction. When the formula bearing for a pile is less than the design bearing, a pile load test should be secured.

The "Foundation Soils Information Chart" is intended to be an effective aid in selecting proper pile lengths. At stream crossings where scour may be a problem, tip penetration should be specified. Preliminary Bridge Design will determine the approximate scour depth.

Where compressible (unconsolidated) soils are under a fill, the fill should be predrilled, and drag forces calculated in accordance with the method described elsewhere.

A steel test pile in Johnson County was tested by pulling. The resultant allowable bearing value for very firm glacial clay fill was 0.3 tons per foot in uplift.

Additional Recommendations

1. Do not end a pile in a foundation material for which N-Value is 4 or less.
2. For wood friction piles, calculate the pile length from the total estimated safe bearing based on the design load and select the nearest pile length in multiples of 5 feet.

3. For a steel pile, the allowable load over the cross sectional area of the tip of the pile shall not exceed the following:

6,000 psi in bedrock for which $N = 20 - 200$

9,000 psi in bedrock for which $N = 200$ or more

4. When driving steel pile into bedrock, the following penetration is recommended:

8 ft to 12 ft in broken limestone, where practicable.

8 ft to 12 ft in shale or firm shale ($N = 20$ to 50).

4 ft to 10 ft in medium hard shale, hard shale or silt stone ($N = 50$ to 200).

3 ft to 6 ft in sandstone, siltstone, or hard shale ($N = 200$ or more).

1 ft to 3 ft in solid limestone.

5. If spread footing foundations are considered for a structure, additional core borings should be obtained to determine the allowable bearing value of the foundation material. In the absence of any other data, the allowable bearing value may be adopted from the following table:

Bedrock	Average N-Value	Allowable Bearing Value, tons/sq ft
Shale	16	2
Firm Shale	25	3
Med. Hard Shale	50+	5
Hard Shale	50+	5
Siltstone	50+	5
Sandstone	50+	5
Limestone	100+	10

Foundation Soils Information Chart

Estimated Allowable Bearing Value for Friction Piles in Tons per Foot
(Factor of Safety = 2.0)

Soil Description	Mean N-Value	Range* of N-Value	Wood Pile	Steel "H" Pile	Concrete Pile		Steel Shell Pile				
					16"	14"	Parallel Sided		Tapered		
							18"	14"	12"	10"	12" (Av.)
<u>Alluvium or Loess</u>											
Very soft silty clay	1	0-1	0.3	0.2	0.5	0.4	0.3	0.3	0.3	0.2	
Soft silty clay	3	2-4	0.3	0.2	0.5	0.4	0.3	0.3	0.3	0.2	
Stiff silty clay	6	4-8	0.5**	0.4	0.8	0.7	0.5	0.5	0.4	0.4	
Stiff silt	5	3-7	0.5	0.4	0.8	0.7	0.5	0.5	0.4	0.4	
Stiff sandy silt	5	4-8	0.5	0.4	0.9	0.8	0.5	0.5	0.4	0.4	
Stiff sandy clay	6	4-8	0.7	0.6	0.9	0.8	0.6	0.6	0.5	0.4	
Silty sand	8	3-13	0.8	0.7	1.0	0.9	0.6	0.6	0.5	0.4	
Clayey sand	13	6-20	0.7	0.6	1.0	0.9	0.6	0.6	0.5	0.4	
Fine sand	15	8-22	1.0	0.6	1.1	1.0	0.7	0.7	0.6	0.5	0.9
Coarse sand	20	12-28	1.2	0.9	1.2	1.1	0.9	0.9	0.8	0.6	1.2
Gravelly sand	21	11-31	1.6	0.9	1.6	1.6	1.3	1.2	1.0	0.9	1.6
<u>Glacial Clays</u>											
Firm silty clay	11	7-15	1.0	0.7	0.9	0.8	0.7	0.6			
Firm silty gl. clay	11	7-15	1.0	0.8	1.0	0.9	0.7	0.6			
Firm clay (Gumbotil)	12	9-15	1.0	1.0	1.0	0.9	0.7	0.6			
Firm glacial clay	11	7-15	1.4	0.9	1.1	1.0	0.9	0.8			
Firm sandy gl. clay	13	9-17	1.4	0.9	1.1	1.1	0.9	0.8			
Firm-very firm gl. clay	14	11-17	1.4	1.2	1.2	1.1	0.9	0.8			
Very firm gl. clay	24	17-31	1.6	1.4	1.6	1.7	1.4	1.3			
Very firm sandy gl. clay	25	15-35	1.6	1.4	1.6	1.6	1.4	1.3			

* Range = mean ± 1 std. deviation.

** Underlined values determined from pile load tests to yield.

Note: Glacial soils with N-values greater than 35 and granular soils with N-values greater than 50 MUST be given special consideration.

Date: January, 1967

Revised: June, 1976